

**Impacts of Past and Future Glaciation-Deglaciation
Cycles on Sedimentary Rocks in Southern Ontario**

submitted by:

Dr. M. Fall
Associate Professor
and
O. Nasir
M.A.Sc., P.Eng

Civil Engineering Department
Faculty of Engineering
University of Ottawa

to

CNSC

Ottawa, Canada, December 15th, 2011



**Safety-Related Aspects of a Radioactive Waste Repository in
Sedimentary Rock Formations - Generation and Migration of Gas from
the Waste Repository**

**Impacts of Past and Future Glaciation-Deglaciation Cycles on
Sedimentary Rocks in Southern Ontario**

submitted by:

Dr. M. Fall
Associate Professor
and
O. Nasir
M.A.Sc., P.Eng

Civil Engineering Department
Faculty of Engineering
University of Ottawa

to

CNSC

Ottawa, Canada, December 15th, 2011

Contract No. and Title: 87055-08-0571: R413.1 - "Coordinated Assessment and Research
Program on Safety-Related Aspects of a Radioactive Waste Repository in Sedimentary Rock
Formations: Stability of the Geosphere under Past and Future Climate Change"

Preface

Proponents for the geological disposal of solid radioactive waste must present safety cases to regulatory agencies, such as the Canadian Nuclear Safety Commission (CNSC). In order to prepare for an objective assessment of such safety cases, CNSC staff is building independent expertise on key safety aspects, such as the impact of glaciation/deglaciation cycles on sedimentary rocks in southern Ontario at the proposed deep geological repository (DGR) site. To that effect, the CNSC is financing the present study which deals with the numerical investigation of the stability of the geosphere under past and future climate changes. The principal investigator of the present project is Professor M. Fall from the Department of Civil Engineering at the University of Ottawa.

Table of Contents

1 Introduction	9
2 Critical Review and Comparison of Climate Change Models	11
2.1 Introduction	11
2.2 The University of Toronto Glacial Systems Model (U of T GSM) “Peltier’s model”	14
2.2.1 3D thermo-mechanically coupled ice sheet model (ISM)	15
2.2.2 Visco-elastic bedrock response	15
2.2.3 Surface mass-balance	15
2.2.4 Ice calving module	16
2.2.5 Drainage solver	16
2.2.6 Climate and margin forcing	16
2.3 UEDIN’s ice-sheet/drainage model - “Boulton’s Model”	16
2.3.1 Climate drive	17
2.3.2 3D TM ice-sheet model	17
2.3.3 Earth model	17
2.3.4 The drainage model	17
2.4 Comparison and conclusion	18
3 Geological and Geotechnical Characteristics of the Study Area	21
3.1 Introduction	21
3.2 The study area	22
3.3 Geological characteristics of the study area	24
3.3.1 Geological formation and structural characteristics	24
3.3.2 Hydrogeological characteristics	30
3.3.3 Geochemical characteristics	32

3.3.3.1 Rock chemistry	33
3.3.3.3 Chemistry of glacial melted water	36
3.3.4 Paleoglaciations and their geological effects in the study area	37
3.4 Geotechnical characteristics of the study area	40
3.4.1 Geomechanical characteristics	40
3.4.2 Hydraulic characteristics	43
3.4.3 Thermal characteristics	44
3.5 Conclusion	45
4 Development of a Thermo-Hydro-Mechanical-Chemical Model for the Analysis of the Impacts of Glaciation-Deglaciation Cycles on Sedimentary Rocks	47
4.1 Introduction	47
4.2 Development of the mathematical model	47
4.2.1 Flow equation	48
4.2.2 Solute transport model	49
4.2.3 Mechanical model	50
4.2.3 Heat transfer model	50
4.3 Conclusions	52
5 Numerical Analysis of the Impacts of Past Glaciation-Deglaciation Cycles on Sedimentary Rocks in Ontario	53
5.1 Introduction	53
5.2 Model conceptualization	53
5.3 Initial and boundary conditions	55
5.4 Simulation results	57
5.4.1 Temperature distribution and evolution	57
5.4.2 Distribution and evolution of the pore water pressure	58

5.4.3 Evolution and distribution of the surface deformation and the vertical effective stress	65
5.4.4 TDS distribution and evolution	70
6 Numerical Analysis of the Impacts of Future Glaciation-Deglaciation Cycles on Sedimentary Rocks in Ontario	72
6.1 Introduction	72
6.2 Model conceptualization, initial and boundary conditions	72
6.3 Simulation results	74
6.3.1 Hydraulic response	74
6.3.2 Mechanical response	80
6.3.4 Simulation of solute transport	83
7 Conclusions	89
8 References	92
9 Disclaimer	97

List of Abbreviation

Abbreviation	Identification
BC	Boundary conditions
CNSC	Canadian nuclear safety commission
DGR	Deep geological repositories
EDZ	Excavation damaged zone
FEM	Finite element method
ILW	Intermediate level radioactive waste
GRIP	Greenland ice core project
GSM	Glacial Systems Model
ISM	Ice sheet model
GCM	Global circulation models
LLW	Low level radioactive waste
NWMO	Nuclear waste management organization
PDE	Partial differential equation
RQD	Rock quality designation
TDS	Total dissolved solid
THMC	Thermo-hydro-mechanical-chemical
UCS	Uniaxial compressive strength

Abstract

This document represents the final report of a study initiated and financed by the Canadian Nuclear Safety Commission (CNSC). It deals with the study of the impacts of past and future climate changes on the Ontario's sedimentary rocks with regards to deep geological disposal of nuclear wastes (Low and Intermediate Level radioactive waste, LLW, ILW).

In the present report, a general review on the fundamental causes and results of the long-term climate change is performed. Moreover, a comprehensive and critical review and comparison of two long-term climate change models is carried out. The results show that the University of Toronto's Climate Change Model can be used to predict the past and future climate changes in Ontario. Published geological, geochemical, mechanical, hydraulic and thermal data on sedimentary rock formations in Ontario, which are relevant to the study of the impacts of past and future glaciations are compiled and critically analysed. These data are used in the development of conceptual models of the study area. A coupled thermo-hydro-mechanical-chemical (THMC) model for the analysis of the impact of glaciations on sedimentary rocks is developed and validated. The verification and validation results show that there is a relatively good agreement between the results predicted by the model and those obtained analytically or experimentally (field data). The developed model is used to numerically analyse the effects of past and future cycles of glaciation and deglaciation on Ontario's host sedimentary rocks. Valuable results are obtained. It is found that past and future glaciations had or will have a significant impact on the pore water pressure gradient, hydraulic gradient and effective stress distribution within the sedimentary rocks in Ontario. Furthermore, the permafrost depth is found to be limited to shallow depth ($\leq 50\text{m}$). It is also found that the past and future climate changes didn't have and will not have significant effects on solute transport in the Ontario's host rock and that solute transport in the rock barrier (limestone, shale) is diffusion dominant. However, the simulation results show, for the case of a deteriorated shaft, that the future climate changes can lead to the development of high vertical effective stresses in the shaft. These stresses could potentially lead to further physical degradation of the shaft seal material. The simulation results reveal that a failed shaft can become a preferential path for contaminant (solute) transport.

1 Introduction

Deep geological repositories (DGR) in a host sedimentary rock formation for the long term containment and isolation of nuclear wastes are currently being proposed in several countries (e.g., Canada, France, Switzerland). In Canada, a repository for low and intermediate levels of radioactive wastes is being proposed in Ontario's sedimentary rock formations. A key aspect of DGR safety is the long-term stability of the sedimentary host rock for very long timeframes of up to 1 Ma.

Glaciation and deglaciation are viewed as the primary natural process that can significantly affect the host rock of a DGR for nuclear waste (Nguyen et al. 1993, Chan et al. 2005). The potential impact of glaciations on the stability of a DGR system can result from different processes, such as mechanical (ice loading-unloading), hydraulic (water pressure due to the melting of ice), thermal (thermal stresses and deformation) and geochemical (changes in ground water and rock chemistry) processes. The understanding and modelling of those thermal-hydraulic-mechanical-chemical (THMC) processes are crucial for a reliable analysis of the impact of future climate changes on the host sedimentary rocks of a DGR in Ontario.

An understanding of the impact of past and future glaciation on sedimentary rocks for a DGR in Ontario is important to reliably assess the safety of underground repositories for radioactive waste. Therefore, CNSC initiated, financed and participated in the present study, which consists of the following tasks:

- to critically review and compare the climate change models by Peltier (University of Toronto) and Boulton;
- to compile published geological and geotechnical (mechanical, hydraulic, thermal) data on sedimentary rock formations in Ontario;
- to develop a mathematical model for the analysis of the impact of past and future glaciation on Ontario's sedimentary rocks;
- to conduct a numerical analysis of the impact of past glaciation-deglaciation cycles on Ontario's sedimentary rocks; and
- to conduct a numerical analysis of the impact of future glaciation-deglaciation cycles on Ontario's sedimentary rocks.

The report comprises seven sections. The content of each section is summarized as follows. **Section 1** provides an introduction to the issues that will be addressed and the objectives of the project. In **Section 2**, the climate change models by Peltier and Boulton are critically reviewed and compared to determine the model that is more suitable for the present study. **Section 3** presents a review and analysis of the existing geological and geotechnical data from Ontario's sedimentary rocks. **Section 4** deals with the development and verification of a mathematical model for the prediction and assessment of the impact of past and future glaciation-deglaciation cycles on Ontario's sedimentary rocks. **Section 5** presents the application of the developed mathematical model to numerically analyse the impacts of past glaciation-deglaciation cycles on Ontario's sedimentary rocks. **Section 6** deals with a numerical analysis on the effects of future a glaciation-deglaciation cycle on Ontario's sedimentary rocks. **Section 7** provides the main findings and conclusions of the project as well as recommendations for future work.

2 Critical Review and Comparison of Climate Change Models

2.1 Introduction

The Earth's climate during the Quaternary period had dynamical characteristics, represented by periodic glaciation-deglaciation cycles. The dynamic features of the Earth's climate could be attributed to its response to external and/or internal forcing mechanisms (Lowe and Walker 1997; Maslin et al., 2007). External forcing mechanisms (e.g., tectonic activities, see Figure 2.1, orbital forcing) are those which are outside the climate system; variations in solar energy are an example of external forcing (Lowe and Walker 1997). On the other hand, internal forcing mechanisms (e.g., atmospheric and oceanic circulation, feedback mechanisms) are those that exist within the climate system; for example, internal oscillations in ocean circulation (Mark et al. 2007) which change the heat and moisture transport between regions (Mark et al. 2007).

Geological evidence has shown that the northern hemisphere has been subjected to a series of intense glaciation-deglaciation cycles over the past millions of years. Each glaciation cycle is associated with the development of large continental ice sheets. The last cycle started approximately 120,000 years ago. In southern Ontario, where the proposed repository would be located, the ice advanced in a NE-SW direction, and its thickness attained a maximum value of 2500 m (personal communication, Nguyen 2011). However, it should be emphasized that a NW-SE direction is suggested by other studies (Piotrowsk 1987; Lowe and Walker 1997). Ice sheet loading was responsible for the significant change in the topography and groundwater regime (Vidstrand et al., 2008). These cycles are likely to reappear in the future within a time frame of several hundred thousands of years and have to be taken into account in performance assessments of DGR for nuclear wastes in Ontario.

The facts mentioned above mean that the reconstruction of past climates and the prediction of future climate changes in the northern hemisphere could have significant implications on the performance assessment of DGRs in Ontario. This is because there are several features of the glaciation process that are pertinent to the understanding of DGR performance. Peltier (2003) identified the following main features: (i) mechanical properties, such as the time dependence of glacial ice thickness that could develop over a

site and the normal stress regime related to the weight of this load, and (ii) the evolution of the temperature at the bottom of the ice-sheet, which could result in various hydraulic and/or thermal boundary conditions (BCs) relevant to DGR performance, such as the generation of melt water (which may be forced to penetrate into the subsurface and thus affect the sub-surface hydrology), and the development of frozen ground (permafrost) (Peltier 2003).

Climate change models are useful tools and commonly used to reproduce past climates and predict future climates. The main objective of a climate change model is to link the different components of an ocean-atmosphere-terrestrial system with climate change. Climate change models are numerical tools to predict and project the weather for different time scales (future and past) based on the integration of different equations. Each of the solved equations represents specific physical, chemical, and sometimes, biological processes, which could be external or internal processes within the climate system (see Figure 2.2). In general, global circulation models (GCM) and conceptual models can be used for the prediction of climate change (Lowe and Walker 1997). Due to both the large scale and huge uncertainties and complexities of the earth climate system, GCM and conceptual models are gross simplifications of the system. The most established and used climate change models include: (i) The University of Toronto Glacial Systems Model (U of T GSM), “Peltier’s model”; (ii) UEDIN’s ice-sheet/drainage model, “Boulton’s Model”.

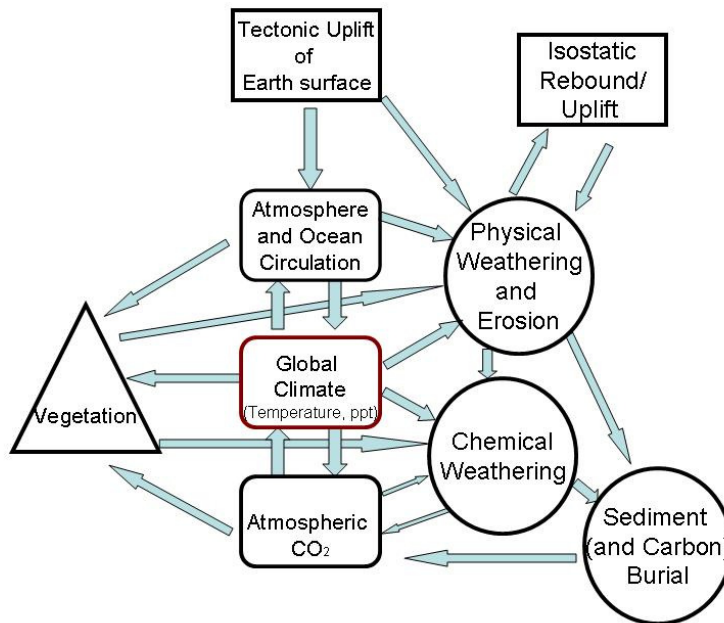


Figure 2.1. Tectonic uplift and climate change (redrawn after Williams 1997)

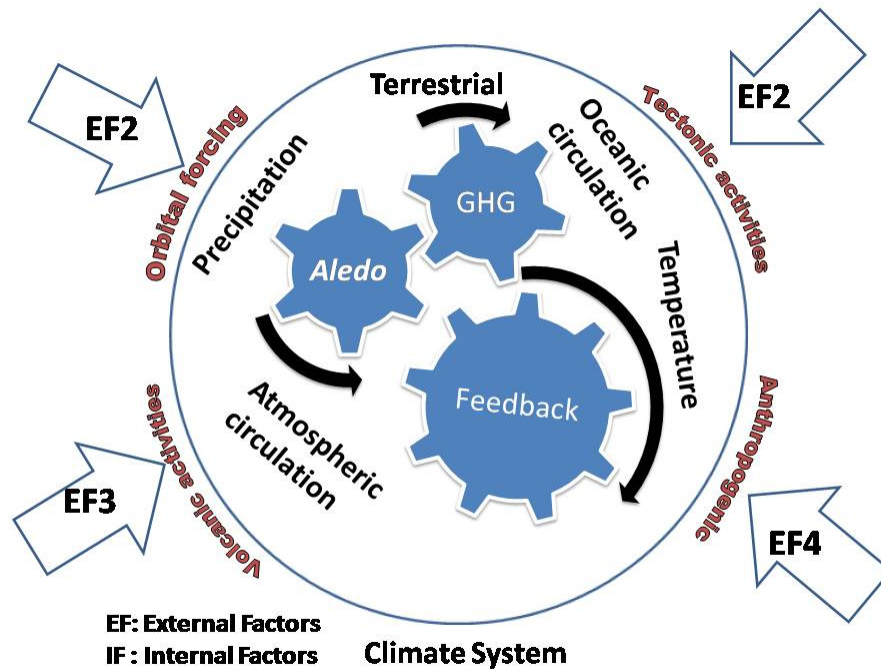


Figure 2.2. Climate system of the Earth

From the synthesis presented above, it can be concluded that the use of a suitable climate change model to predict past and future climate changes is crucial for the determination of adequate hydraulic, thermal and mechanical BCs in a DGR system, i.e. for a reliable assessment of a DGR performance in Ontario.

Hence, the objectives of this section are:

- to review the U of T GSM, “Peltier’s model”;
- to review UEDIN’s ice-sheet/drainage model, “Boulton’s model”;
- to compare the above models and analyze their suitability to predict the climate in Ontario; and
- to select the climate change model that would specify the thermal, mechanical, hydraulic and chemical BCs at the earth surface based on sound scientific principles, and have an acceptable degree of validation with existing field records to predict the past and future climate changes in Ontario.

2.2 The University of Toronto Glacial Systems Model (U of T GSM) “Peltier’s model”

Recently, Peltier (2003) constructed a new class of Laurentide (North American) glaciation models that are able to meet relative sea levels and surface geomorphologic constraints as well as recent geodetic observations. The Peltier’s model can be used to generate required BCs in the process of reconstructing a past climate system. The Peltier’s model incorporates a number of interacting components, such as a 3D thermo-mechanically coupled ice-sheet model that includes a model of sub-surface thermal evolution, a representation of fast flow due to subglacial till-deformation, model of visco-elastic bedrock response, surface mass-balance module, an ice calving module, and finally, a fast dynamical melt water surface routing and storage solver (Tarasov and Peltier, 2004) as explained in more detail in the following sub-sections. The most important element is a deterministic model of continental ice sheet evolution (Tarasov and Peltier, 1999; 2002; 2004; 2006). Peltier (2008) executed the GSM over the past 120 ka in North America with a 1.0° longitude by 0.5° latitude grid resolution in order to produce a data set for surface elevation, ice sheet thickness, relative sea level and subglacial melt rate. The GSM model has a large number of parameters, many of which

are well known. Many parameters are “ensemble parameters” that lie within a given range. The ensemble parameters have been undergoing calibration for North American deglaciation against a large set of observational constraints, including a large set of high-quality relative sea-level histories, a space geodetic observation of the present-day rate of vertical motion of the crust from Yellowknife, and a traverse of absolute gravity measurements from the west coast of Hudson Bay southward into Iowa (Tarasov and Peltier, 2004).

2.2.1 3D thermo-mechanically coupled ice sheet model (ISM)

The ice sheet model (ISM) is the core of the U of T GCM model. In this model, shallow-ice approximation and the Glen flow law are used for ice rheology. In addition to that, the ISM model includes some components to simulate the real changes in BCs. These components include: sub-surface thermal evolution, and fast flow due to subglacial till-deformation (Chan et al. 2005). Moreover, the best fit dynamical models for the Greenland Ice Sheet is used to find an ice flow enhancement factor (Tarasov and Peltier 2002, 2003).

2.2.2 Visco-elastic bedrock response

For the modelling of the earth’s surface deformation due to glaciation-deglaciation loads, a linear visco-elastic field theory is used (Peltier 1974, 1976). In this model, radial viscosity and elasticity of the earth were employed by Peltier (1996) and Dziewonski and Anderson (1981), respectively. This model of “the glacial isostatic adjustment” is coupled to the ISM.

2.2.3 Surface mass-balance

This part of the model includes the computation of the key parameters for ice and water mass balance parameters. These parameters include ice and snow ablation by using a positive-degree day methodology, and rain–snow fraction, by using a normal statistical model (Tarasov and Peltier 2002, 2006). However, ensemble parameters are used to overcome the uncertainties in the surface mass-balance. In addition to that, the basal melting of water ice (wet-basal conditions), due to pressure and temperature (melting point), is included in the model.

2.2.4 Ice calving module

Both the effects of buoyancy and ice blockage of drainage channels have been taken into account in the calving model by considering the influence of temperature. Due to the poor constraints on calving dynamics, three ensemble parameters are assigned to the calving model (Tarasov and Peltier 2002).

2.2.5 Drainage solver

In this model, calculations of the surface drainage of melt water are based on a depression fill and down-slope flow drainage algorithm. In addition to that, the model includes the changes in the inland lake levels by considering the existing level and the change due to the drainage input (over-flow is included in the model) (Tarasov and Peltier 2002).

2.2.6 Climate and margin forcing

In this model, uncertainties due to poorly constrained dynamical processes and transitions from interglacial to glacial atmospheric states are captured based on large ensembles of model runs, with 22 ensemble parameters (Tarasov and Peltier 2004) by using geophysical observations. In addition to that, a strong regional topographic feedback on precipitation is also included through the desert-elevation effect. Furthermore, a glacial index (It) is used to control the time dependence of the climate forcing. It is used to linearly interpolate between a present day observed climatology and LGM climate. This index is derived from the temperature history of the Greenland summit region by using the $\delta^{18}O$ records from the Greenland Ice Core Project (GRIP) (Tarasov and Peltier 2002). Due to the limitation in the mentioned ensemble parameters in capturing the complexities of glacial climate variations, modifications to the surface mass-balance by using the inferred ^{14}C to control the margin chronology are included in the model (Chan et al. 2005).

2.3 UEDIN's ice-sheet/drainage model - "Boulton's Model"

This model was developed at the University of Edinburgh to generate transient hydraulic and mechanical surface BCs that resulted from glaciations on a continental-scale (Boulton et al. 2004). The model contains four main components as described in the following sub-sections.

2.3.1 Climate drive

In this part of the model, the climate force responsible for climate change is derived by using a simple linear regression correlation between the Greenland ice sheet palaeoclimate records and local climate change records (Chan et al. 2005). Moreover, some geological evidence has been used to fit the ice sheet model with the geological data.

2.3.2 3D TM ice-sheet model

The Ice Sheet Model is the main component of UEDIN's ice-sheet/drainage model; in this model, three processes are included. The first process is the temperature dependent flow of ice sheet due to possible sliding (Mahaffy 1976). In this model, the Glen flow law is used for the ice strain rate. In addition to that, the ICM is coupled with heat transfer due to advection from the flow of the melted water. Changes in the BCs have also been taken into consideration. The included changes in the ice sheet BC are: (i) basal BC which includes temperature-dependent basal sliding, and time dependent lithosphere deflection which depends on the diffusivity of the asthenosphere, (ii) the upper BC which includes temperature and mass balance, and marine BC, which includes sliding, floating and calving of ice blocks (Boulton et al. 2001).

2.3.3 Earth model

In this part of the model, the isostatic response of the earth's surface due to the loading and unloading effects of glaciation-deglaciation cycles by using the results by Lambeck et al. (1998) is included, and coupled with ISM (Boulton et al. 2004). To measure the earth's surface deformation, it was assumed that the surface is a plastic plate subjected to normal load, floating on a non-viscous medium (Lambeck and Natiboglu 1980; Le Meur and Huybrechts 1996). The asthenosphere, where most of the deformation occurs, is approximated by a Maxwell solid allowing for a full visco-elastic treatment according to the correspondence principle (Peltier 1974).

2.3.4 The drainage model

In this part, the flow of melt water is determined by using two components. The first component is a subglacial stream tunnel, which is responsible for the longitudinal

discharge of water. In addition to the discharge, the pressure inside the tunnel is determined and the melting due to pressure is taken into consideration (Chan et al. 2005). The second component is the groundwater flow and water pressure at the ice/bed interface. In this part, the source of the groundwater flow is the melting water from the ice sheet; hence, the tunnels will work as a sink for the underground flow. However, the underground flow will be due to diffusivity, and the pressure inside the stream tunnel can be determined at equilibrium (Chan et al. 2005), which can be used as hydraulic BCs on the ground surface.

2.4 Comparison and conclusion

From the literature review presented above, it can be concluded that a climate change model should as much as possible, fulfill the following three main criteria.

- The climate change model should have adequate input data. Since climate change is mainly triggered by external factors, and affected by internal factors, the input values for the relevant parameters are the key in the successful prediction of the future climate.
- The model should include information about the main processes within the ice sheet and ground surface-ice sheet interface because of the specific purpose and objectives of this project, including the analysis of THMC coupled processes in sedimentary rocks. This information will be used as the BCs which include the temperature, ice thickness and water pressure.
- The model should be validated with globally (by using ice core records) and locally (by using geomorphological records) available climate change evidence.

Table 2.1 shows a comparative summary between the U of T GSM and the UEDIN model.

Table 2.1. Summary of comparison between the UoT GSM and UEDIN models.

Criteria	General Model Should Include	UEDIN's Model	U of T's Model	Comments
Forcing factors	External	NA	NA	Interpolation with $\delta^{18}O$
	Internal	NA	NA	Interpolation with $\delta^{18}O$
Model output	Mechanical ice thickness	Applicable	Applicable	Constant ice profile density
	Hydraulic surface water pressure	Applicable wet-based glacier	NA	Can be initiated from UEDIN's model as 80% of the normal ice pressure
	Thermal surface temperature	Applicable	Applicable	
	Chemical water chemistry	Applicable	NA	
Model validation	Global Temperature ($\delta^{18}O$ records)	Applicable	Applicable	
	Sea level	Applicable	Applicable	
	Local geomorphological records	Applicable	Applicable	Ensemble parameters

Based on the results of the comparisons presented in Table 2.1, the following conclusions can be drawn:

- both models, UEDIN and the U of T GSMs, could be used to reconstruct past climate changes and predict future climate changes in Ontario. Each model presents certain advantages and some weakness with regards to its applicability to Ontario;
- UEDIN's model has more applicable parameters within the model. Nevertheless, it does not fully capture the uncertainties related to the geomorphological evidence; and

- the U of T GSM model could be applied because it has more validation in geographical areas relevant to the present study through the use of the ensemble parameters, with more extensive amounts of validation data through the use of existing field records (sea level, δ O18, geomorphology, etc.). However, the U of T GSM is not supported by information on surface water pressure and water chemistry.

3 Geological and Geotechnical Characteristics of the Study Area

3.1 Introduction

Understanding and predicting the impacts of glaciation-deglaciation cycles on Ontario's sedimentary rocks require numerical modelling of the various coupled processes, such as mechanical (e.g., ice loading-unloading, deformation), hydraulic (e.g., water pressure due to the melting of ice, pore water), thermal (e.g., thermal stresses and deformation) and chemical (change in ground water and rock chemistry) processes that have occurred in Ontario's sedimentary rocks. The numerical modelling of these THMC processes necessitates the development of a representative geological framework that characterizes the geometrical, physical and chemical properties and processes of the rock formations in the study area as well as the use of sufficient and adequate data to validate the model with respect to the THMC processes. This means that there is the need to gather sufficient technical data with regards to the geological and geotechnical characteristics of the area investigated.

The objectives of this section are to:

- describe the study area, and
- collect sufficient technical data on sedimentary rock formations in Ontario, which is necessary to build and validate a conceptual model for the area of study.

In this chapter, two main data categories are used. The first category includes the geological data (e.g., regional geology, geological formations, and geochemical data). The second category contains geotechnical data, such as the mechanical, hydraulic, and thermal properties of sedimentary rocks. Figure 3.1 presents a diagram of the data collected in this report.

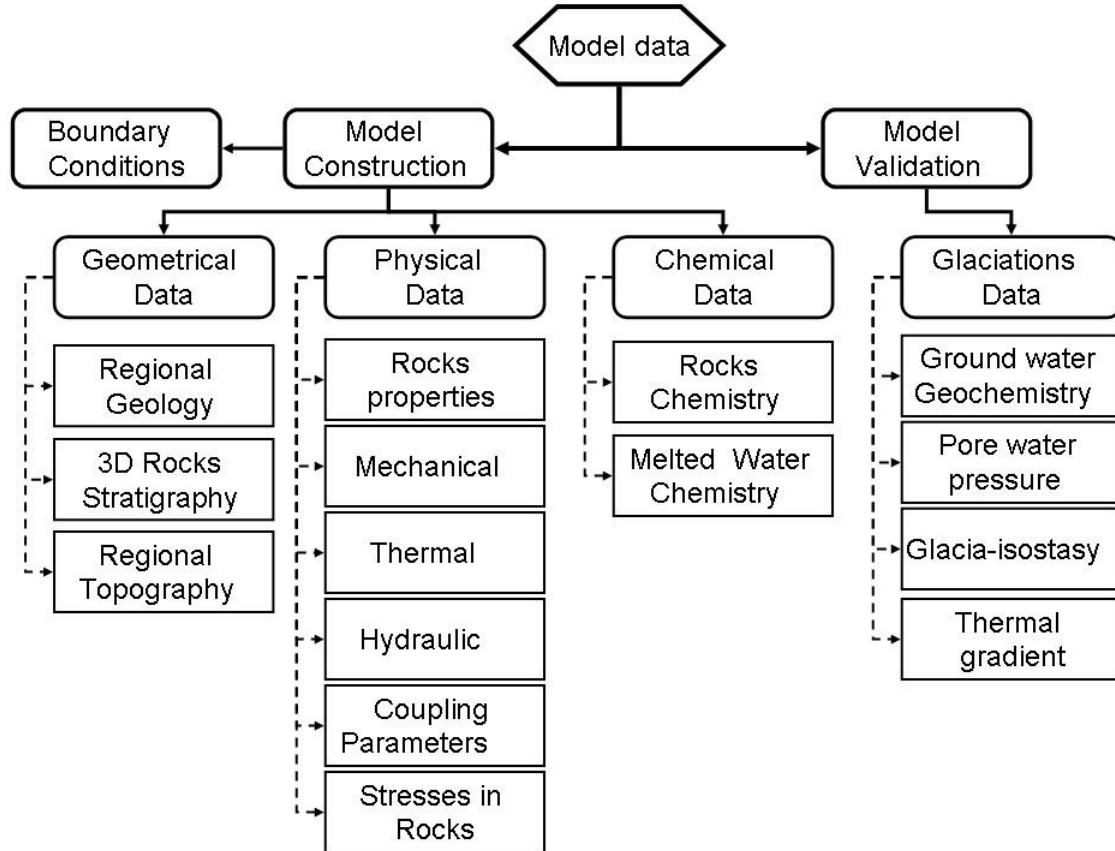


Figure 3.1. Diagram of the collected data

3.2 The study area

The study area is located in southern Ontario, near the eastern margin of the Michigan Basin, on the eastern side of the Huron Lake as shown in Figure 3.2. A DGR for low and intermediate levels of nuclear waste is being proposed at a depth of approximately 680 m in an argillaceous limestone formation within the study area (Figure 3.3). A multi-year site investigation program has been conducted at the site of the proposed DGR, consisting of seismic surveys, and a series of deep vertical and inclined boreholes, and hydraulic, petrographic, geochemical and mechanical testing that have been performed in-situ and in the laboratory (e.g., Gartner Lee Limited, 2008; Jensen et al. 2009; NWMO, 2011a; NWMO, 2011b).

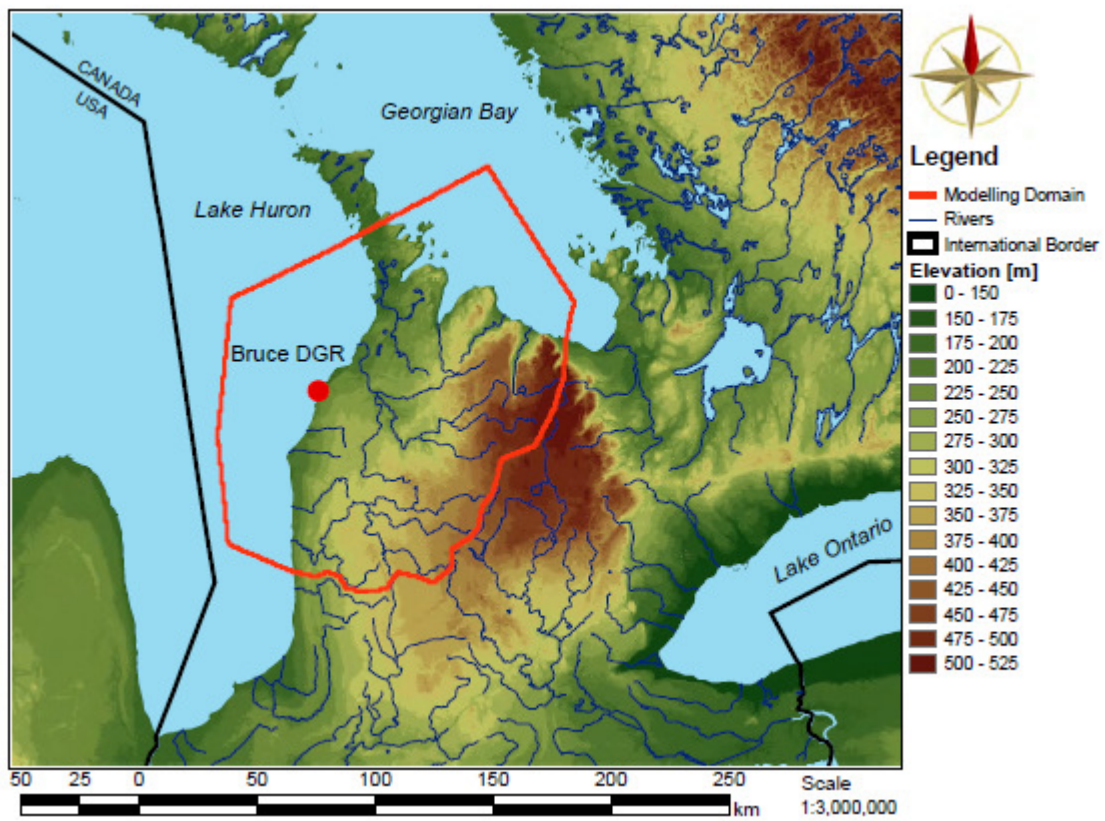


Figure 3.2. Map that shows the location of the OPG proposed deep geological repository for low and intermediate level waste (NWMO, 2011c)

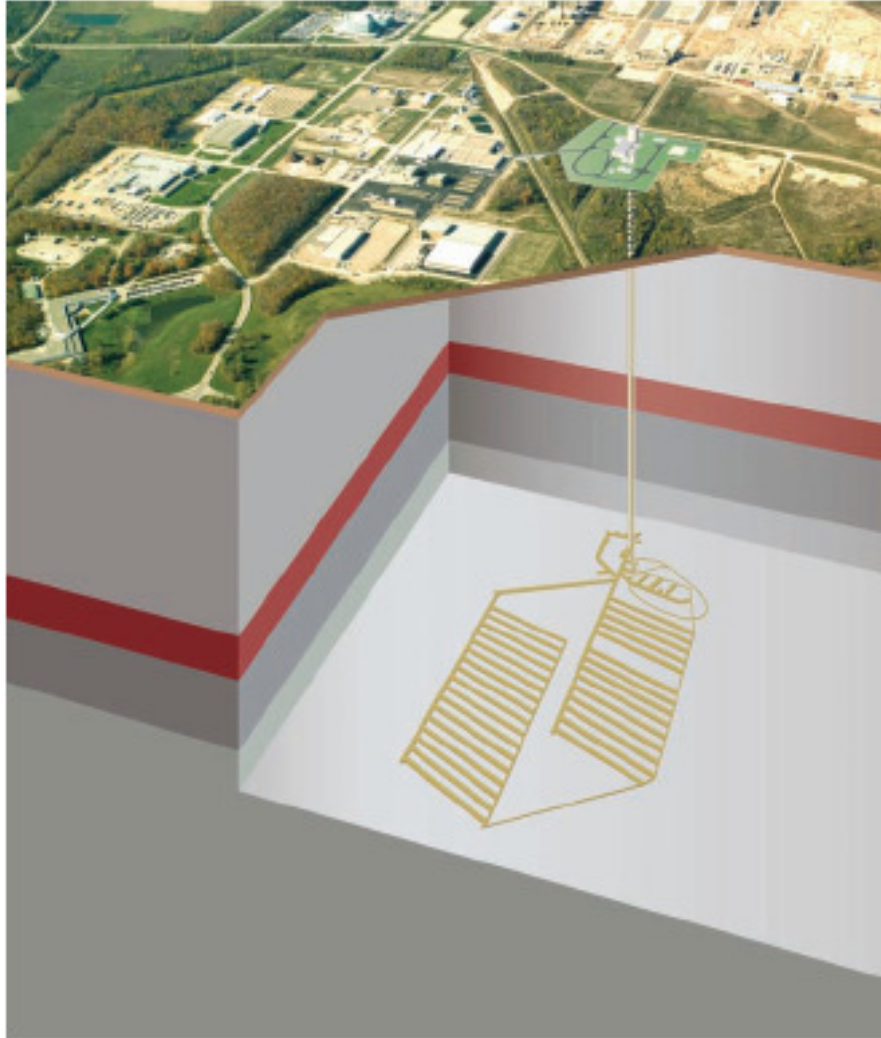


Figure 3.3. Conceptual layout of the proposed DGR (replace with the most recent conceptual design (NWMO, 2011a))

3.3 Geological characteristics of the study area

3.3.1 Geological formation and structural characteristics

The bedrock formations in the study area are layers of sedimentary rocks that had formed within the depression of the Michigan Basin. The Michigan Basin is one of four basins of subsidence and sedimentation southeast of the Transcontinental Arch. The other basins include the Eastern Interior, Appalachian and Western Interior Basins as shown in Figure 3.4. Sedimentary rock formations in the Michigan Basin typically include: carbonates, shale, evaporite and sandstone which are located above the Pre-Cambrian crystalline basement. The thicknesses and dips of each layer in the Paleozoic formation

vary with increasing thicknesses towards the southwest direction until a maximum is reached at the center of the Michigan Basin, and decreasing thicknesses towards the Algonquin Arch as shown in Figures 3.5 and 3.6.

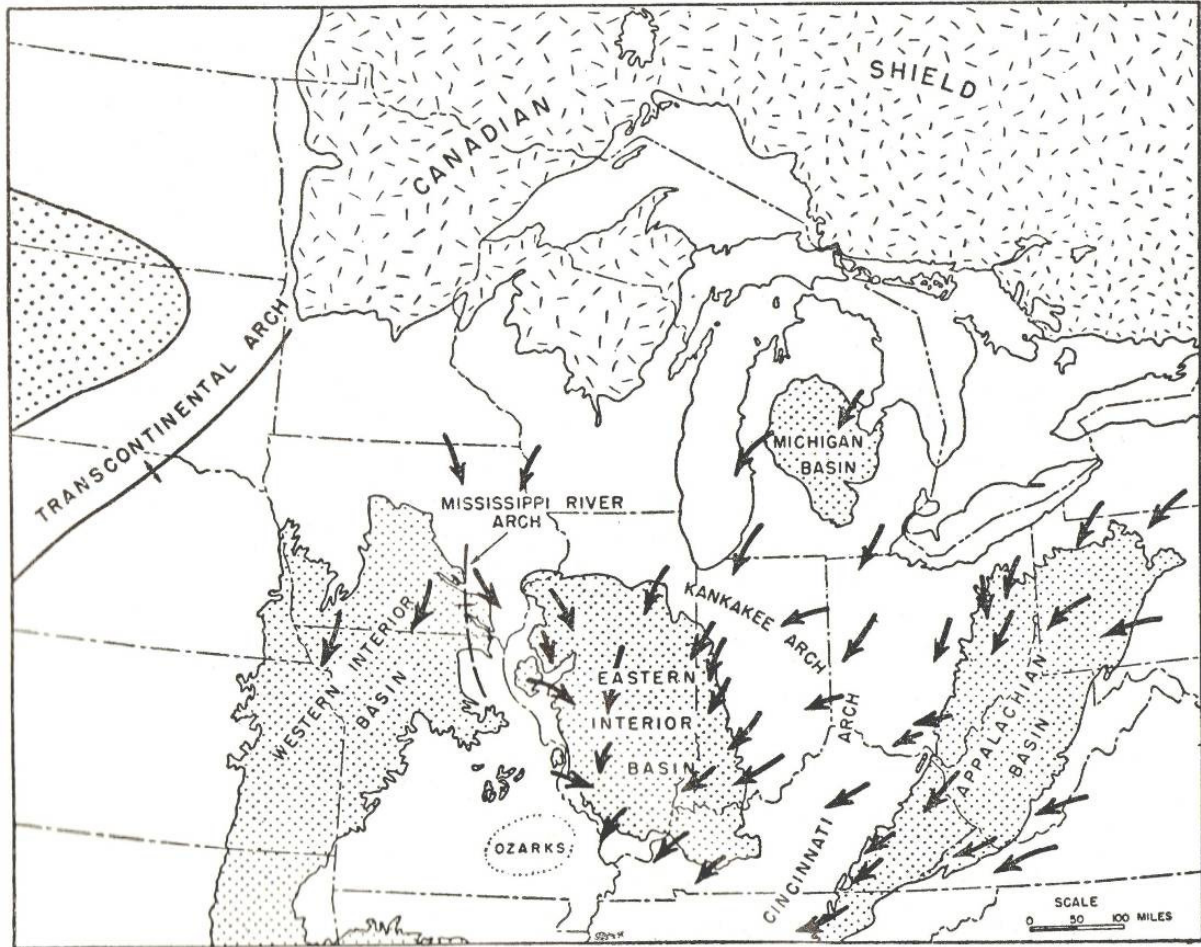
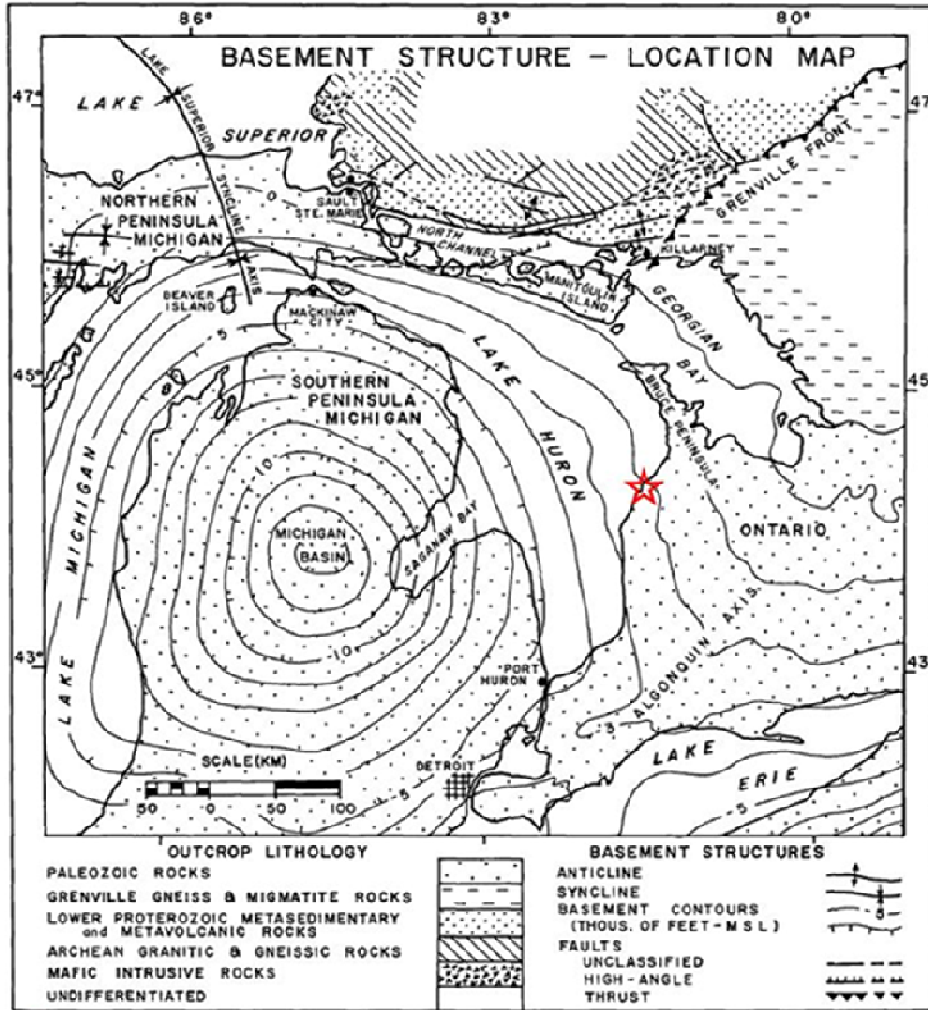


Figure 3.4. Basins that are southeast of the Transcontinental Arch (Eardley 1962).
(Arrows = direction of the stream transport)



★ Site for OPG's Proposed DGR for Low and Intermediate Level Wastes

Figure 3.5. Geology of the Michigan Basin (O'Hara and Hinze, 1980)

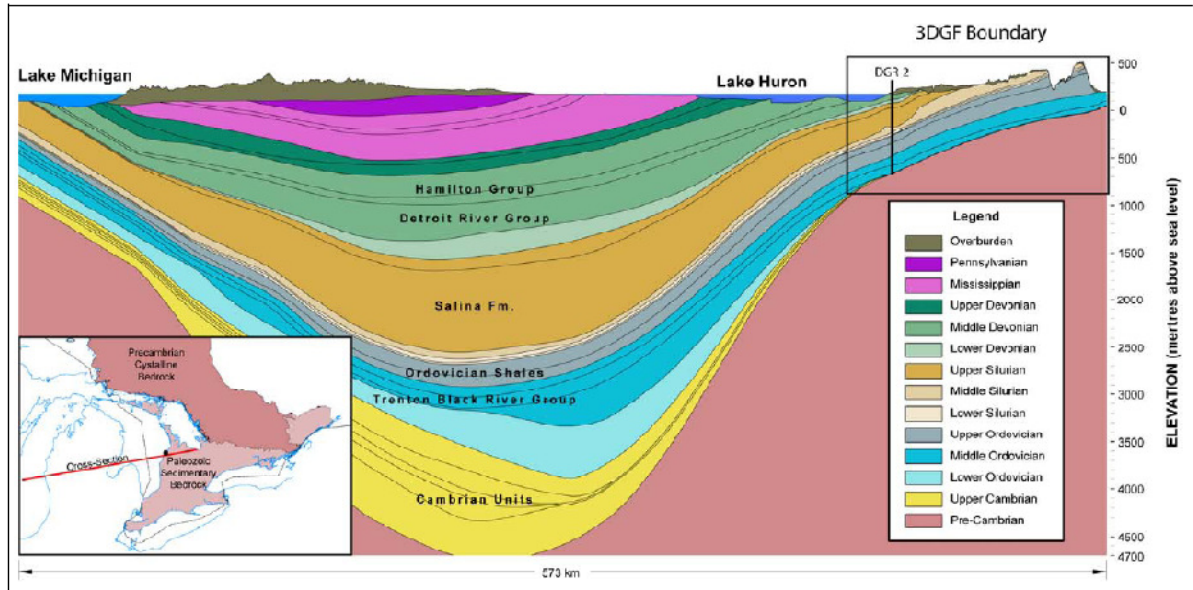


Figure 3.6. Cross section of the Michigan Basin (Gartner Lee Limited, 2008)

Based on the mapping of major fractures obtained by satellite imagery, Sanford et al. (1985) defined several megablock boundaries. He subdivided Southern Ontario south of the Canadian Shield into a number of tectonic blocks (megablocks) based upon the characteristics of basement structures, subsurface faults and surface lineaments. Among these megablocks, the megablock that includes the study area (red circle in Figure 3.7) is tectonically stable and less active than the surrounding megablocks. The overall patterns of joints from all sources in southern Ontario, Michigan, Ohio and New York are compiled in Gartner Lee Limited (2008). The latter compiled the data from surficial joint sets; this does not necessarily imply that these joint sets will be consistent with depth at any one location. The collected data indicates a consistent EW joint set that ranges from ENE to ESE in the upper 300 m. At a greater depth, the NE-ENE trend becomes more consistent. An SSE set is found below 760 m. In general, the NE-ENE is present across all depths, but other minor joint directions show no discernable pattern (Hill et al., 2002).

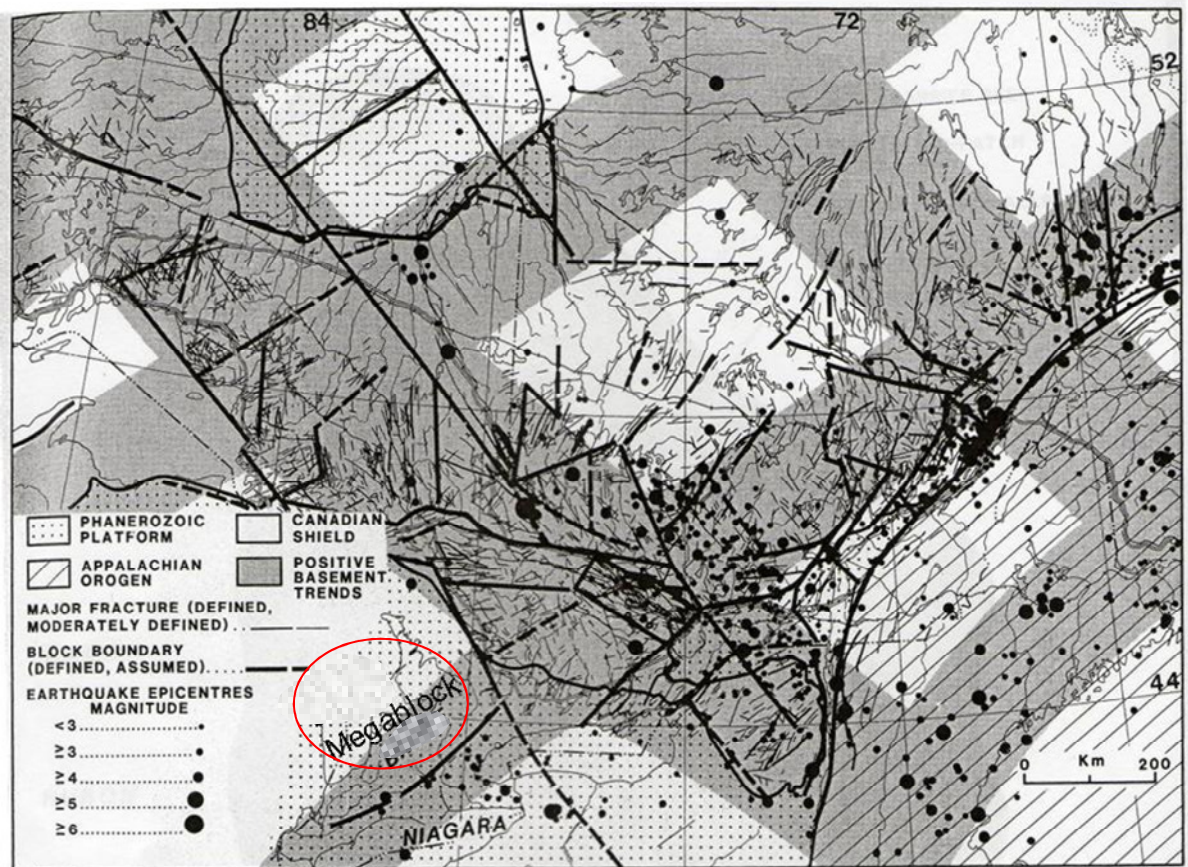


Figure 3.7. Major fracture system and block boundaries (Sanford et al., 1985)

The results of a site characterization program have provided a conceptual model of the site and allowed refinement to the geology and hydrogeology aspects of the model for the study area (Figure 3.8). The conceptual model shows that the DGR, located within the Cobourg Formation, is overlain by multiple low permeability formations, including 280m of low permeability limestone, shale and dolostone before the first permeable formation (Guelph Formation- Figures 3.8-3.9). The shale and anhydrite units with lower permeability are above the Guelph Formation within the Silurian deposits.

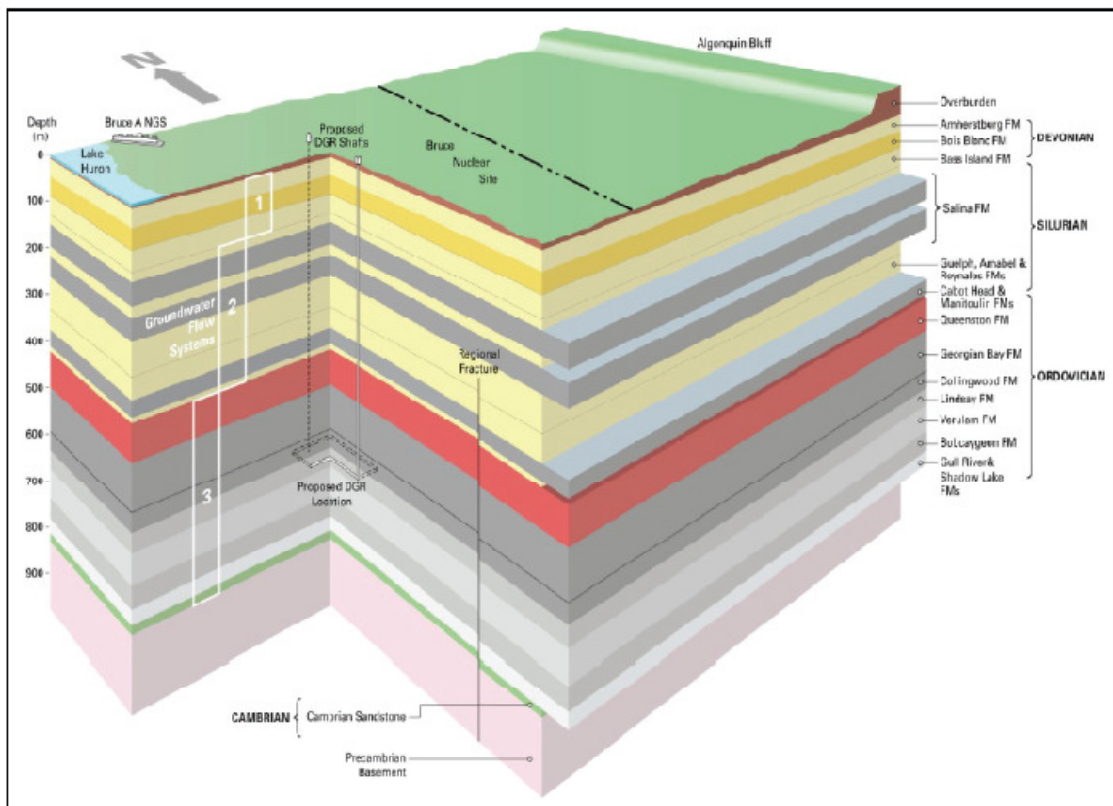


Figure 3.8. Conceptual geosphere model of the proposed DGR (Gartner Lee Limited, 2008)

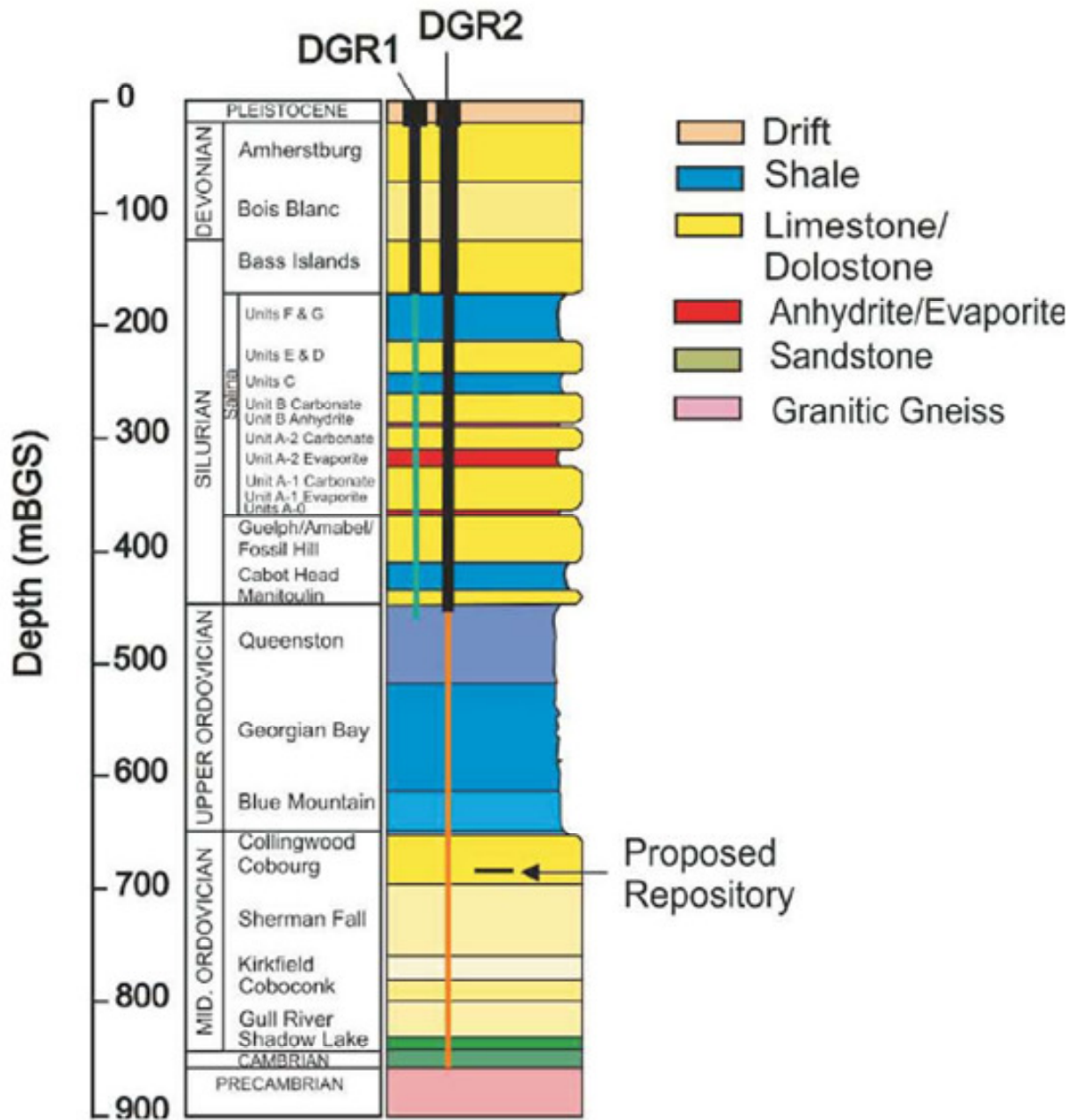


Figure 3.9. Phase I of the deep drilling program: DGR-series boreholes (Gartner Lee Limited, 2008)

3.3.2 Hydrogeological characteristics

The hydrostratigraphy of the study area consists of three underground water aquifer systems (McIntosh and Walter, 2006) located at different levels as shown in Figure 3.10. The modern flow is restricted to the first one in the Great Lakes region. It can be seen

that the study area includes two of these aquifer systems, the Silurian-Devonian aquifer and the Cambrian-Ordovician systems.

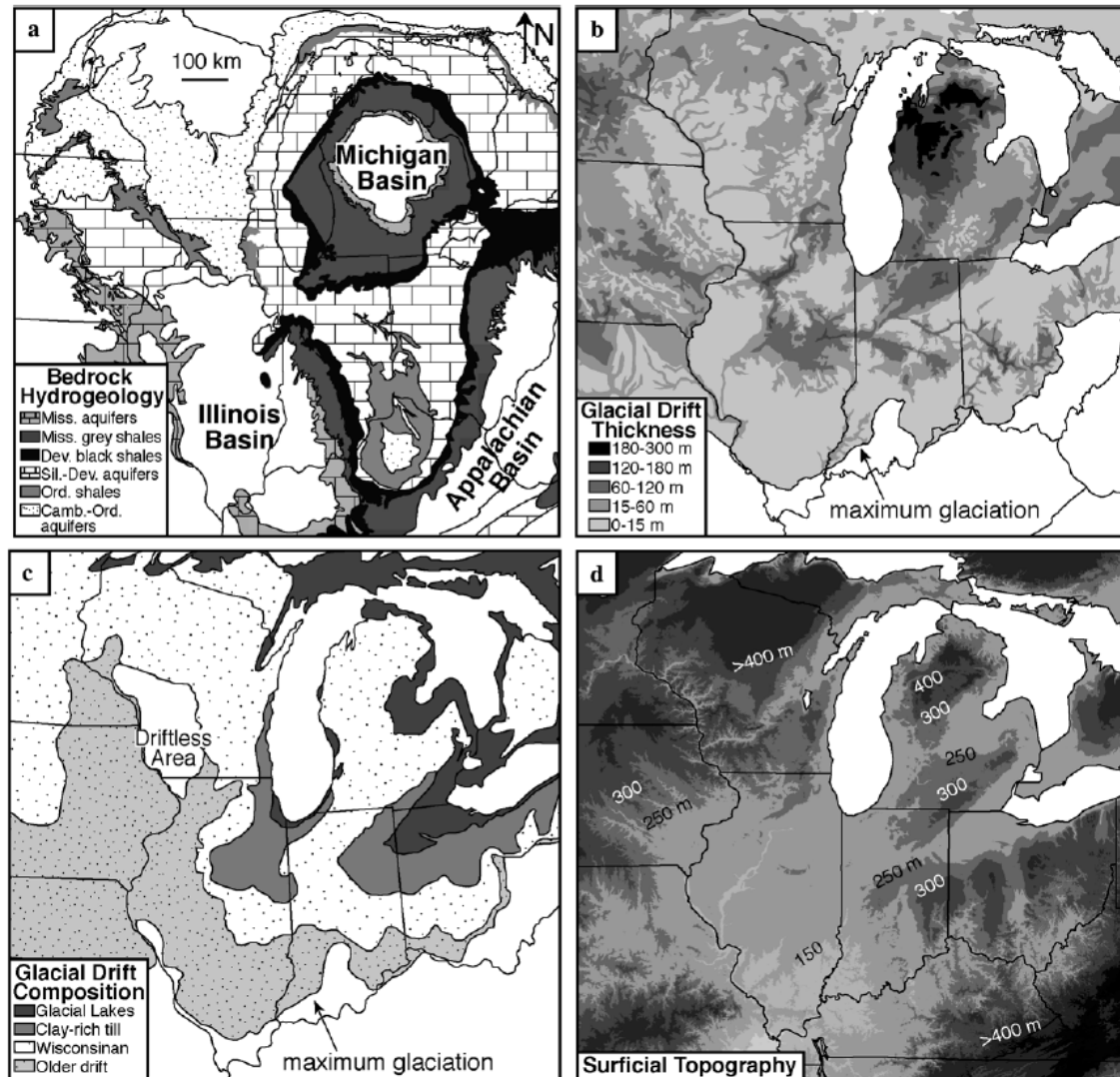


Figure 3.10. Hydrogeology of the study area (McIntosh and Walter, 2006)

High fluid pressures have been measured (up to 1.7 times greater than hydrostatic pressures) in argillaceous Paleozoic rocks of low permeability in southern Ontario and western New York State (Raven et al. 1992) as shown in Figure 3.11 (located in the Huron domain). Based on a literature review, Raven et al. (1992) summarized ten mechanisms as potential explanations for supernormal fluid pressures in sedimentary rocks, including: regional groundwater flow, variations in formation fluid density, sediment loading, uplift and erosion, thermal effects, mineral diagenesis, osmosis,

tectonic compression, gas generation, and gas migration, and found that the most reasonable explanation for the observed supernormal pressures is the upward migration and accumulation of gas generated from deeper distant sources in the Michigan and Appalachian Basins or underlying basement rocks (Raven et al. 1992).

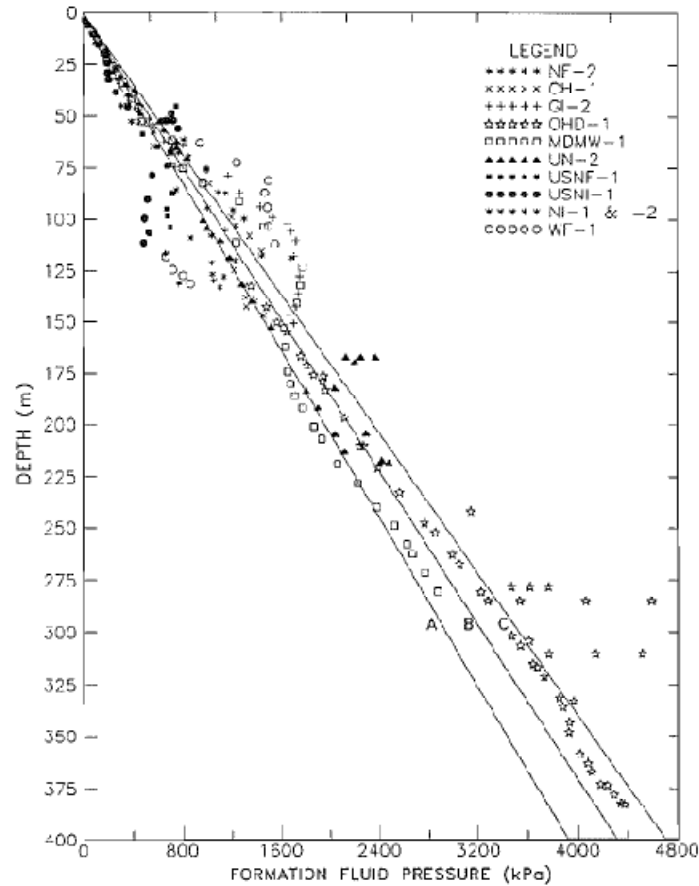


Figure 3.11. Measured formation fluid pressure vs. depth. Lines A, B, and C are hydrostatic pressure lines for fluid densities of 1000, 1100, and 1200 kg/m³, respectively (Raven et al. 1992).

3.3.3 Geochemical characteristics

The gathered geochemical data were divided into three groups. The first group comprise the chemical properties of rock formations within the study area. The second group is data on the ground water geochemistry. The third group consists of data on the chemistry of the glacial melted water.

3.3.3.1 Rock chemistry

The chemistry of rock formations could be an important mechanism in the enrichment and depletion of isotopic components (^{18}O , ^2H) in the fluid phase (McNutt et al. 1987). Strontium isotope is used as a geochronological tool and indicator of the changes in water chemistry due to water-rock interaction in situ (McNutt et al. 1987). Figure 3.12 shows the strontium isotope composition from the Michigan and Appalachian Basins. The differences in $^{87}\text{Sr}/^{86}\text{Sr}$ for seawater and underground waters are attributed to water-rock interactions.

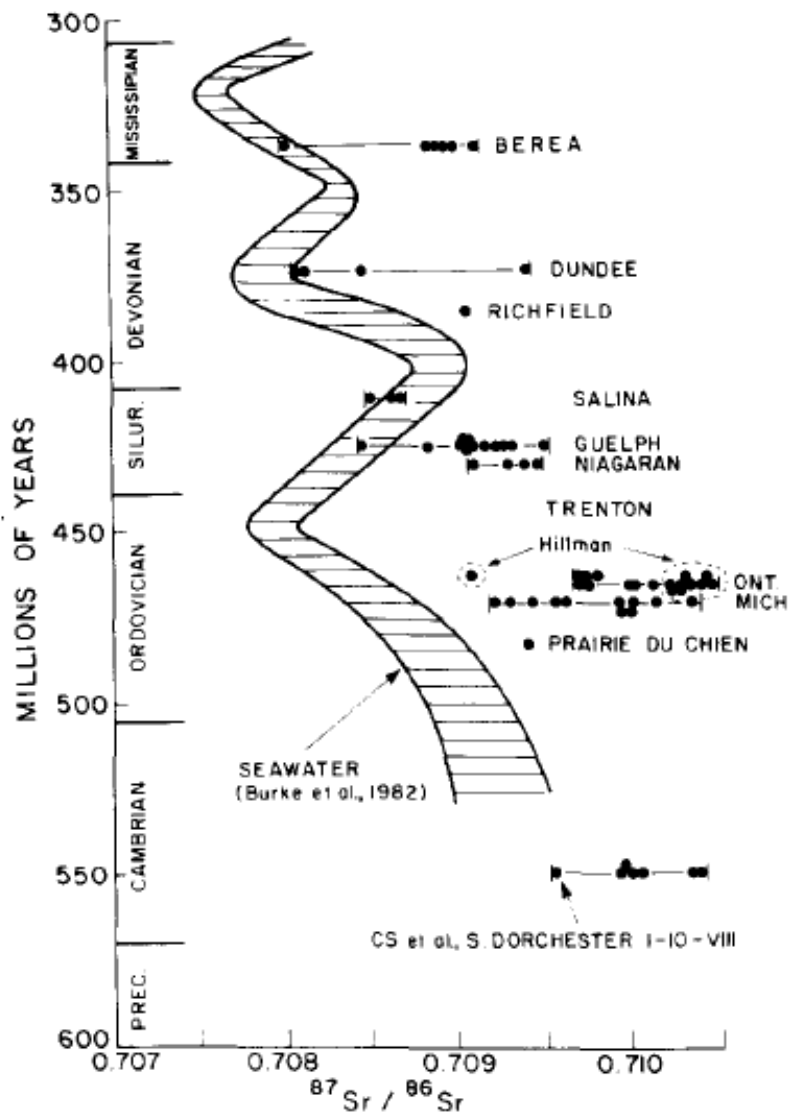


Figure 3.12. Strontium isotope composition from the Michigan and Appalachian Basins (McNutt et al. 1987)

To evaluate the degree of underground water-reservoir rock interaction, the isotopic compositions of minerals and rocks can be analyzed, such as the strontium isotope. Table 3.1 shows the strontium isotopic composition of rocks for some formations in the study area (McNutt et al. 1987).

Table 3.1. Strontium isotopic composition of rocks for some formations (McNutt et al. 1987).

Stratigraphic unit	$^{87}\text{Sr}/^{86}\text{Sr}$
Cambrian Rock	0.73302
Trenton Rock	0.70858

3.3.3.2 Ground water chemistry

Data of the ground water geochemistry for southern Ontario and the deeper parts of the Michigan Basin in the Michigan area were mainly collected from oil- and gas-producing wells (Mazurek 2004; McNutt et al. 1987). The collected data consisted mainly of ionic concentrations, water stable isotopes and $^{87}\text{Sr}/^{86}\text{Sr}$ ratios. Table 3.2 shows the main ionic concentrations for the formation waters.

Table 3.2. Representative compositions of formation waters (Mazurek 2004; McNutt et al. 1987)

	Precambrian	Cambrian	Trenton	Guelph	Salina	Dundee
Ca (mg/l)	65000	48000	32500	31300	8200	31500
Na (mg/l)	16900	43800	49700	65500	100000	70600
Mg (mg/l)	10	6090	5960	7770	2850	5410
K (mg/l)	120	1390	2070	1880	2600	3030
Sr (mg/l)	1390	1210	620	435	215	750
Cl (mg/l)	156000	179800	150290	189000	207000	179000
Br (mg/l)	1090	1530	1190	1390	590	1050
So ₄ (mg/l)	1140	260	335	250	750	165
TDS (mg/l)	241000	282000	242700	297600	322200	291600

The deep groundwater system that exists in these Ordovician formations is very old and highly saline (~300 g/L). The intermediate system covers all of the Silurian Formations. This zone has mixed permeability formations (e.g., high permeability Guelph Formation and low permeability shale/anhydrite beds in the Salina Formation) with groundwater salinity that ranges from saline to slightly salty. The Devonian and Quaternary formations represent the shallow groundwater system for the successive formations and layers over the proposed DGR (Hobbs et al. 2008).

Figure 3.13 shows the relationship between the $\delta^{18}\text{O}$ and $\delta^2\text{H}$. As compared to the global meteoric waterline, it can be seen that there are large enrichment in ^{18}O and small enrichment in ^2H (McNutt et al. 1987). This can be attributed to the exchange of isotopes between water and carbonate minerals.

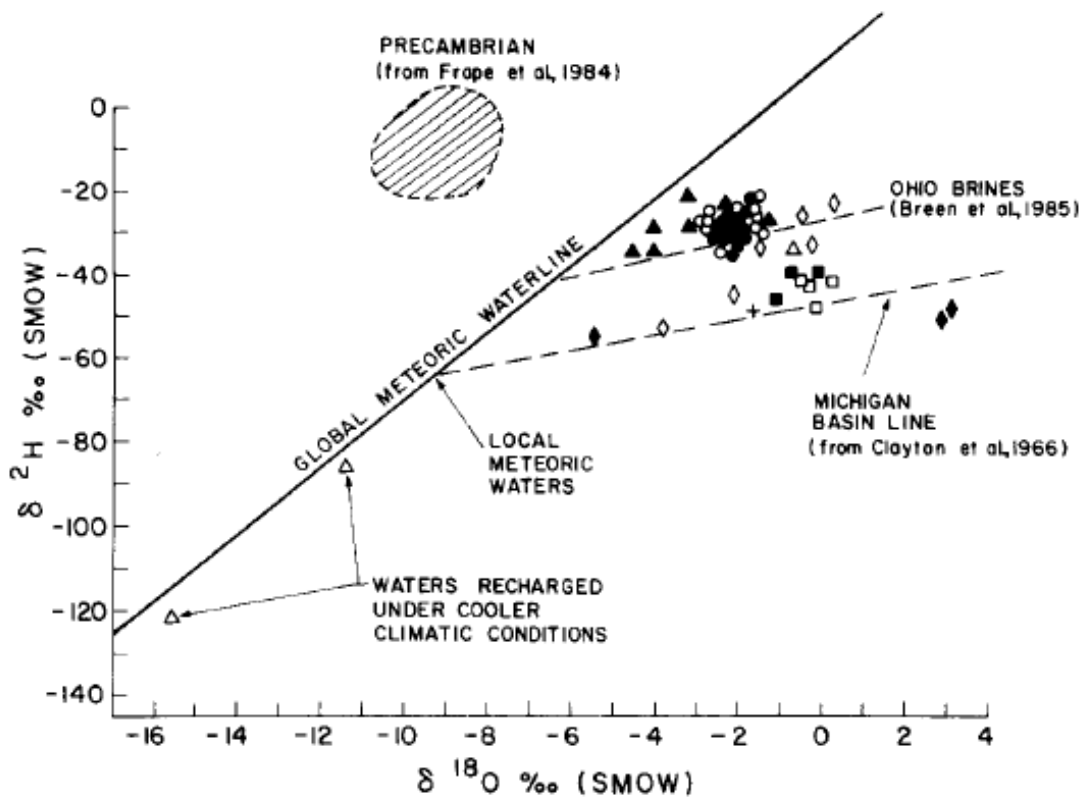


Figure 3.13. Relationship between $\delta^{18}\text{O}$ and $\delta^2\text{H}$ (McNutt et al. 1987)

3.3.3.3 Chemistry of glacial melted water

To trace the hydrological processes as a result of glacial melted water, it is advantageous to obtain the chemistry of the melted water. Both oxygen and hydrogen isotopic compositions may provide information about the history of a given water mass (Jeonghoon et al. 2009). During the ice ages, the water vapor that contained light oxygen moved toward the poles, condensed and fell onto the ice sheets where it stayed. As temperatures started to increase, and ice started to melt, there was an isotope exchange between the ice and melted water, in which the melted water became enriched with heavier isotopes (Jeonghoon et al. 2009). However, the melted water had a lighter isotope ratio as shown in Figure 3.14 (Hobbs et al. 2008), which made it possible to distinguish between groundwater from glacial melted water and old resident water.

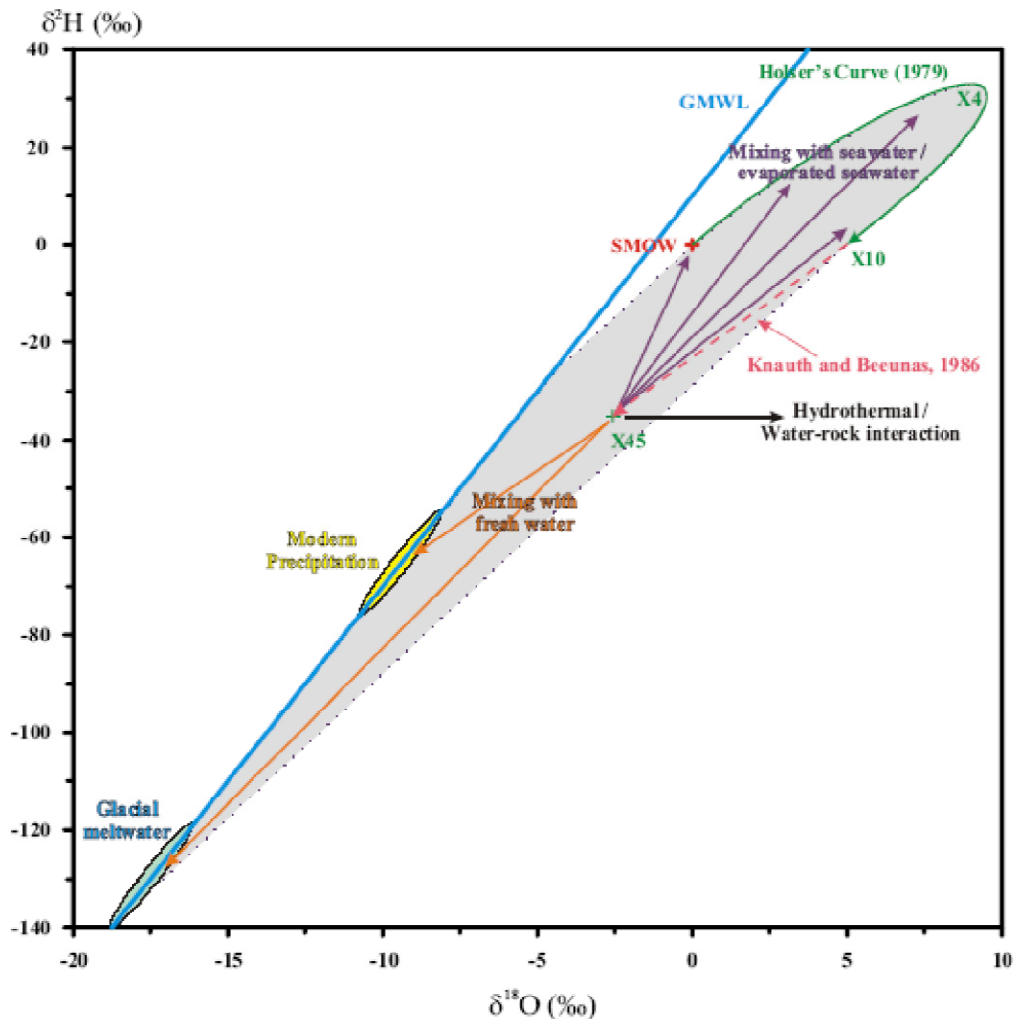


Figure 3.14. Relationship between $\delta^{18}\text{O}$ and $\delta^2\text{H}$ (Hobbs et al. 2008)

3.3.4 Paleoglaciations and their geological effects in the study area

In geological history, the Earth has been characterized by several intense glaciation events. Therefore, one of the most distinctive features of the Quaternary has been the periodic glacier activity during the cold periods of about 100,000 years in duration (Lowe et al. 1997, Vidstrand et al. 2008). The glacier stages were interspersed with warm episodes of deglaciation. Furthermore, glacier activities were accompanied with periodic advances and retreats of major continental ice sheets in many parts of the world, for example in the northern hemisphere, which includes the study area. Figures 3.15 and 3.16 show the extent of the Quaternary glaciers and ice sheets in North America (Lowe et al. 1997). Figure 3.16 was produced by using a computer model developed by Boulton et al. (1985). The study area is located in the Great Lakes region, which has been subjected to repeated fluctuations of an ice margin, and produced large numbers of end moraines as shown in Figure 3.15. In Figure 3.16, a maximum ice thickness of about 2500 m is found in the study area, with a predominant NE-SW direction of ice movement. Modelling research work (e.g., Vidstrand et al. 2008, Nguyen et al. 1993, Selvadurai and Nguyen 1995, Karrow et al. 2002) has suggested that glaciation and permafrost comprehensively re-organised the geometry and magnitudes of both groundwater flow and pressures. In addition to that, geomorphological observations give an indication of the significant mechanical responses in the sub-surface due to glacial loading (Vidstrand et al. 2008, Nguyen et al. 1993, Karrow et al. 2002). Moreover, during the late Pleistocene, advance and retreat of a kilometer thick ice sheet (McIntosh et al. 2006) recharged a large volume of glacial meltwater to great depths, which affected the groundwater flow and salinity gradient (McIntosh et al. 2006). Siegel (1991) showed that the Cambrian-Ordovician aquifers in Iowa state (USA) had been invaded by glacial melt water that penetrated hundreds of meters of fractured confining beds. There is increasing evidence that significant subglacial recharge into aquifers was caused by high fluid pressure at the base of continental ice sheets (Weaver et al. 1995; Grasby and Chen 2005). As a result, the hydrodynamic boundary conditions were significantly disrupted (Grasby and Chen 2005), including fluid flow direction and fluid pressure as shown in Figures 3.17 and 3.18. It is obvious that the reconstruction of a hydrological system by using paleohydrological data of the area will help in understanding the origin of recharge as

well as groundwater flow and mixing. This kind of data will greatly help with the validation of both the hydraulic and chemical aspects of the conceptual model.

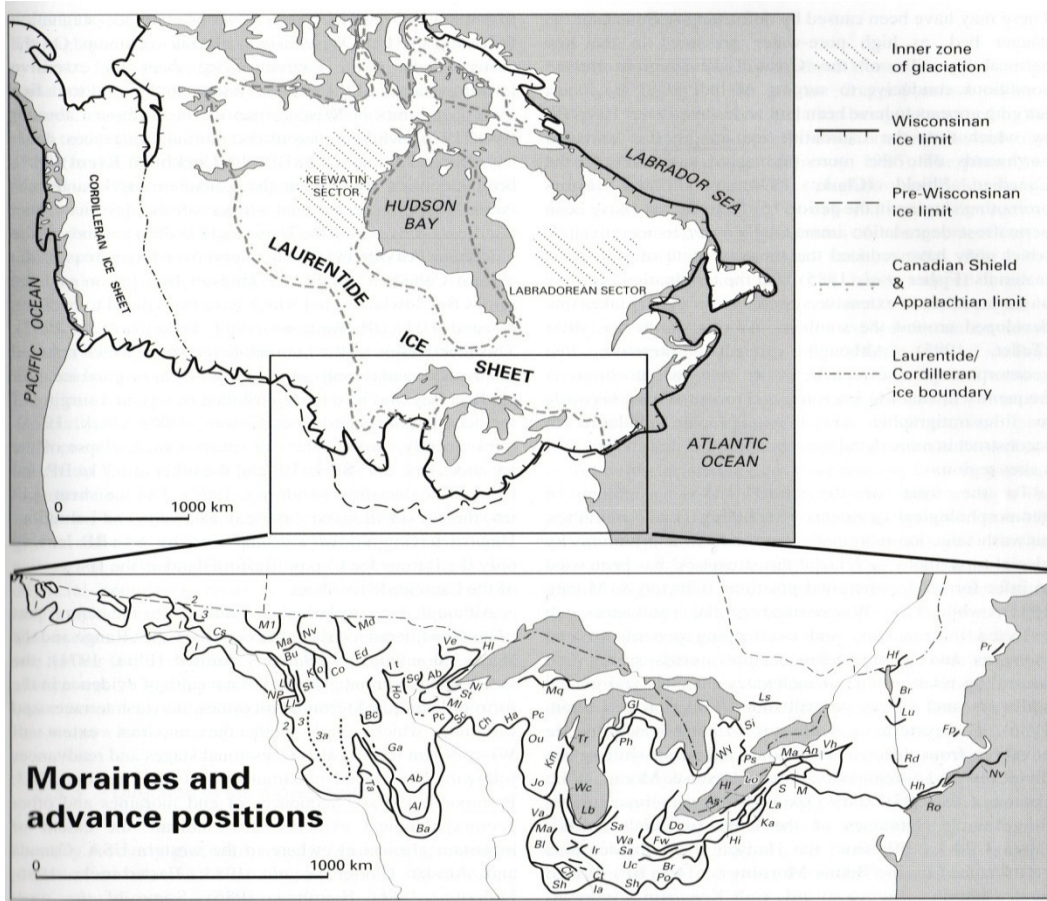


Figure 3.15. Moraines and ice limits in southern Ontario (Lowe et al. 1997)

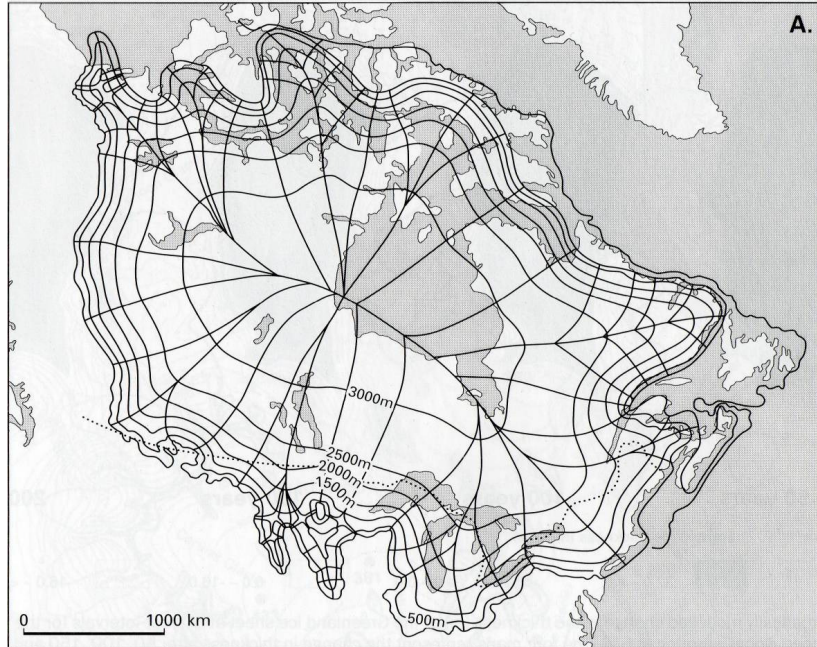


Figure 3.16. Computer model of ice sheet (Mongelli et al. 1982, reproduced by Clauser and Huenger 1995)

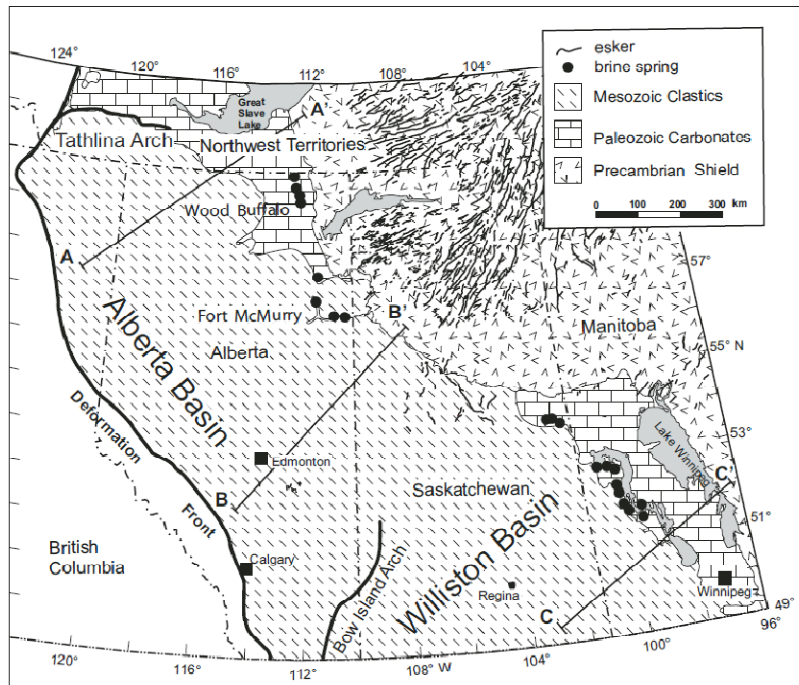


Figure 3.17. Western Canada sedimentary basin (Grasby and Chen 2005)

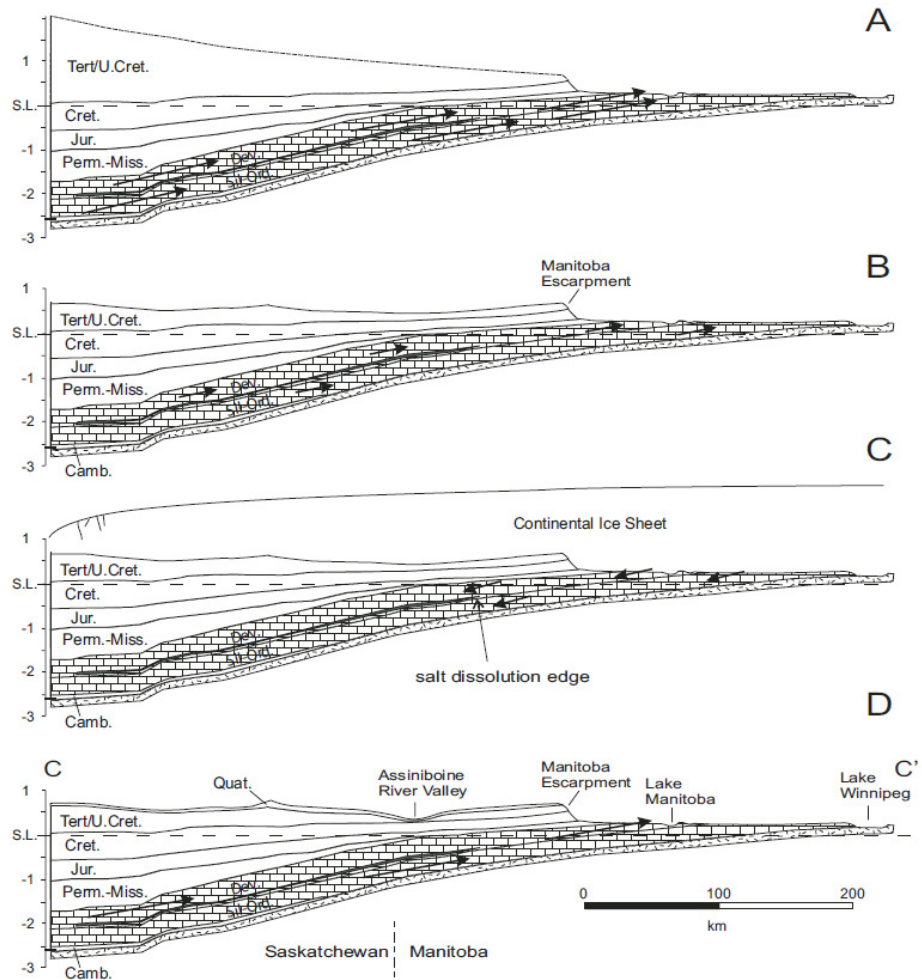


Figure 3.18. Schematic series of diagrams that show evolution of basin hydrodynamics for the past 50 m.y. (based on Section C–C' Figure 23) (Grasby and Chen 2005)

3.4 Geotechnical characteristics of the study area

The geotechnical data gathered and analysed include geomechanical, hydraulic and thermal data as presented below.

3.4.1 Geomechanical characteristics

The geomechanical data compiled were divided into two main categories. The first category included the stress distribution in the study area, whereas the second category presented the mechanical properties of the rocks present in the study area. The above two categories will include the available data for each layer in the site from the ground surface to the rock basement (Pre-Cambrian).

3.4.1.1 Stress distribution

Results of in situ stress measurements in southern Ontario showed that the horizontal stresses are much higher than the vertical stresses (Lo 1978; Zoback 1980). These results were supported by surface evidence, such as folds, faults and natural pop-ups, and underground evidence, such as the performance records of shallow and deep engineering structures (O'Hara and Hinze 1980; Lo 1978). Most of the available in-situ stress data in Paleozoic rock (Gartner Lee Limited, 2008) were collected from over 20 sites in the Great Lakes region. Figure 3.19 shows a plot of the maximum and minimum horizontal stresses (σ_H and σ_h) as a function of depth. There are only a few deep boreholes with in-situ stress measurements drilled within a few hundred kilometers of the selected repository site. Some of these boreholes were completed in Ordovician limestone between 45 and 208 m in depth. Based on these measurements, the σ_h varies between 8.3 and 9.5 MPa within the Ordovician Formations (75 – 208 m). The σ_H for the two rock types was determined to vary between 10.6 MPa and 15.4 MPa in the Ordovician rock and between 17.2 MPa and 19.6 MPa in shield rock.

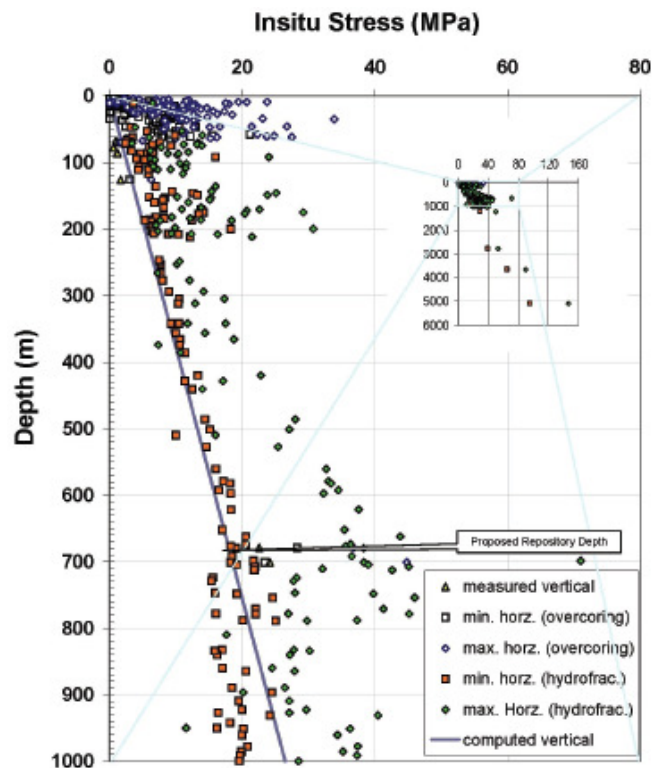


Figure 3.19. Distribution of the principal stresses with depth in the Appalachian and Michigan Basins. Included are both hydro-fracturing and over-coring results (Gartner Lee Limited, 2008).

3.4.1.2 Mechanical properties

Table 3.3 includes a summary of the mechanical properties for the rock in the area of study collected from published data. Figure 3.20 shows the profile of the modulus of elasticity (E) in the study area. Based on the numerical value of E, three primary levels can be recognized: the first level (0-650 m in depth) which includes the Devonian and Silurian Formations with an E that ranges from 20 to 25 GPa, the second level (650-900 m in depth) which includes the Upper and Mid-Ordovician Formations with an E of about 35 GPa, and the third level (900-1000 m depth) which includes the Cambrian Formation with an E of about 10 GPa. An estimated value of 0.2 was used for the value of Poisson's ratio based on the available published field data (Lo, 1978; Mazurek, 2004).

Table 3.3. Primary material properties of the rock in the study area (data from NWMO, 2011a).

Subdomain number	Rock formation	Depth	Poisson's ratio	Young's modulus (Gpa)	Hydraulic conductivity Kh (m/s)	Kh/Kv	Thermal conductivity W/(m.K)	Specific heat capacity J/(kg.K)	Diffusion m ² /s
1	Overburden Aquifer	0-20	0.2	10	8.0E-10	2:1	2	700	6.0E-10
2	Dolostone Aquifer	20-169.3	0.2	40	1.0E-5	10:1	2	700	8.0E-12
3	Silurian Aquifer	169.3-178.6	0.2	18	5.0E-12	10:1	2	700	1.0E-12
4		178.6-325.5	0.2	6	5.0E-12	10:1	2	700	1.0E-12
5	Silurian Aquifer	325.5-328.5	0.2	38	2.0E-7	1:1	2	700	7.0E-12
6		328.5-374.5	0.2	38	5.0E-12	10:1	2	700	1.0E-12
7	Silurian Aquifer	374.5-378.6	0.2	38	3.0E-8	1:1	2	700	3.0E-11
8		378.6-411	0.2	38	5.0E-12	10:1	2	700	1.0E-12
9		411-447.7	0.2	16	5.0E-12	10:1	2	700	1.0E-12
10	Ordovician shale	447.7-659.5	0.2	16	2.0E-14	10:1	2	700	1.0E-13
11	Ordovician limestone	659.5-688.1	0.2	39	1.0E-15	10:1	2	700	3.0E-13
12		688.1-762.0	0.2	24	1.0E-15	10:1	2	700	3.0E-13
13	Ordovician limestone	762.0-838.6	0.2	24	6.0E-12	100:1	2	700	3.0E-13
14	Cambrian	838.6-860.7	0.2	24	1.0E-7	1:1	2	700	1.0E-11
15	Precambrian	>860.7	0.2	60	1.0E-11	1:1	1.375	700	3.0E-13

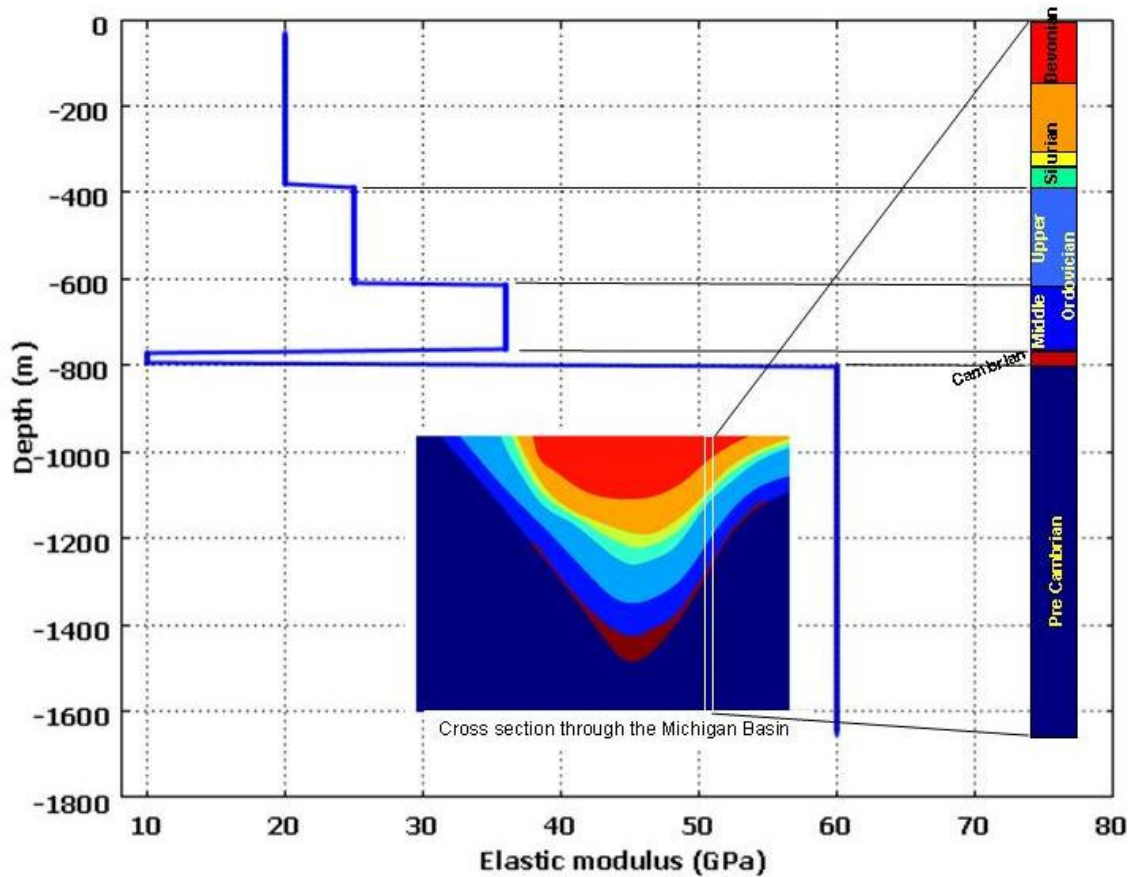


Figure 3.18. Variation of elastic modulus with depth (Nasir et al. 2011; interpreted from data from NWMO 2011a)

3.4.2 Hydraulic characteristics

Table 3.3 contains the values of the horizontal and vertical hydraulic conductivities for the different formations. Figure 3.21 shows the profile of the horizontal hydraulic conductivity (K_h) for the study area. Based on the numerical value of K_h , three main levels can be identified: the first level (0-600 m in depth) which includes the Devonian and Silurian formations with a K_h range from 10^{-11} m/s to 10^{-9} m/s, the second level (600-900 m in depth) which includes the Upper and Mid-Ordovician formations with a K_h range from 10^{-14} m/s to 10^{-12} m/s, and the third level (900-1000 m in depth) which includes the Cambrian formation with a K_h about 10^{-8} m/s.

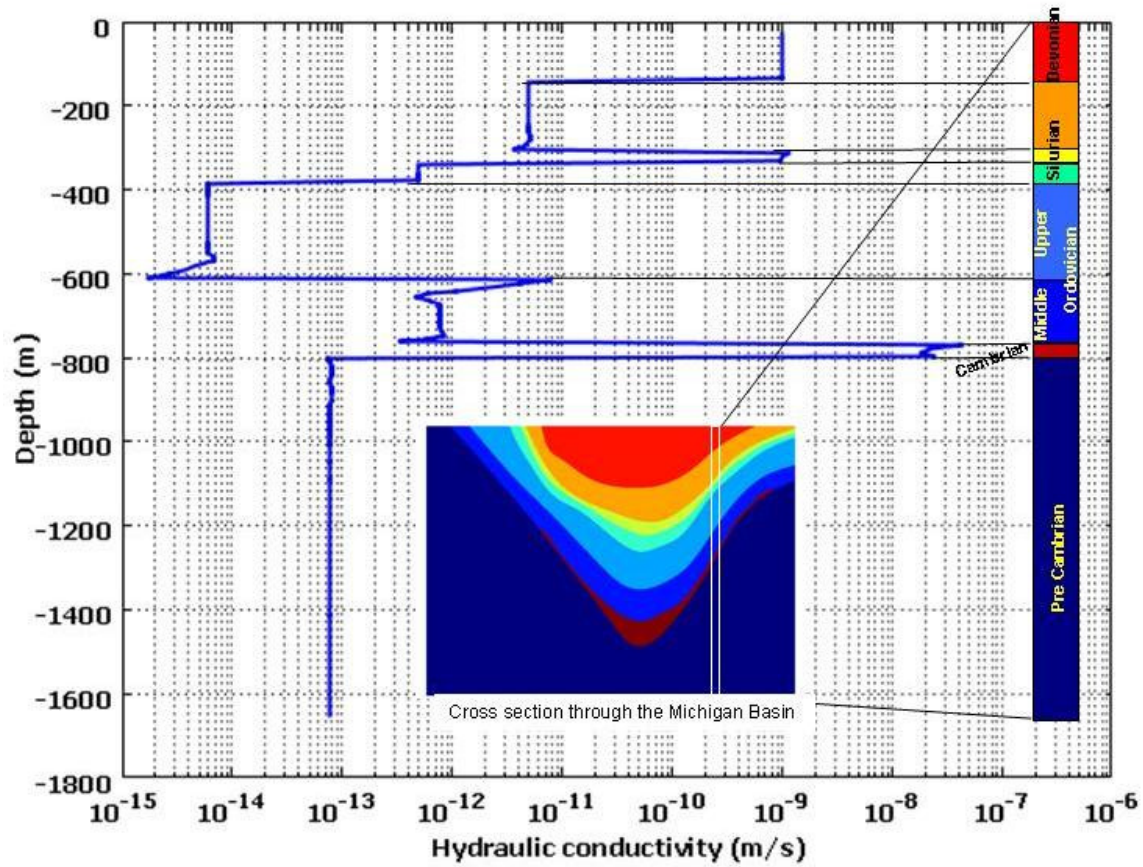


Figure 3.21. Variation of hydraulic conductivity with depth (Nasir et al, 2011; interpreted from data from NWMO 2011a)

3.4.3 Thermal characteristics

By using the linear regression of records from deep borehole temperature measurements versus depth in the Lower Peninsula of Michigan (Vugrinovich 1989) as shown in Figure 3.22, the following equation is proposed for the geothermal gradient in the Michigan Basin: $(T(^{\circ}\text{C}) = 14.5 + 0.0192 \times \text{depth}(\text{m}))$. The thermal properties of the formations are listed in Table 3.3. The experimental results show that the thermal properties of rocks are temperature dependent so that there is a decrease of thermal conductivity and diffusivity, and an increase in specific heat with increasing temperature as shown in Figure 3.22 for various kinds of rocks (Mongelli et al. 1982).

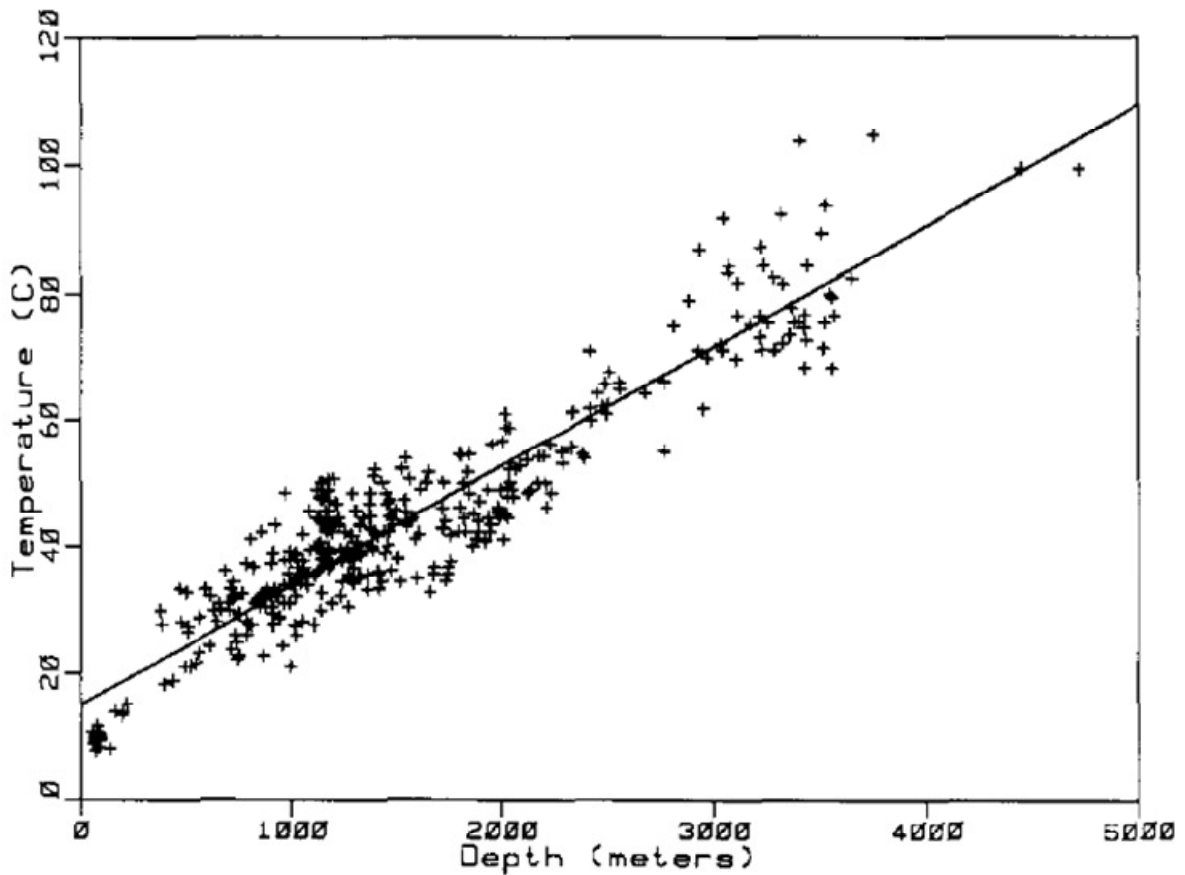


Figure 3.22. Subsurface temperatures vs. depth. Straight line is the least-squares 'best-fit' (Vugrinovich 1989).

3.5 Conclusion

A significant amount of data on the properties of sedimentary rock formations (which are potential host rocks for nuclear waste disposal repositories) in Ontario are presented and discussed in this section of the report. The data are mainly obtained from Gaertner Lee (2008); NWMO (2011a.b). The data can be classified into two main groups: geological (e.g., geochemical, glaciation, hydrogeological, in-situ stress) and geotechnical (mechanical, geochemical, hydraulic, thermal) data. These data are important for the development of a THMC model to predict the response of a hypothetical underground repository in Ontario to past and future climate changes and to analyze the safety of the repository with respect to climate change. Furthermore, these data are pertinent to the calibration and validation of the mathematical models to be developed. It is noted that for

the Michigan Basin, in general, formations with higher horizontal hydraulic conductivity are exposed to the surface in some of the areas. This could suggest that it would be more appropriate (at least for the study of the effects of past climate changes) to adopt a large scale model, especially for ice sheet loading/unloading, and flow of melted water. However, a site scale model is still necessary for the coupled impact of both climate and a potential DGR. It is found also that the site of the proposed DGR is “relatively” tectonically stable. However, for the entire region comprising southern Ontario, some major fracture and fault blocks appear, dividing the region into megablocks. For more accurate and representative results, the boundaries of these megablocks could be included in the domain of the numerical model to include their impact.

4 Development of a Thermo-Hydro-Mechanical-Chemical Model for the Analysis of the Impacts of Glaciation-Deglaciation Cycles on Sedimentary Rocks

4.1 Introduction

The objective of the present chapter is to develop constitutive and mathematical models to predict and analyze the impacts of climate changes on the sedimentary rocks in Ontario. To achieve the above objective, a THMC model is developed to predict and analyze the impacts of climate changes on the sedimentary rocks. The model development is described below.

4.2 Development of the mathematical model

Here, a set of governing equations is developed to simulate coupled heat, solute and fluid transfer or transport in deformable porous media. The governing equations are derived based on the basic laws of force equilibrium, mass conservation and heat conservation. The governing equations presented describe four models: (i) groundwater flow, (ii) solute transport, (iii) heat transfer, and (iv) mechanical (deformation). A number of assumptions have been made in the formulation of the governing equations. These assumptions include: (i) the host rock is considered as a continuous porous medium made of two constituents, a solid (solid skeleton) and a fluid (water). The two constituents are distributed in two phases: solid (referred to as solid skeleton) and liquid (l); (ii) the liquid moves through the connected voids of the medium. The liquid phase is composed of liquid water; (iii) small strain is assumed; (iv) local thermal equilibrium is assumed for the two-phase system; and (v) the constituents of the porous medium are not reactive. The details of the developed mathematical model have been published (e.g., Nasir et al. 2009, 2011) and summarized in the next sections. The mathematical model was numerically implemented with the FEM code COMSOL Multiphysics. COMSOL Multiphysics is a well known commercial software for solving partial differential equations (PDEs), numerical analyses, and simulations.

4.2.1 Flow equation

The conservation of mass for both fluid and solid are expressed by Equations 4.1 and 4.2, respectively (De Marsily, 1986):

$$\nabla \cdot (\rho_f U_f) + \frac{\partial}{\partial t} (\rho_f n) + \rho_f q = 0 \quad \dots\dots\dots (4.1)$$

$$\nabla \cdot (\rho_s U_s) + \frac{\partial}{\partial t} (\rho_s (1-n)) + \rho_s q = 0 \quad \dots\dots\dots (4.2)$$

where: ρ is density, U are fictitious velocities, t is time, n is porosity, q is mass source, s is the solid and f is the fluid.

In the above equations, the mean velocities for the fluid and solid can be expressed as:

$$u = \frac{U}{n}, \text{ and } u_s = \frac{U_s}{(1-n)} \quad (4.3)$$

Darcy's law can be written in terms of the mean velocities as:

$$(u - u_s) = -\frac{\kappa}{\eta} (\nabla p + \rho_f g \nabla D) \dots\dots\dots (4.4)$$

where: κ is permeability, η is dynamic viscosity, P is pressure, and D is the direction of the gravitational acceleration (g).

Combining Equations 4.1 and 4.2, and by using Darcy's law, we obtain (De Marsily, 1986):

$$\nabla \cdot \left[\rho_f \frac{\kappa}{\eta} (\nabla p + \rho_f g \nabla D) \right] = n \frac{\partial \rho_f}{\partial t} + \frac{\rho_f}{1-n} \frac{\partial n}{\partial t} - \frac{\rho n}{\rho_s} \frac{d\rho_s}{dt} \dots\dots\dots (4.5)$$

Based on the compressibility of the fluid, solid and skeleton of the rock components, the term $\frac{\partial n}{\partial t}$ (time variation in porosity) can be represented with (Nguyen, 1995):

$$\frac{dn}{dt} = \left(\left((\alpha - n) \frac{de_{ff}}{dt} + \frac{(\alpha - n)}{K_s} \frac{dp}{dt} \right) + (-(\alpha - n)\beta + (1 - n)(\beta - \beta_s)) \frac{dT}{dt} \right) \dots\dots (4.6)$$

As well, Equation 3.5 can be written as:

$$\nabla \cdot \left[\rho_f \frac{\kappa}{\eta} (\nabla p + \rho_f g \nabla D) \right] = (n\gamma) \frac{\partial C}{\partial t} + \rho_f \alpha' \frac{de_{ff}}{dt} + \rho_f \left(\frac{\alpha'}{K_s} - \frac{n}{K_s} + \frac{n}{K_f} \right) \frac{dp}{dt} + \rho_f (n\beta_s - \alpha' \beta + (\beta - \beta_s) - n\beta_f) \frac{dT}{dt}$$

...(4.7)

where $\alpha' = \frac{(\alpha - n)}{(1 - n)}$, $\alpha = 1 - \frac{K_D}{K_s}$, K_D , K_s and K_f are the bulk moduli of the solid matrix, solid grains and water fluid, respectively, β , β_s and β_f are the thermal expansion coefficients for the solid matrix, solid grains and water fluid, respectively.

Equation 4.7 includes the concentration (C) of the dissolved solids in the pore fluid and the local average temperature (T) of the porous medium. The density of the pore fluid is assumed to vary with dissolved solid concentration.

4.2.2 Solute transport model

For the purpose of solute transport modelling, the advection-dispersion module (Comsol 2009), given by Equation 4.8, is used:

$$\theta_s \frac{\partial c}{\partial t} + \nabla \cdot [-\theta_s D_L \nabla c + uc] = S_c$$

.....(4.8)

where: θ_s is porosity; D_L is the hydrodynamic dispersion tensor; u is the vector of pore fluid velocities; and S_c is the solute source or sink.

Equation 4.8 is coupled with Equation 4.1 in two ways, via pore fluid velocities and rate of solute change with time (in this work, the concentration of total dissolved solid (TDS) is represented by C):

$$\frac{\partial c}{\partial t}$$

The density of the pore fluid is assumed to vary with dissolved solid concentration according to the following equation:

$$\rho_f = \rho_{fo} + \gamma C$$

.....(4.9)

where ρ_{fo} is the initial fluid density, and γ is a concentration–density coefficient. The numerical values of both ρ_{fo} and γ are taken to be 1000 kg/m³ and 2/3 and for a range of C from 0 to 300 kg/m³ (Sykes et al. 2008).

4.2.3 Mechanical model

By assuming linearly elastic rocks, the mechanical process is included by taking the equation of momentum conservation, coupled with water pressure by using Biot’s effective stress principle (Nguyen, 1995):

$$G \frac{\partial^2 u_i}{\partial x_j \partial y_j} + (G + \lambda) \frac{\partial^2 u_j}{\partial x_i \partial y_j} - \alpha \frac{\partial p}{\partial x_i} - \beta K_D \frac{\partial T}{\partial x_i} + F_i = 0 \quad \dots\dots(4.10)$$

where: u is the displacement, G is the shear modulus, λ is Lamé’s first parameter, α is the Biot coefficient, and T is the temperature.

Mechanical deformation is an important process because it can affect the porosity and the intrinsic permeability, hence, the hydraulic conductivity of sedimentary rocks. In this work, the change in intrinsic permeability due to change in porosity is modeled by using the Carman–Kozeny relationship (Carman, 1937; Kozeny, 1927):

$$k^t = \left[\frac{n^3}{(1-n^2)} \right]^t \left[\frac{(1-n^2)}{n^3} \right]^{initial} k^{initial} \quad (4.11)$$

where k^t [L²] represents permeability at time t, and $k^{initial}$ [L²] represents the initial permeability. In this work, initial porosity and permeability are assumed to be equal to the current field values.

4.2.3 Heat transfer model

Convection and conduction modes are used to analyse the heat transfer by assuming a single fluid moving through a porous media:

$$C_{eq} \frac{\partial T}{\partial t} + \nabla \cdot (-K_{eq} \nabla T) = -C_L \mathbf{u} \nabla T + Q_H + Q_G \dots\dots\dots(4.12)$$

where: (T) represents the average temperature of the porous medium, C_{eq} is the effective volumetric heat capacity; K_{eq} is the effective thermal conductivity; C_L is the volumetric heat capacity of the moving fluid; \mathbf{u} is the fluid velocity vector, and Q_H and Q_G both denote general and geothermal heat sources.

Temperature is coupled with hydraulic processes by both water density and viscosity. The dynamic viscosity of water [Pa s] is taken to be temperature dependent by using a built in material function within COMSOL (COMSOL 2009). On the other hand, water and solid densities are taken as temperature and pressure dependent by:

$$\rho_f = \rho_{fo} e^{\frac{(p-p_o)}{k_f} - \beta_f (T-T_o)} \dots\dots\dots(4.13)$$

$$\rho_s = \rho_{so} e^{\frac{(p-p_o)}{k_f} - \beta_f (T-T_o)} \dots\dots\dots(4.14)$$

Equations 4.13 and 4.14 are included during the derivation of Equation 4.1.

Frozen ground and phase change (liquid-ice-liquid) are considered in this work by evaluating the volumetric ice content (θ_i) as a function of temperature by using the freezing curve equation (Weismüller et al., 2011):

$$\theta_i = \left[1 - \frac{1}{\phi} \left(-\frac{a}{T-b} + cT + d \right) \right] \theta_w \text{ if } T < 0 \text{ C}^\circ \quad (4.15)$$

$$\theta_i = 0 \text{ if } T \geq 0 \text{ C}^\circ$$

where a,b,c and d are constants assumed based on the work of Weismüller et al. (2011) as $a=8 \times 10^{-12}$, $c=8 \times 10^{-4}$, $d=9 \times 10^{-2}$ and $b=a/\phi-d$; ϕ is the total porosity; and θ_w is the total water volumetric content (liquid + ice). Water-ice-water phase change and latent heat are evaluated through effective volumetric heat capacity (C_{eq}) and thermal conductivity by using the following equations:

$$C_{eq} = C + \rho_w \cdot L_f \frac{\partial \theta_i}{\partial T} \quad (4.16)$$

$$C = (\theta_i \times C_i + \theta_w \times C_w) + ((1 - \theta) \times C_s) \quad (4.17)$$

$$K_{eq} = (\theta_i \times K_i + \theta_w \times K_w) + ((1 - \theta) \times K_s) \quad (4.18)$$

where C_i, C_w are the heat capacities of ice and water, respectively, and K_i, K_w are the thermal conductivities of ice and water, respectively.

4.3 Conclusions

The developed THMC model will be used to simulate the effects of past and future glaciation cycles on sedimentary rocks in southern Ontario for the study area. Furthermore, the reliability of the prediction ability of the developed model is tested in this section by comparing the predicted values with those measured in the field or obtained by using an analytical model. Transient boundary conditions are applied by using ice sheet loading and temperature history adopted from the U of T GSM or “Peltier’s Model”, model nn9930 (Peltier, 2008). The main results are presented in the following chapter.

5 Numerical Analysis of the Impacts of Past Glaciation-Deglaciation Cycles on Sedimentary Rocks in Ontario

5.1 Introduction

The developed model was implemented by using various boundary condition scenarios, particularly, surface pore water pressure due to glacial melting water to simulate the impacts of past glaciations-deglaciation cycles on the sedimentary rocks in Ontario. However, in this report, only one scenario will be presented in detail, and that is zero surface pore water pressure. The main results of the simulation are presented below.

5.2 Model conceptualization

The conceptualization of the model is mainly taken from the work by Nasir et al. (2011) as follows. The host rock could be conceptualized as a porous medium with a solid skeleton and pores, cracks and microcracks filled with a fluid such as water (pore water) or a mixture of fluids (water, gas and/or air). When an ice sheet forms on the surface of a host rock, it imposes a mechanical load that reaches maximal values in the order of 30 MPa during the last glaciation cycle. The ice sheet, in addition to the mechanical load due to its weight, would also affect the thermal and hydraulic conditions at the interface between its base and the surface of the host rock. Permafrost conditions might prevail at that interface, at the forefront of the advancing ice sheet. The following assumptions are also adopted:

- 1- ice loading and surface water pressure due to the last glaciation-deglaciation cycle is generated by the U of T GSM, “Peltier’s model” (Peltier, 2008) as shown in Figure 5.1. Different loading scenarios are used to apply the top BCs of the model;
- 2- the main PDEs are developed to include the THMC processes in porous media based on the conservation of mass (solid and fluid) and momentum for porous media fully saturated with water. This assumption is based on the fact that the host rock is mainly located under the groundwater table.

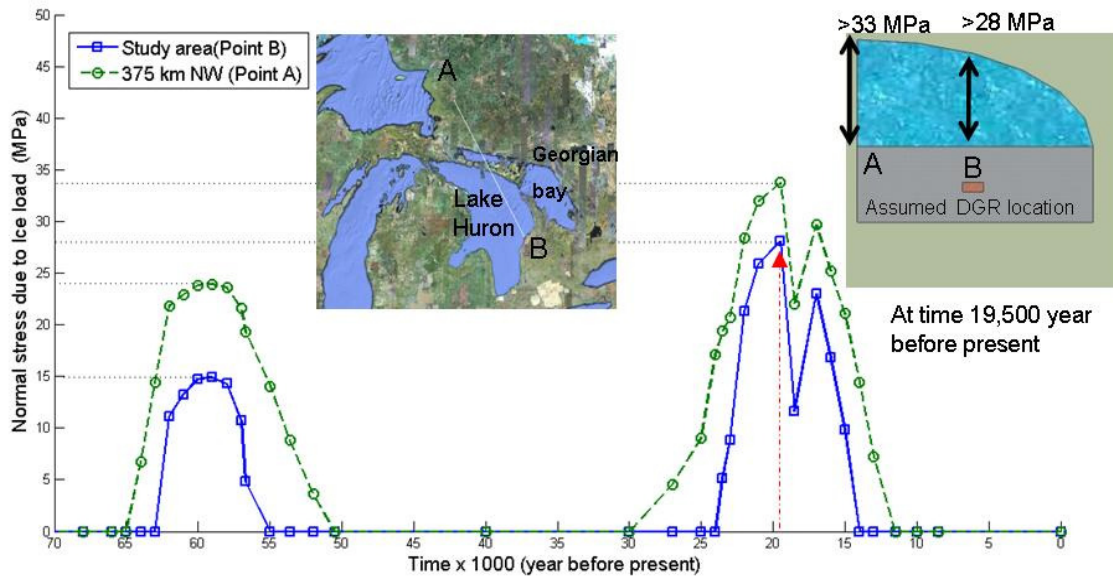


Figure 5.1. Ice loading (interpolated from U of T GSM, “Peltier’s Model”, model nn9930 Peltier 2008) (Nasir et al. 2011)

The direction of line A-B (NW-SE) (Figure 5.1) will be assigned an assumed x-coordinate parallel to the direction of the ice sheet movement. The selected NW-SE glacial direction is based on the work published by Piotrowski (1987). It should be emphasized that the modeling works performed by Peltier (2011) suggest NE-SW glacial direction in the local area of the Bruce Peninsula. However, the glacial direction will have no effect on the 1D-modeling simulation results. In order to take into account the actual parabolic shape of the ice load distribution with respect to time and location in southern Ontario, a steady-state ice sheet on a horizontal bed is assumed with a parabolic ice sheet distribution which can be represented by the following equation:

$$h = 3.4(L - x)^{1/2} \dots\dots\dots(5.1)$$

This equation can be used to estimate the length of the covered area (L, in the direction of the ice sheet movement) beyond the highest thickness h point (at x=0):

$$L = \frac{h^2}{11.56}$$

The history of the maximum thickness of the ice used to estimate L is adopted from Peltier's model (Peltier, 2008).

5.3 Initial and boundary conditions

For the 2D model shown in Figure 5.2, the initial hydraulic conditions are set as linear hydrostatic, and at the same time, the self-weight of the rock formations is assumed to be based on a rock density of 2500 kg/m³ for the initial mechanical stresses at 10 million years before the present. The above time is selected after several trials for achieving self-weight mechanical and hydraulic equilibrium. At the time of equilibrium, both hydraulic pressure and effective stresses were used as initial conditions for the analysis before the application of ice loading.

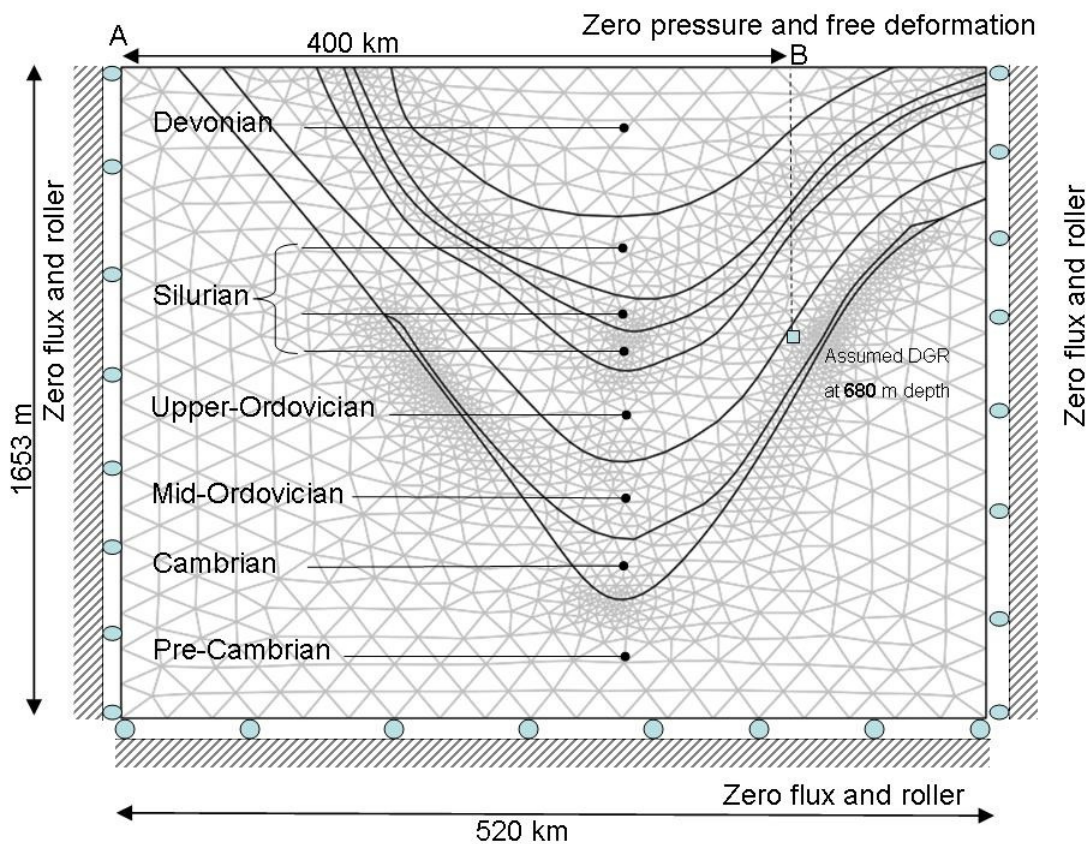


Figure 5.2. Two dimensional model mesh (Nasir et al. 2011)

Four sets of boundary conditions (B.Cs), including hydraulic, mechanical, thermal and chemical, are used to simulate the effect of past glaciation. The assumed BCs can be divided into two groups: the first group comprises fixed BCs, and the second group is transient BCs.

In this work, hydraulic BCs are set as no flux at both sides and the bottom. On the other hand, to cover the diversity in theories, spatial and temporal variations of subglacial pore water pressure (e.g., Boulton et al. 2007a, and 2007b, Jansson and Näslund 2009); two cases of surface hydraulic BCs, are assumed. The first case is zero pressure hydraulic BCs, and the second case is a transient condition as a function of the ice loading history. However, in this report, we mainly focus on the former. The stress at the ground surface due to ice is directly adopted from the main outputs of the U of T GSM (Peltier, 2008) and the geometry of water pressure at the ice/bed interface is assumed to be linearly related to the surface stress and taken as a fraction of the ice load at the surface with different fraction values (0, 1/3 and 80%) to cover a wide range of potential ice/bed interface BC results.

For the mechanical conditions, roller BCs are assumed for the two sides and bottom, and free deformation at the surface. Transient normal stress which represents the ice load is applied at the surface. The surface thermal boundary conditions are given in **Figure 5.3**.

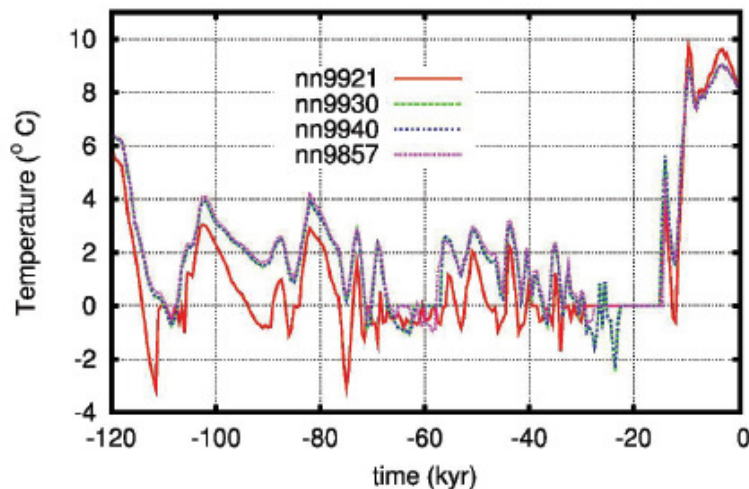


Figure 5.3. Thermal boundary conditions considered at the surface of the solid earth at the repository site (nn9930 considered in the present model as boundary conditions) (Figure from Peltier 2011)

5.4 Simulation results

5.4.1 Temperature distribution and evolution

Figure 5.4 illustrates the history of the ground temperature (depths of 20 m, 45 m and 70 m) for the past 120,000 years, whereas Figure 5.5 shows a comparison of the permafrost depth predicted in front of the glacier by using the model developed in the current study and that of Peltier (2008). The water freezing temperature is considered to be equal to 0°C in front of the glacier. The sequence of the ground temperature is similar to the sequence of ground temperature BCs. From the aforementioned Figures, it can be seen that the maximum depth of the permafrost (with temperature of 0°C) did not exceed 45 m in depth and there is a relatively good agreement between the permafrost depth predicted by the two models (current study and Peltier's model, Figure 5.5). Peltier's model for realization 9930 gives a maximum permafrost depth that is slightly over 40 m (Peltier, 2008). Thus, it can be concluded that permafrost is limited to shallow depths.

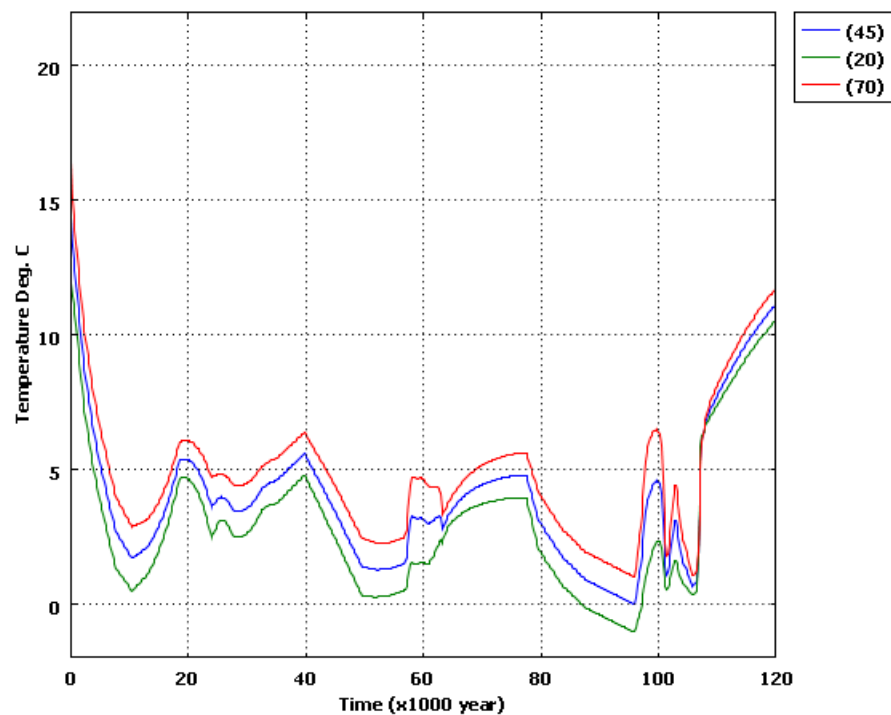


Figure 5.4. Ground temperature history at depths of 20, 45 and 70 m

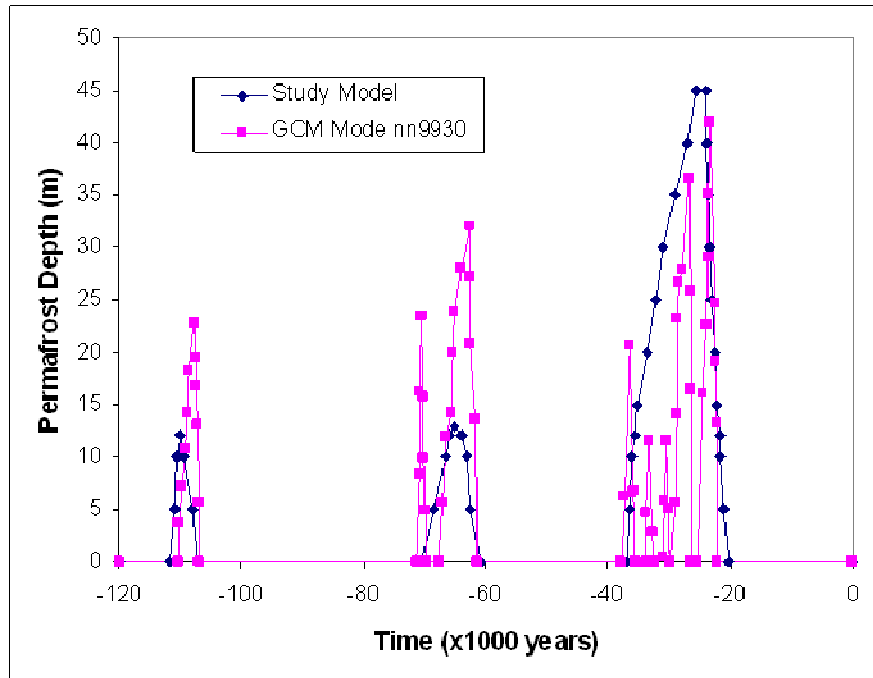


Figure 5.5. Permafrost depth predicted by the developed THMC model vs Permafrost depth predicted by Peltier’s GCM model

5.4.2 Distribution and evolution of the pore water pressure

Trial 1D simulations showed that the thermal processes have no major effects on the pore water distribution pertinent to the DGR. So, the simulations with regards to the impact of past glaciations on the pore water distributions in the study area were conducted by performing a hydro-mechanical-chemical analysis in order to increase the computational efficiency. Some selected simulation results are presented here.

Figure 5.6 illustrates an example of the results of the prediction of the present pore pressure profile in response to the past glaciation cycle; furthermore, the predicted results are compared with the measured field pore water pressure for free draining hydraulic boundary conditions. It can be observed that despite some differences in the predicted results and field data at a greater depth, relatively good agreement is achieved for the depth range of 0 to 700 m which includes the location of the potential DGR. These results are consistent with the field measurements. The differences in results may be due to some assumptions adopted in this work, such as a linear elastic model, homogenous and isotropic materials in addition to some influencing factors such as uncertainties in

geological and glacial data. Moreover, similar results were obtained for the two other hydraulic boundary conditions studied: (i) Case 2: hydraulic head equal to 30% of the ice thickness at the surface ($1/3 p$, Figure 5.7); and (ii) Case 3: hydraulic head equal to 80% of the ice thickness at the surface ($80\% p$).

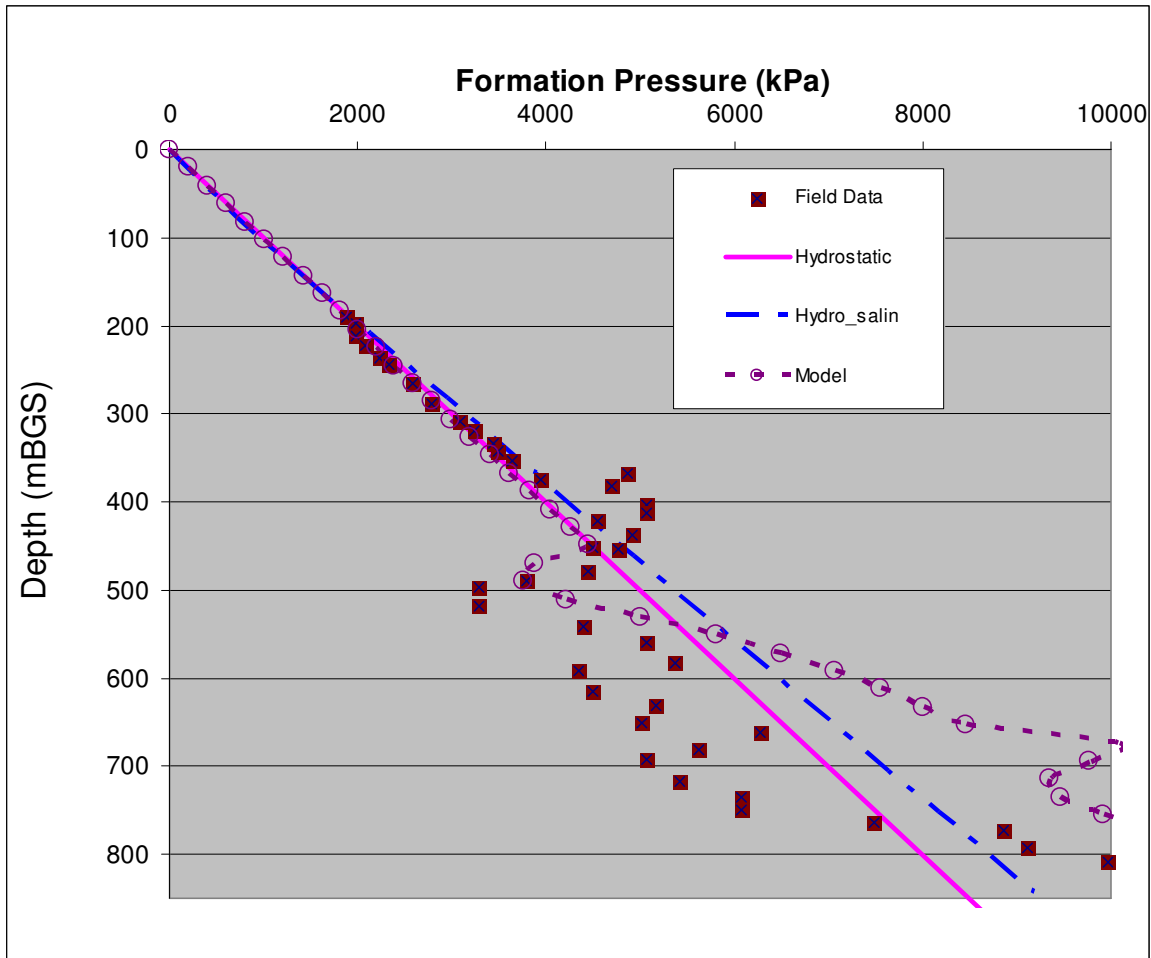


Figure 5.6. Pore water pressure profile for free draining hydraulic boundary conditions (zero pore water pressure B.Cs at surface).

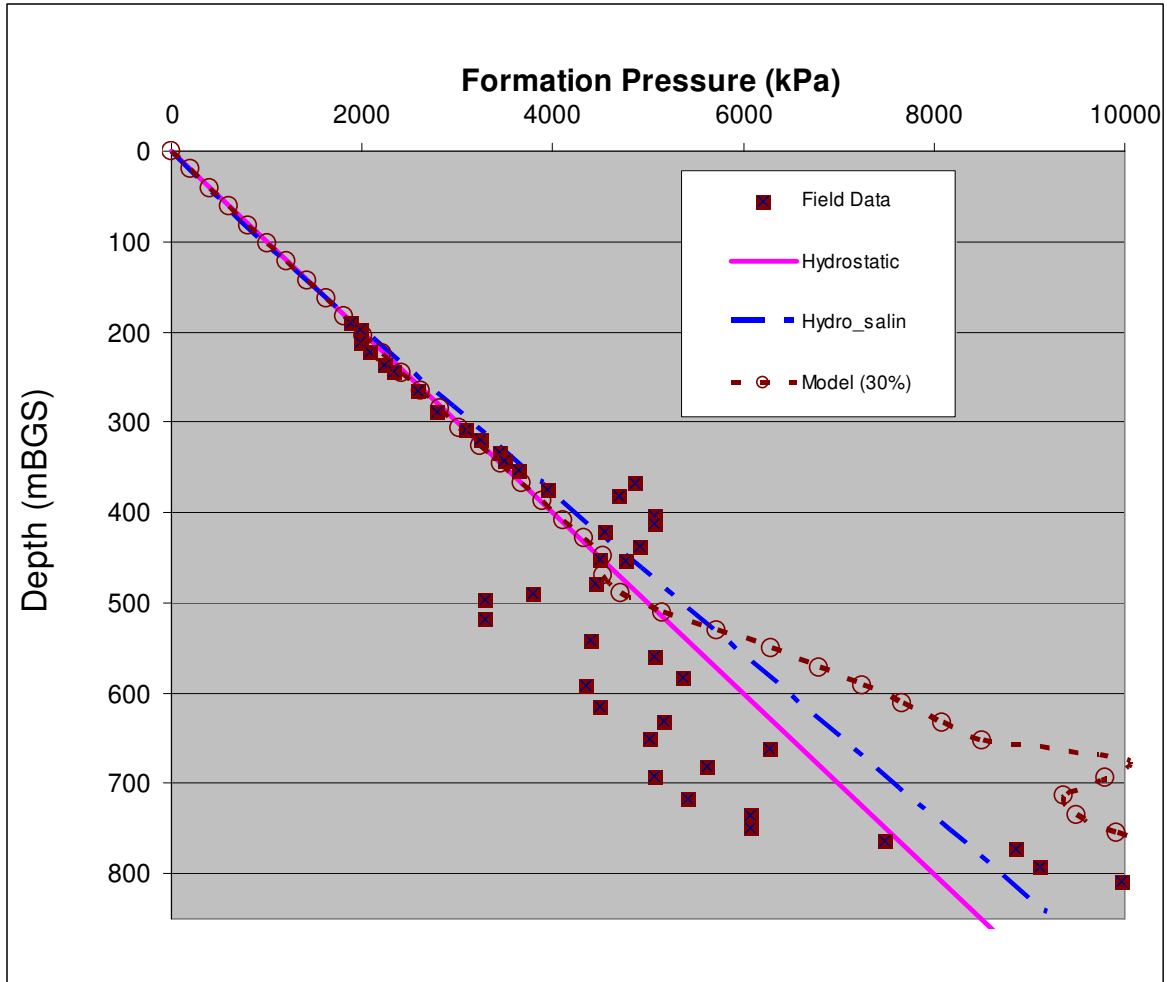


Figure 5.7. Pore water pressure profile for Case 2 (30% pore water pressure BCs at surface).

The variation of water pressure with time at a depth of 680m (the same depth as the proposed DGR) is presented in Figure 5.8. Two peaks are noticed which are related to each glaciation episode with a slight drop in water pressure after the second ice unloading (around 11,000 years before the present). That drop is induced by an elastic rebound. It takes a significant amount of time for the pressure drop induced by unloading to recover. The model predicts that the pressure at 680 m in depth is slightly lower than the hydrostatic pressure. In general, the shape of the time history of pore water pressure at a depth of 680 m is still similar to the ice loading history (Figure 5.1) due to the fast consolidation as compared to the loading rate.

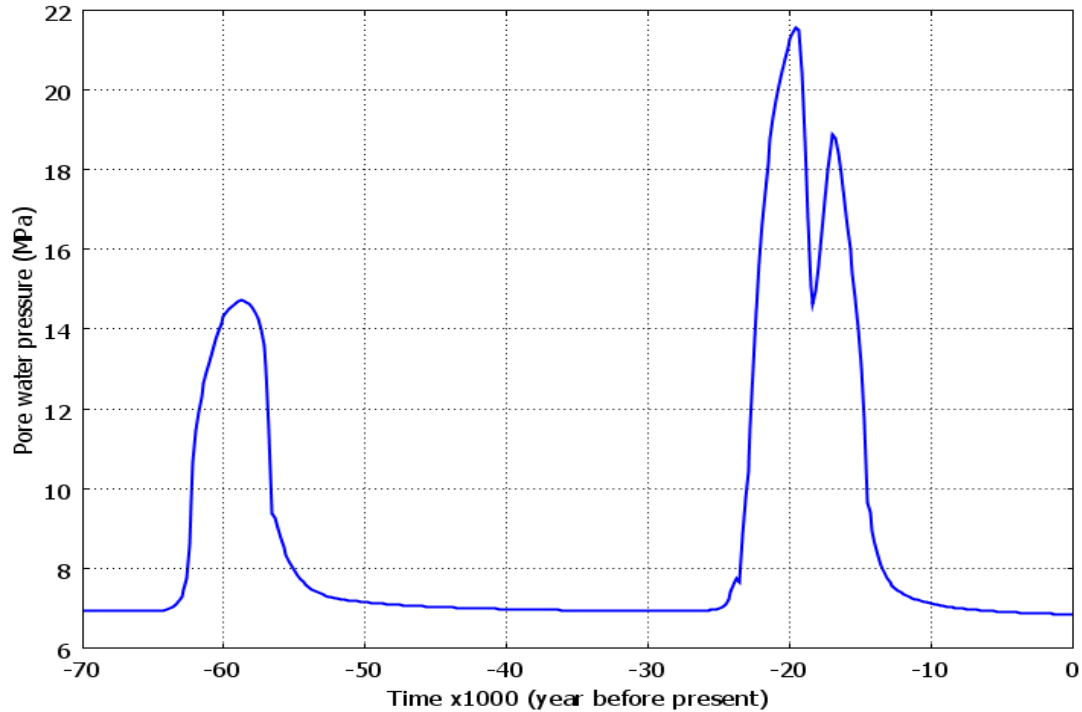


Figure 5.8. Pore water pressure history at the proposed DGR (Nasir et al. 2011)

The hydro-mechanical response of the host rock is mainly affected by two main factors; first, the location within the host rock with respect to its surface boundary, and second, the hydro-mechanical properties. Figure 5.9 shows the history of the pore water pressure at different depths. At a depth of 650 m where the hydraulic conductivity is very low, the hydraulic response is characterized by a significant drop in the pore water pressure following the unloading stage. This prediction is consistent with field measurements from boreholes at the site which shows an underpressure zone at the same level. However, the values of the predicted underpressure at the present are smaller than the measured values.

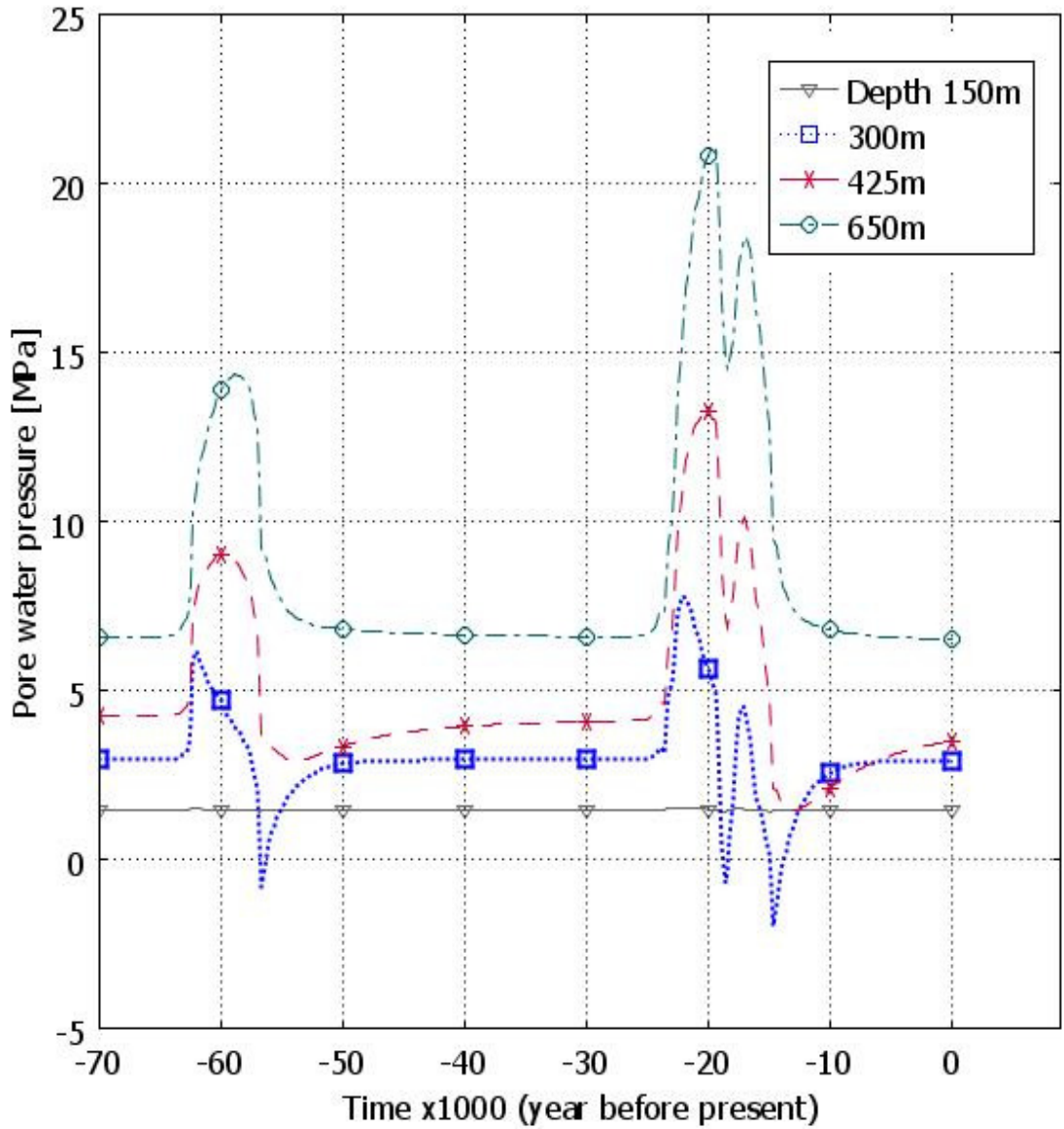


Figure 5.9. History of pore water pressure at different depths.

Figures 5.10 and 5.11 show the predicted changes in water pressure for selected times during the last 65,000 years. It can be noted that the maximum water pressure is accrued at around 19,500 years before present (Figure 5.11) in the Cambrian Formation, with an excess water pressure of about 15 MPa, which caused a pressure of up to 25 MPa at a depth of 1000 m. However, the water pressure in the upper formation (Devonian) has a higher dissipation rate due to its location near a free draining surface, as well as a

relatively high hydraulic conductivity of 10×10^{-8} m/s. Starting from 14,000 years before present (ybp), the pore water pressure distribution started to return to hydrostatic conditions, with some underpressure and overpressure that are still evident as shown in Figure 5.11.

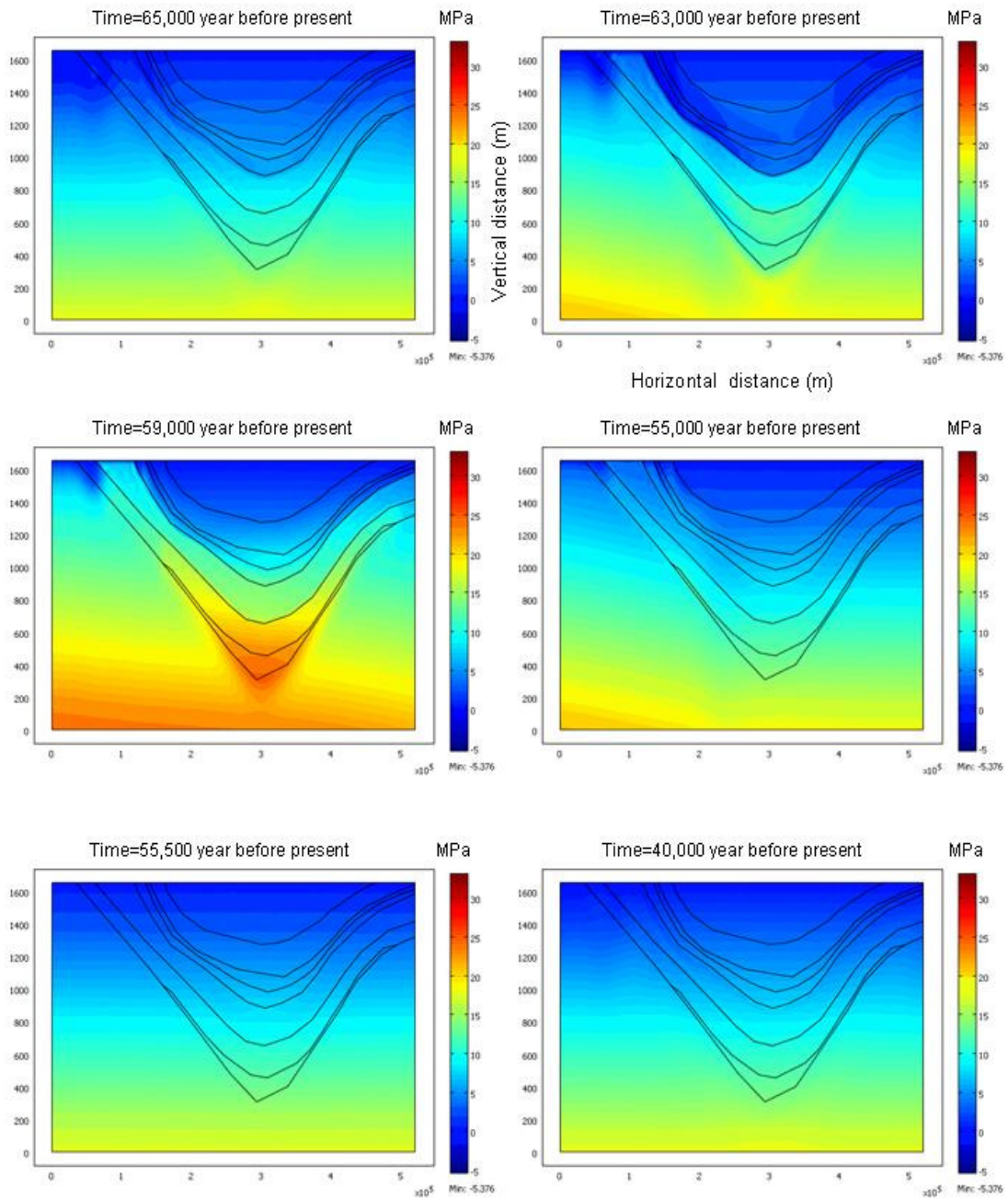


Figure 5.10. Pore water pressure history and distribution at 65,000 to 40,000 years before present.

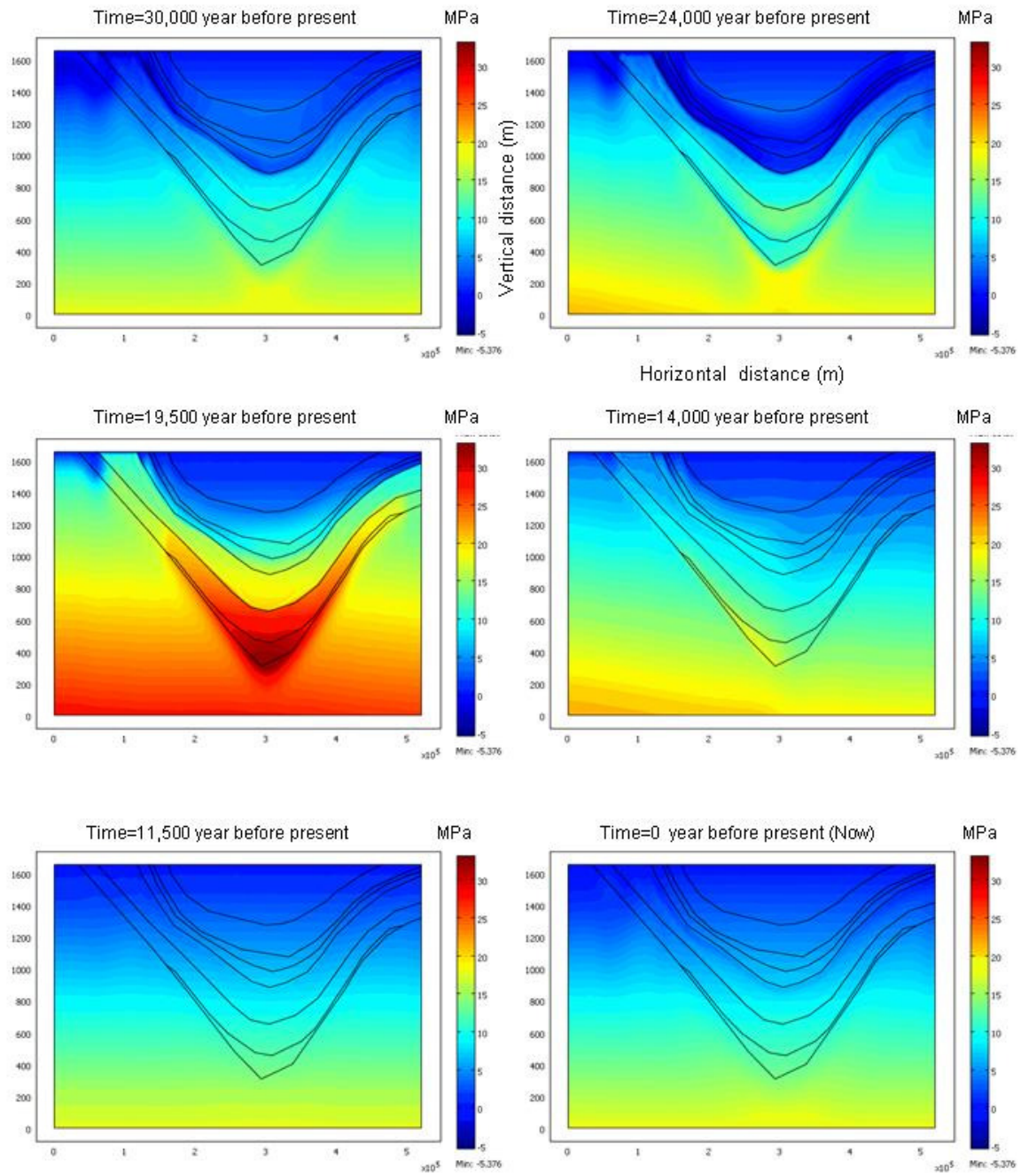


Figure 5.11. History and distribution of pore water pressure from 30,000 years before present

5.4.3 Evolution and distribution of the surface deformation and the vertical effective stress

Figure 5.12 shows the surface displacement under the impact of past glaciation cycles. Two main episodes of loading-unloading, with peaks at approximately 60 and 20 kilo years before present (kybp) can be detected; each one is mainly characterized by the shape of surface loading with a maximum surface displacement of about 1.2 m. This displacement is only due to the mechanical deformation and consolidation of the rock formations relative to the base of the model. It does not include the flow of the mantle underneath the earth crust, which contributes to the majority of the absolute displacement of the earth surface. It can be seen that the surface displacement is consistent with the ice loading history (Figure 5.1). This is a result of fast consolidation as compared to the time of loading.

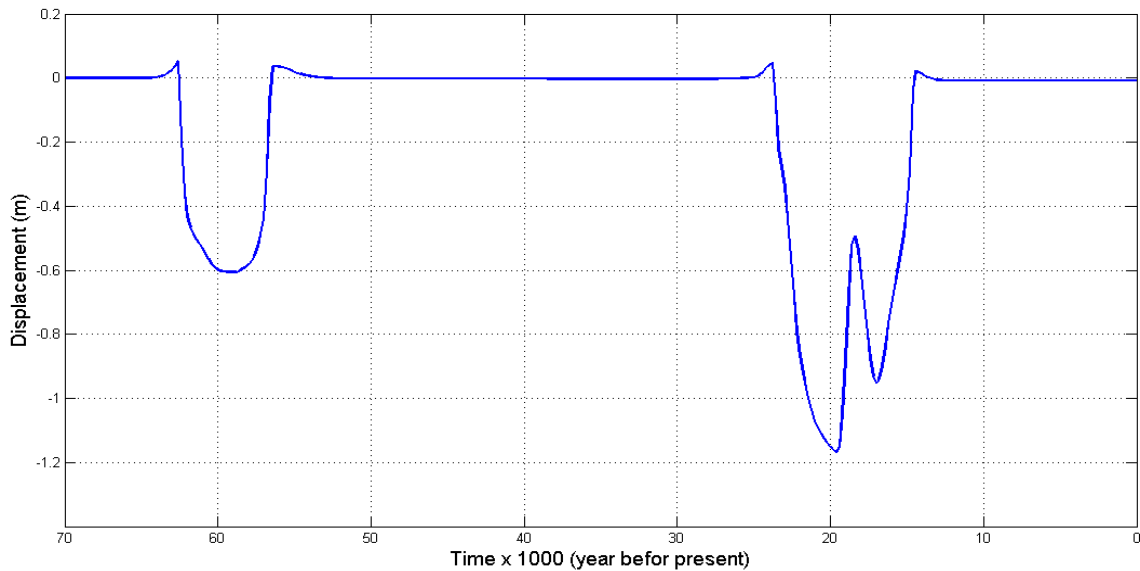


Figure 5.12. Surface displacement history at the location of the study area

Figure 5.13 shows the change in vertical effective stresses with depth for three time periods: (i) 120,000 years before present; (ii) first peak of ice loading (see Figure 5.1); (iii) second peak of ice loading (see Figure 5.1). It can be seen that the ice loading has a significant effect on the effective stress and the magnitude of change in effective stress. However, this change depends on the depth (Figure 5.13). For example, at the DGR level,

a small amount of effective stress reduction is observed during the early times of loading (65,000 and 23,000 ybp) due to high excess of pore water pressure at the early loading stages, and then, the evolution of the effective stress starts to follow that of the ice load as the time of loading is much longer than the time of excess pore water pressure dissipation. On the other hand, a significant change in effective stress is noted in the upper 300m, particularly at 200m. For example, at a depth of 100 m, the change in effective stress is about three times the change in effective stress at a depth of 680 m.

One key question with regards to the integrity of the rock is to estimate or assess if the observed changes in effective stresses could result in the failure of the rock in the study area. A comparison of the simulated effective stresses and measured rock strength values can provide a relatively good indication of a potential rock failure or fracturing due to excessive effective stresses. Figure 5.14 illustrates the distribution of the strength (UCS) of the rock with depth in the study area. It should be emphasized that higher strength should be expected when the confinement is taken into account. However, currently we do not have data on the effects of confinement on rock strength for the upper rock layers. Therefore, a semi-quantitative analysis of rock failure is performed. The analysis of the Figures 5.13 and 5.14 reveals that the vertical effective stresses induced by the 2nd ice loading could exceed the uniaxial compressive strength of some rocks in the upper 280m, whereas for a depth more than 280m the rock uniaxial compressive strength is always significantly higher than the effective stresses regardless of the ice loading period. These observations could suggest that the glaciations induced increase in the effective stress could potentially lead to failure and fracturing of some rocks at shallow depths ($\leq 280\text{m}$) only. This is in agreement with the rock quality designation (RQD) profiles measured in the study area (Figure 5.15). From Figure 5.15, it can be observed that the RQD value is close to 100% for a depth higher than 280m. This is also supported by the results presented in Figure 5.16. This figure shows a comparison of the stresses induced by peak glaciations with the best-fit Hoek-Brown envelopes for various rock units (Cobourg, Collingwood, Georgian Bay and Salina), in the study area. From this figure, it can be noted that only the Salina rocks at the depth of 260m fail. Furthermore, the safety factor with respect to strength of the rock units mentioned (Figure 5.16) is equal to 4.78 for the Georgian Bay, 6.80 for the Collingwood, 6.94 for the Cobourg and 0.83 for the Salina

rock unit, respectively. This means that only the Salina rock at the depth of 260m has failed due to the ice loading. This could provide an additional argument for long term safety under the impact of future glaciations.

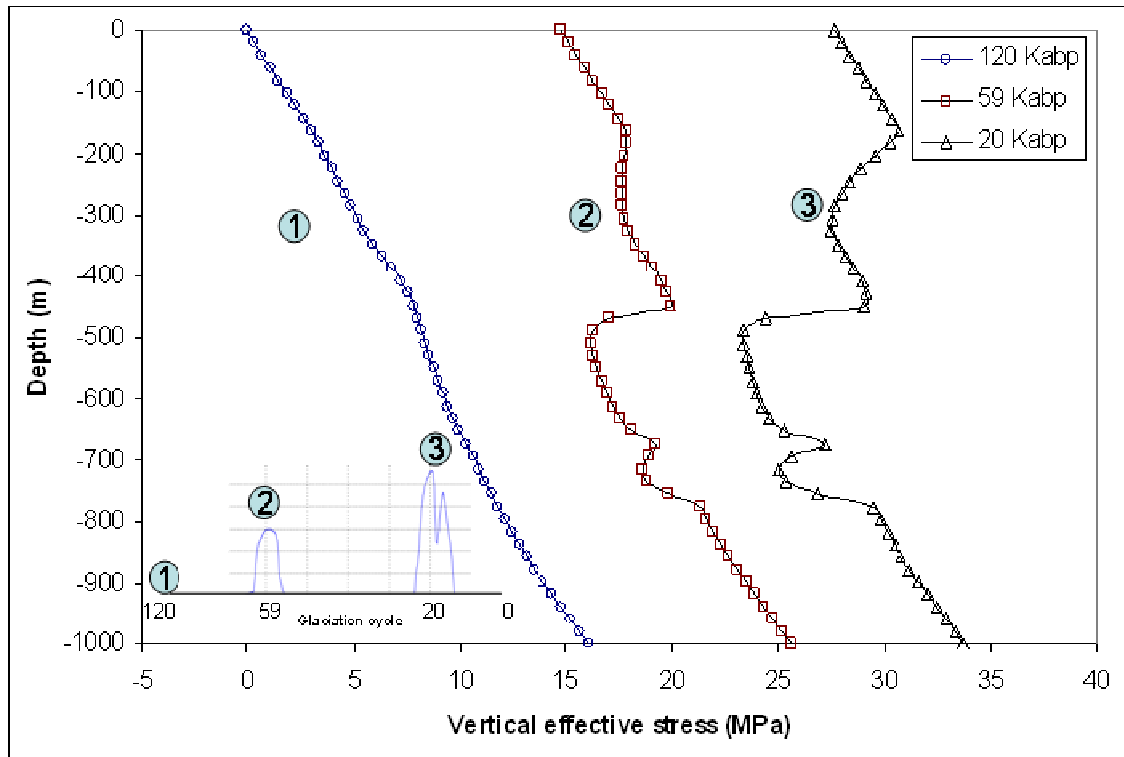


Figure 5.13. Vertical effective stress profile at three periods: (i) 120,000 year before present (noted 0); (ii) 1st ice loading peak (Peak #1: 59 Kabp); 2nd ice loading peak (Peak # 2; 20 Kabp).

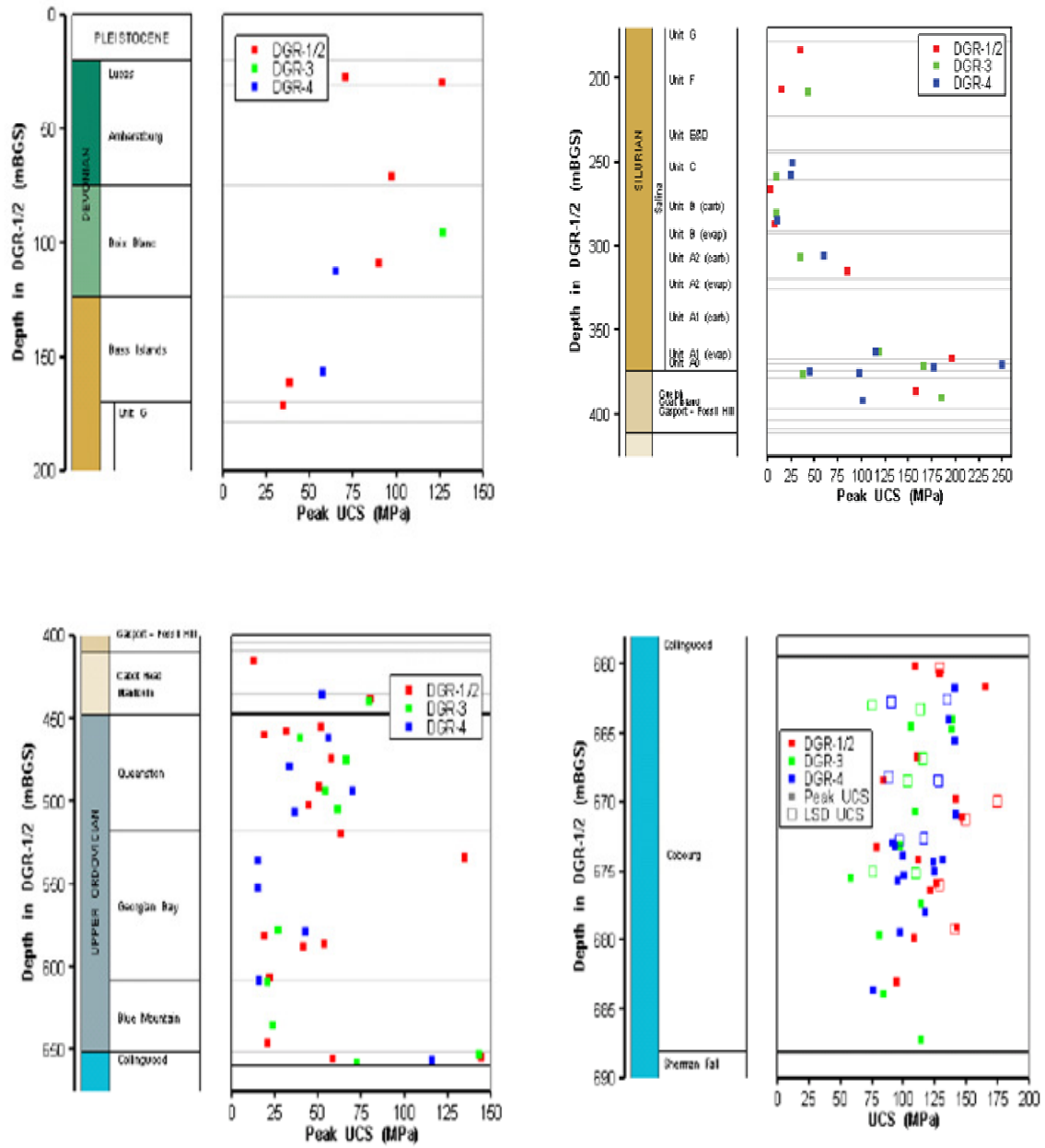


Figure 5.14. Distribution of the rock strength (UCS) with depth in the study area (NWMO 2011d)

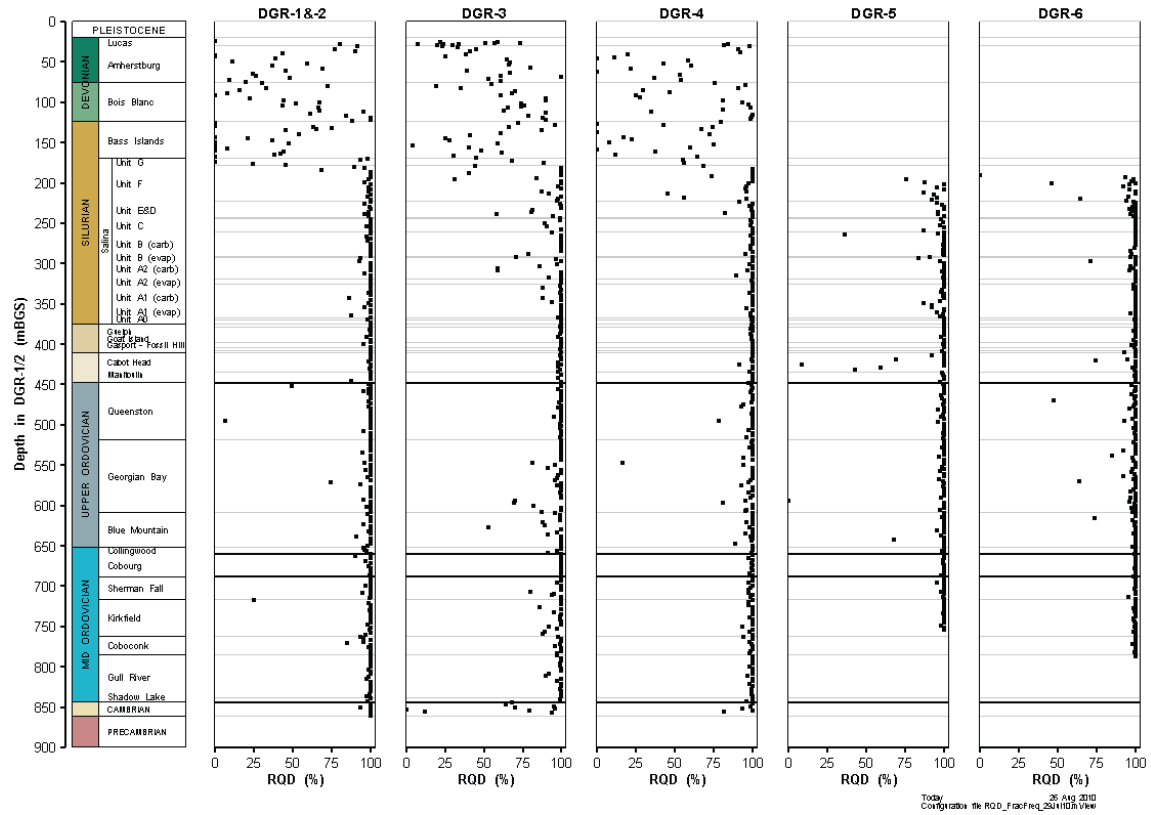


Figure 5.15. RQD profiles in the study area (NWMO 2011d)

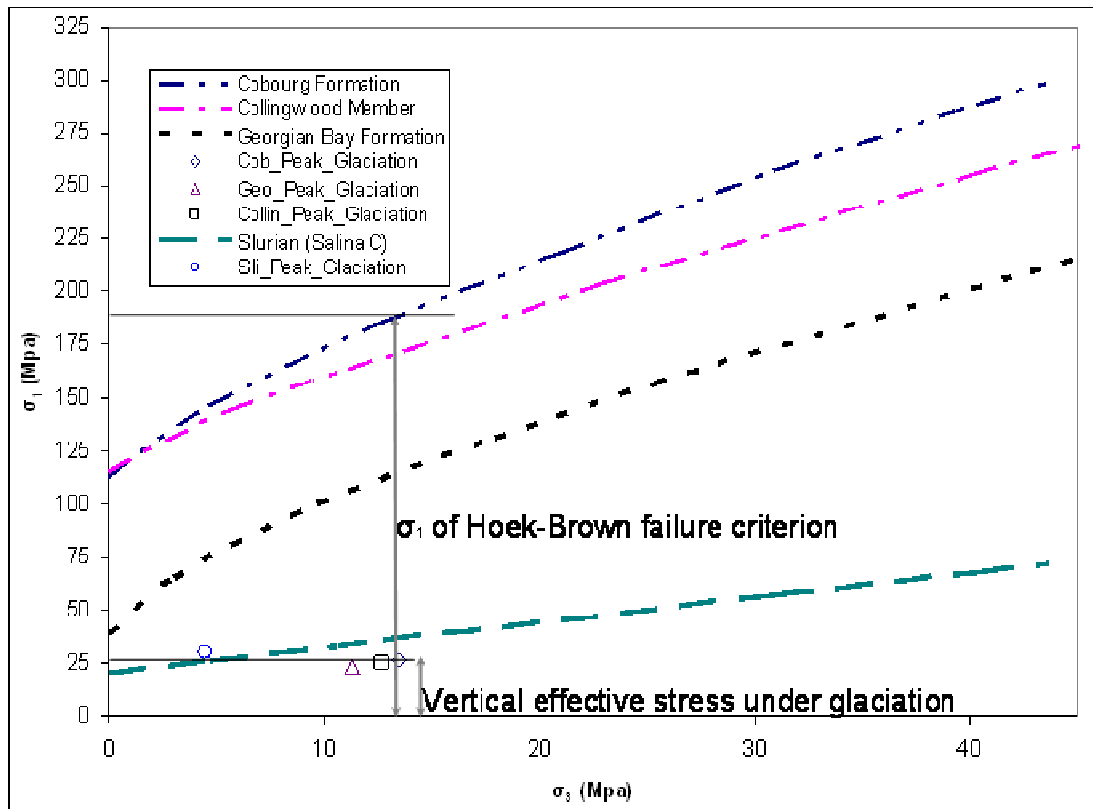


Figure 5.16. Peak glaciation induced stresses compared with best-fit Hoek-Brown envelope (Hoek-Brown failure envelopes of the Cobourg, Collingwood and Georgian Bay rocks are obtained from NWMO2011a; failure envelope of the Salina rock is determined by assuming the following parameters $\sigma_c = 20$ MPa $m_i = 10$ $s = 1.0$ and $a = 0.5$)

5.4.4 TDS distribution and evolution

Figure 5.17 shows the simulated TDS profile compared with the actual field geochemical distribution. This result comes from advection-diffusion solute transport modelling. The following initial TDS boundary conditions are considered: $TDS = 0 \text{ kg/m}^3$ at the top, 150 kg/m^3 in the Precambrian, and initial conditions of 300 kg/m^3 for the rock formations above the Precambrian. The penetration of the glacial melt water is also considered. The model is run for a period of 400 million years equivalent to the approximate time since the rock units were formed. The comparison shows a good agreement between the simulated and actual profile. Moreover, additional TDS simulation results (performed by considering the diffusion solute transport only) have shown that the advective solute

transport is negligible because the TDS profile obtained by diffusion and advection-diffusion solute transport are similar. These results support the diffusion dominated solute transport at the DGR site in the past. Furthermore, additional simulations have shown that this diffusion dominant solute transport in the host rock barrier (limestone, shale) is insensitive to glaciation and deglaciation.

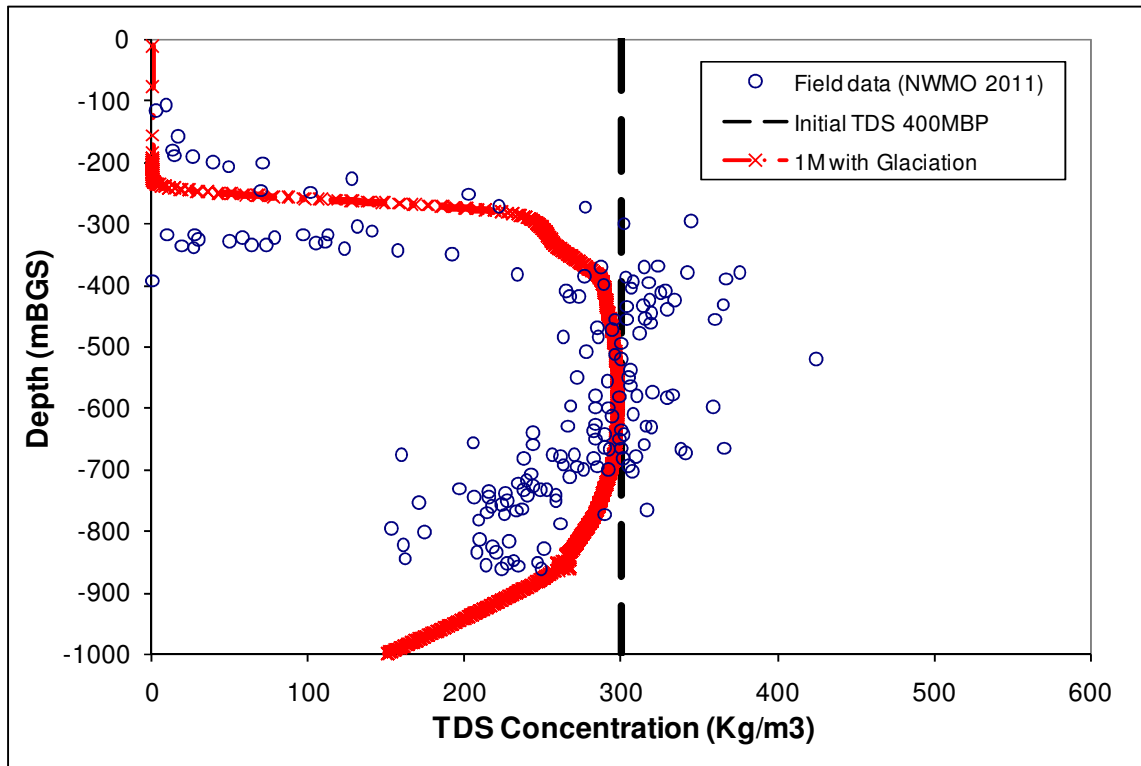


Figure 5.17. Simulated vs measured actual TDS profile field geochemical distribution.

6 Numerical Analysis of the Impacts of Future Glaciation-Deglaciation Cycles on Sedimentary Rocks in Ontario

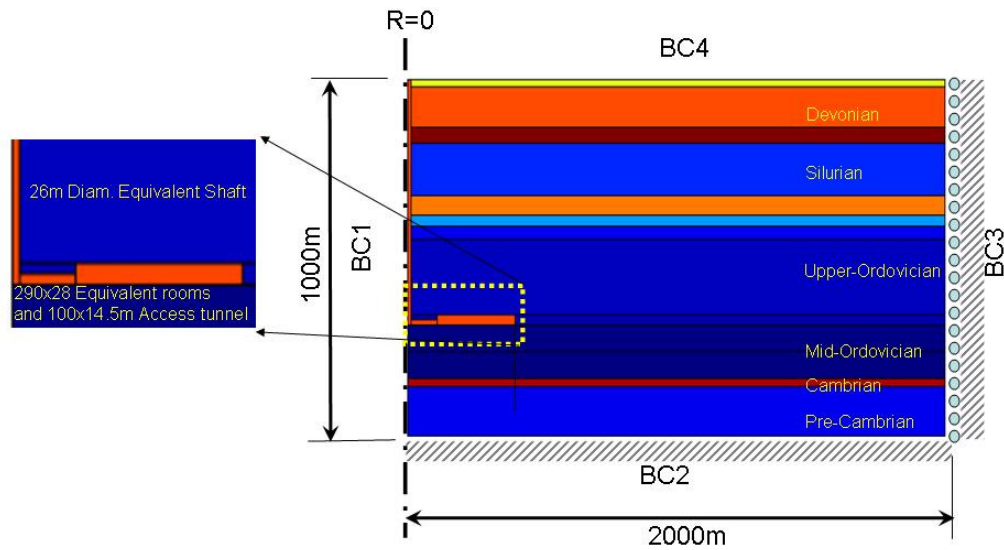
6.1 Introduction

The model was implemented by using various boundary condition scenarios to simulate the impact of future glaciation-deglaciation cycles on the sedimentary rocks and a DGR system in Ontario. Thermal effects were neglected, and only HMC processes were considered. The main results of the simulation are presented below.

6.2 Model conceptualization, initial and boundary conditions

It was decided to focus the modelling of the impact of future climate changes on the part of the sedimentary rocks pertinent to the assessment of the safety of the DGR. This allowed us to conduct a more detailed numerical investigation and to adequately capture the complexity of the coupled HMC processes that occur within the sedimentary host rock. Thus, a smaller domain (compared to the domain selected for the simulation of the past climate changes) of the sedimentary rock was considered that allowed a more refined mesh. Figure 6.1 shows the model geometry and the finite element mesh with the boundary conditions. In this work, an equivalent shaft area with a radius of 13m including the EDZ effects is used to model the two shaft proposed by the OPG's design. Axisymmetric conditions are assumed with the axis of symmetry centred along the equivalent shaft. The initial hydraulic, mechanical and thermal properties of the host rocks are the same as those utilized in chapter 5. The host rock is considered as a saturated porous medium, i.e. it is made of a solid skeleton and pores, cracks and microcracks filled with water.

The initial hydraulic, mechanical and thermal properties of the shafts and the repository and their associated EDZ are obtained from NWMO (2011e); and assumed to be equivalent to one material for the sake of simplicity. Two case scenarios are considered with regards to the properties of the shaft: (i) a normal scenario and (ii) a failed shaft scenario where the material properties (e.g., permeability, porosity) are deteriorated. The properties of the shaft for the failed shaft scenario case are summarized in Table 6.1.



Liquid - Mechanical Boundary conditions

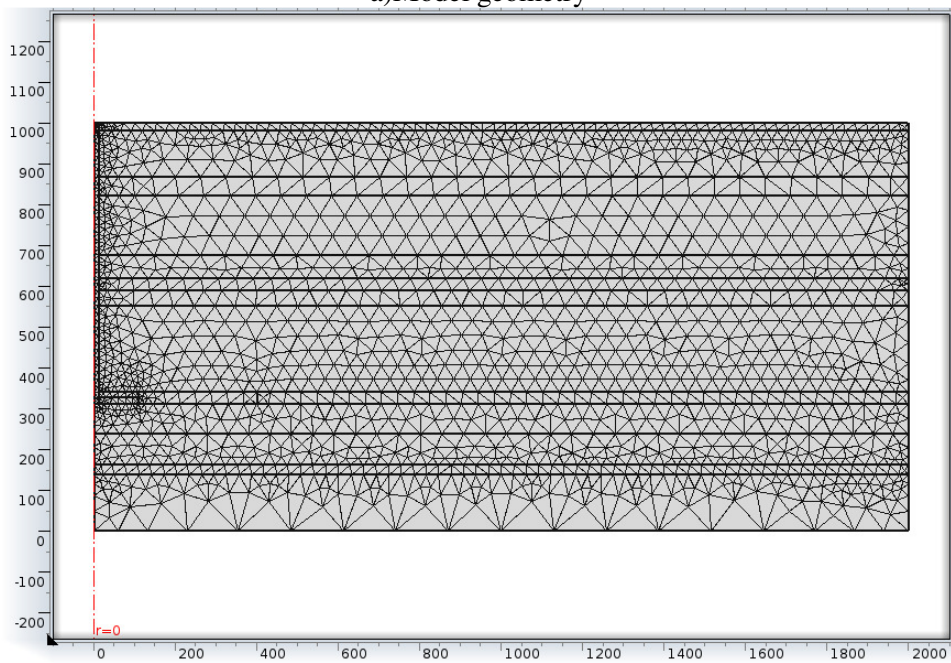
BC1= Axi - symmetric axis

BC2= Zero flux - fixed deformation

BC3= Zero flux - Roller

BC4= Zero pressure - free deformation, transient applied pressure

a)Model geometry



b)2D FEM Mesh

Figure 6.1. A 2D view of the conceptual model and the scheme of the boundary conditions for coupled modeling of the impact of future climate changes on DGR

Table 6.1. Main properties of the shaft adopted (worst case scenario for a failed shaft; data from NWMO2011e)

Property	Value
Hydraulic conductivity (m/s)	10^{-7}
Permeability (m ²)	10^{-14}
Density (kg/m ³)	2500
Poisson ratio (-)	0.2
Modulus of elasticity (GPa)	20
Porosity	0.5
Biot coefficient	0.9

The University of Toronto Glacial Systems Model (GSM) “Peltier’s model” (Peltier, 2008) is used to derive the spatially and temporally varying thermal, hydraulic and mechanical boundary conditions during the future glaciation-deglaciation events. The thermal boundary conditions and ice loading stress shown in Figure 5.3 (nn9930) and 5.1 respectively, are applied for the future glaciations. Since Peltier (2011)’s studies revealed that if a reglaciation of the Canadian land mass should occur again in the future, such an event is most likely to begin in approximately 60,000 years from present, 60,000 years are considered as the time of the first peak of the first glaciation cycle, where the second peak will occur in approximately 100,000 years. Up to four glaciations cycles are considered in the present study; this corresponds to a total time of approximately 480,000 years.

6.3 Simulation results

6.3.1 Hydraulic response

The results for the hydraulic response of the DGR system to future glaciation-deglaciation cycles have shown that the hydraulic characteristics (e.g, water pressure, flow velocity) of the study area follow the advance/growth and retreat/decrease of the ice sheet. Typical results for the worst case scenario for a failed shaft are presented below.

Figure 6.2 illustrates the temporal evolution of the water pressure at the centre of the equivalent DGR repository. From Figure 6.2, it is obvious that the temporal evolution of the water pressure is strongly related to the advance/increase and retreat/decrease of the ice sheet. The two observed water pressure peaks correspond to two distinct glaciation events with maximum ice sheet thickness. The consolidation effects induced by glacial loading increase the water pressure. Furthermore, the simulation results show that the DGR system appears to have some memory of the previous glaciation cycle, with water pressure returning (relatively) slowly to non-glacial conditions shortly after each cycle (Figure 6.2).

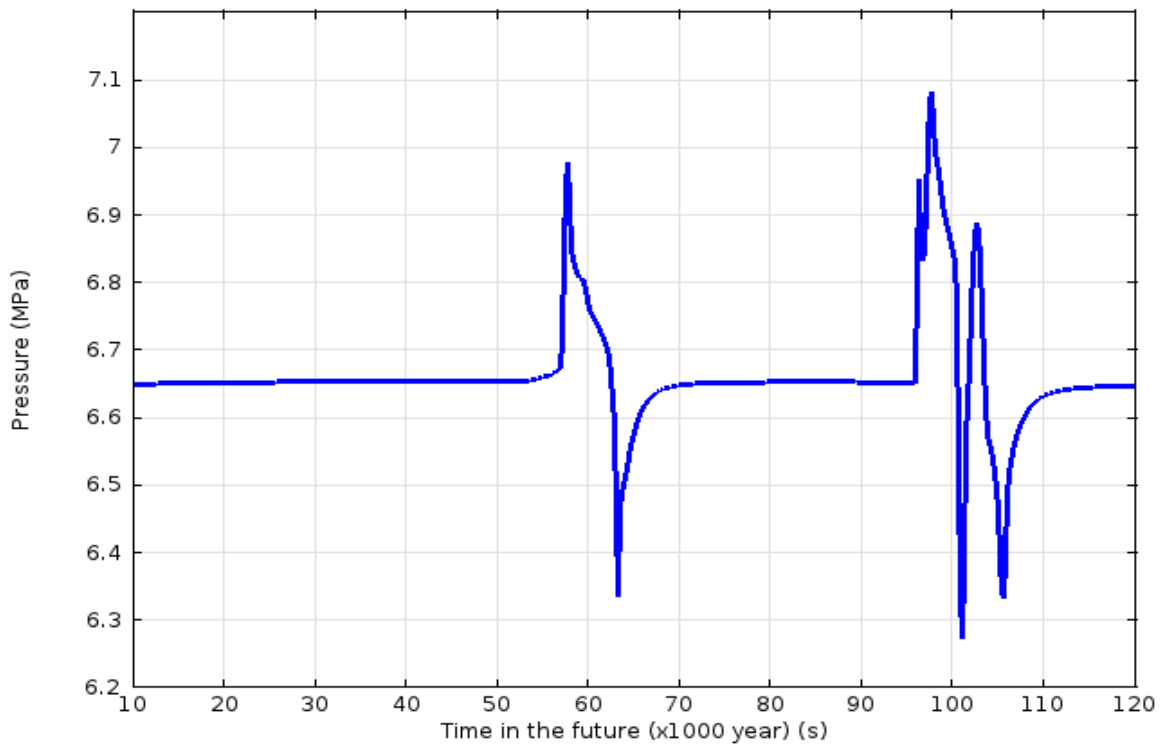


Figure 6.2. Evolution of the pore water pressure at the DGR level – failed shaft

Figure 6.3 and 6.4 show the effect of two glaciation events (first peak at 60,000 years, 2nd peak at 99,000 years) and deglaciations on the pore water pressure profile (Figure 6.3) and distribution (Figure 6.4) in the host rock of the study area, respectively. It can be observed that, during the glaciation events the study area shows an overpressure from a

depth of 300m to 1000m. This overpressure is attributed to the load applied by the ice sheet. This overpressure will affect the hydraulic gradient in the study area, and thus the groundwater flow direction as shown in Figure 6.4.

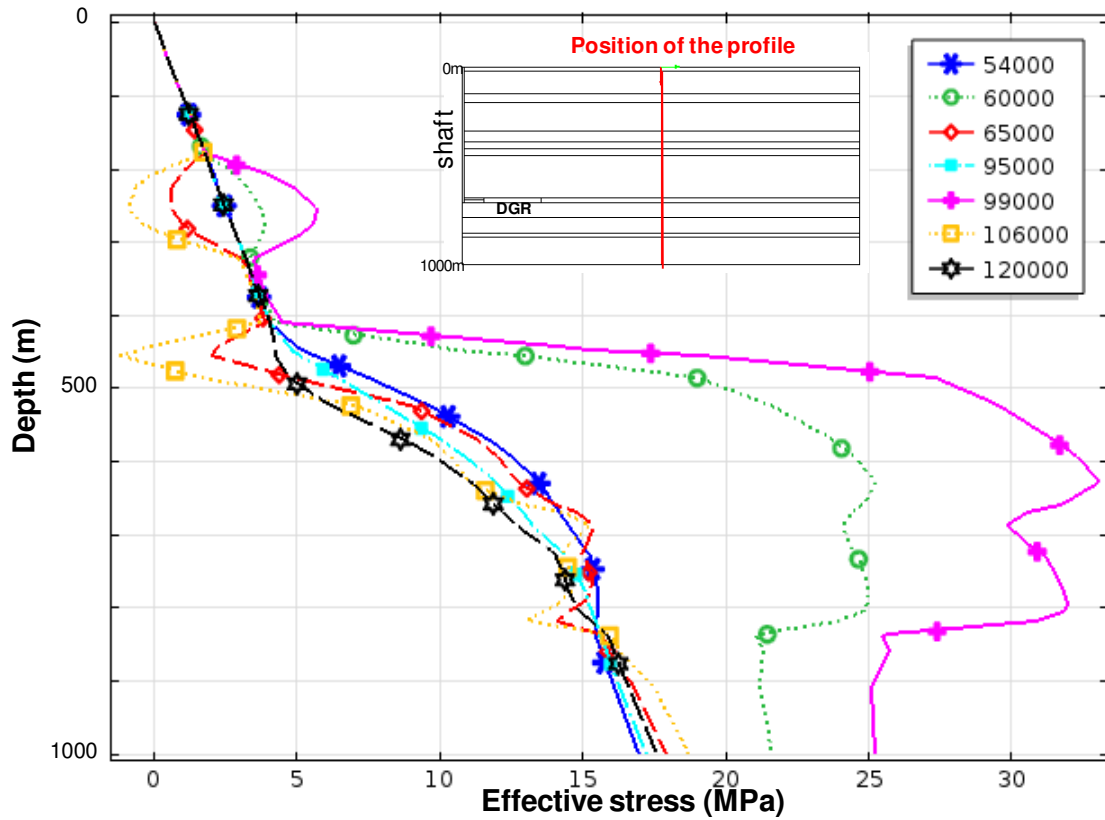
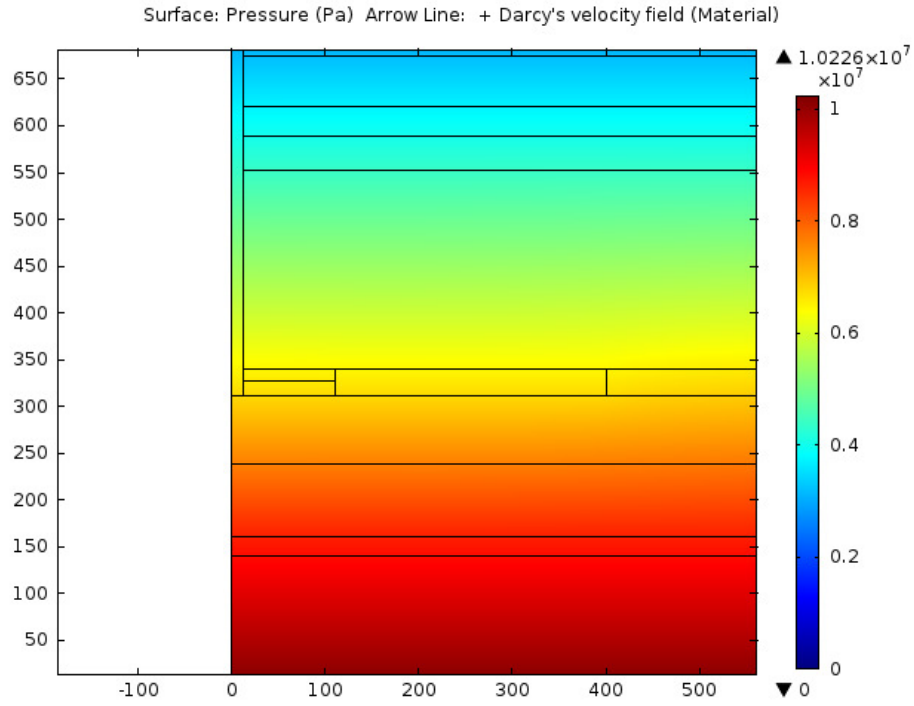
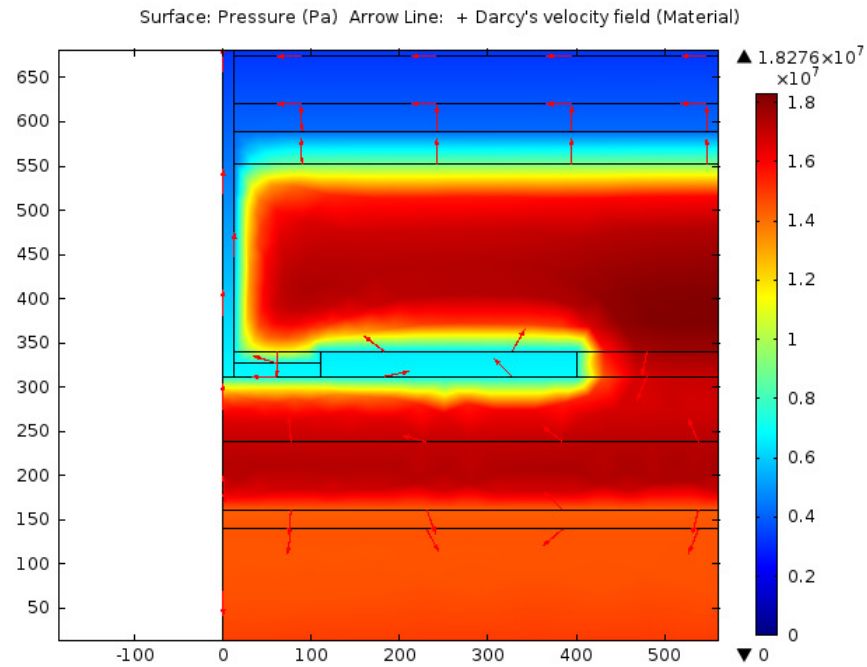


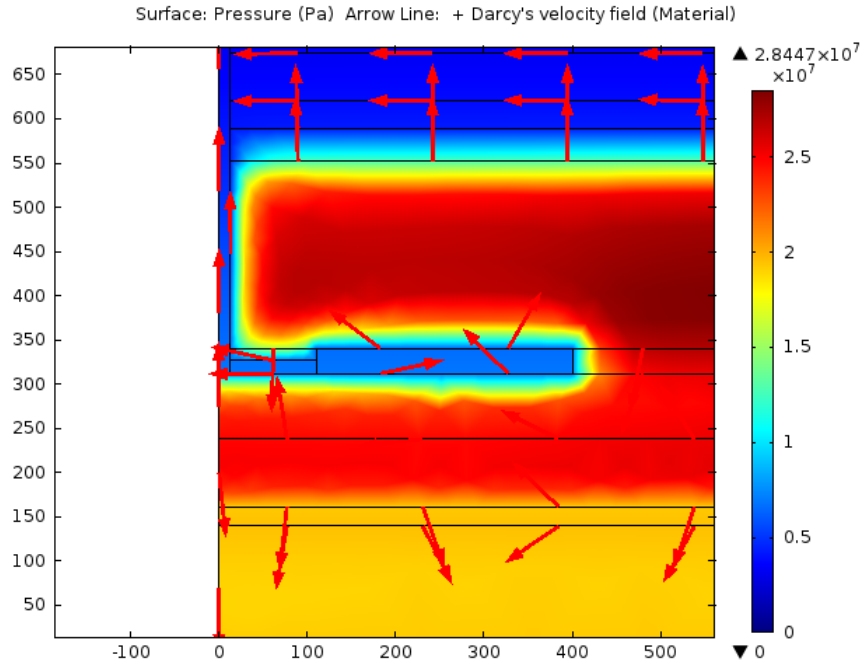
Figure 6.3. Temporal evolution of the water pressure profile in the host rock (free draining surface hydraulic conditions) – failed shaft



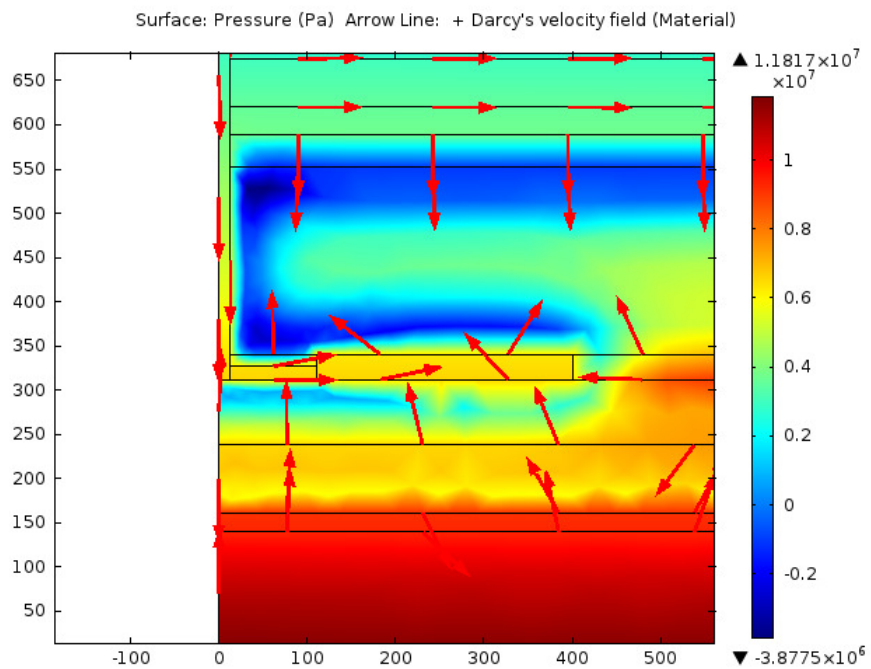
a) initial pore water pressure



b) Pore water pressure at the first peak of the glaciation cycle showing the velocity field and direction of flow – failed shaft



c) Pore water pressure at the second peak of the glaciation cycle showing the velocity field and direction of flow



d) Pore water pressure after unloading of the second peak of the glaciation cycle showing the velocity field and direction of flow

Figure 6.4. Temporal evolution of the flow velocity in the study area (distance given in meter) - failed shaft

Figure 6.5 illustrates the influence of the aforementioned two glaciation events and deglaciations on the pore water pressure on a vertical profile along the shaft. It can be noted that the glaciations did not lead to a significant increase in the pore pressure within the shaft. It can be seen that, down to approximately 700m (bottom of the shaft), the water pressure is close to the hydrostatic pressure. This insignificant impact of the glaciation events on the water pressure within the shaft (worst case) can be attributed to the high permeability (10^{-7} m/s) of the latter.

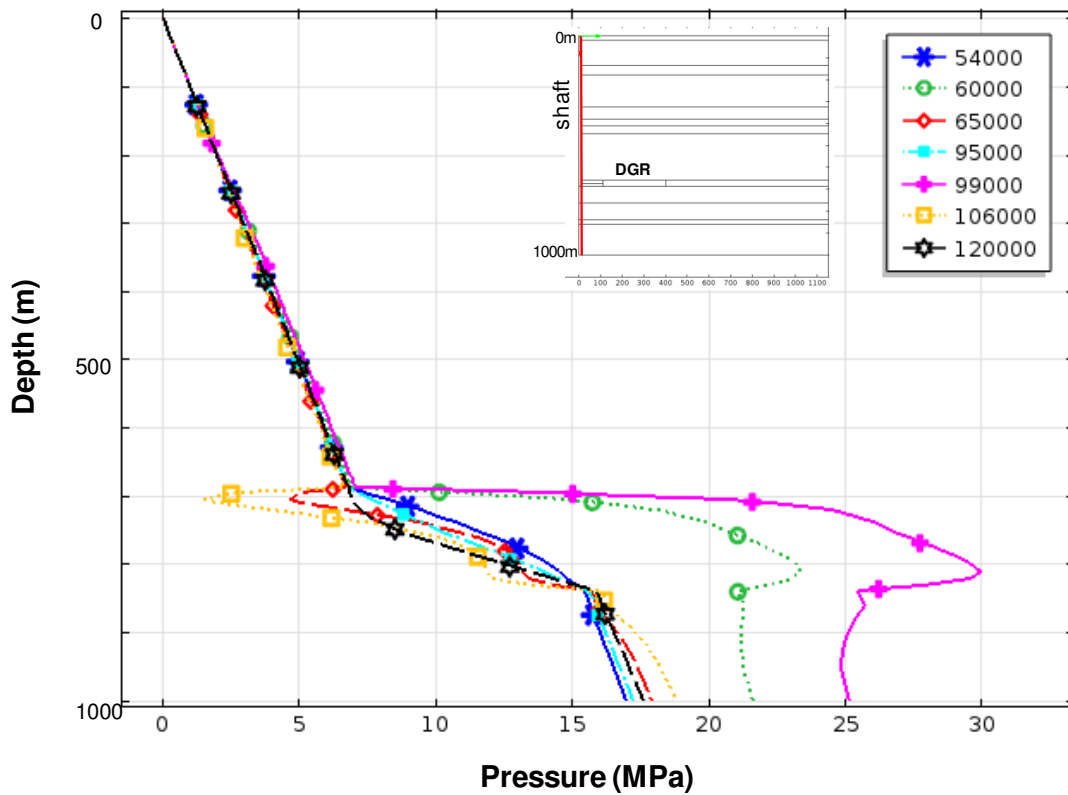
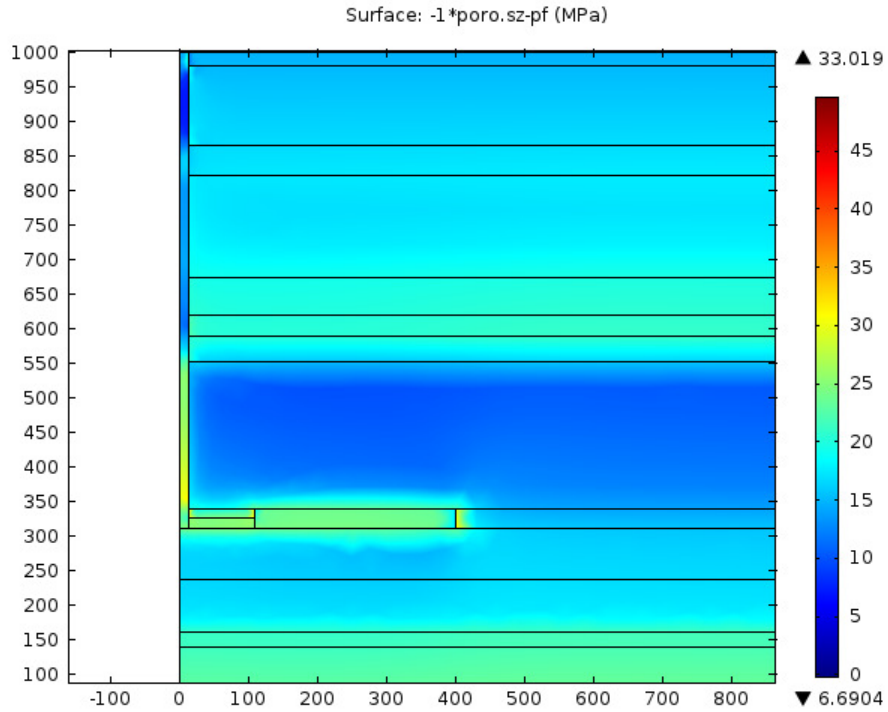


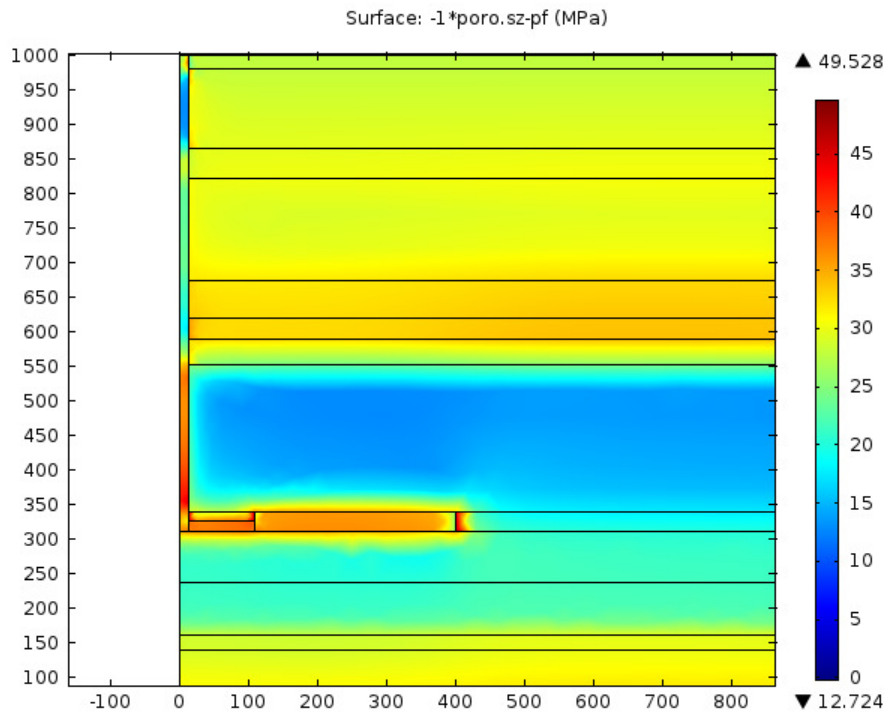
Figure 6.5. Temporal evolution of the water pressure profile along the shaft (free draining surface hydraulic conditions) – failed shaft

6.3.2 Mechanical response

In addition to its effect on the hydraulic responses of the host rock, large normal stress induced by ice loading also contributes to significant changes in effective stress. Figure 6.6 illustrates the effect of the ice loading on the vertical effective stress and its distribution in the host rock, shaft and the proposed DGR. Again, it can be noted that the ice loading has a significant effect on the effective stress and its distribution. The changes in effective stresses due to the ice load is not uniform. The magnitude of the change depends on the depth and formations. Some formations, the shaft and the DGR have a different response than others (e.g., Cobourg) due to different poroelastic response. This discrepancy is attributed to the differences in both hydraulic conductivity and modulus of elasticity. It can be observed that the glaciation loads induce larger increase in effective stress at depths lower than 400m, at the DRG level and in the shaft. The highest effective stress is observed in the bottom 200 m of the shaft and in the repository zone during the second glaciation peak. A vertical effective stress up to 45 MPa is predicted. It should be noted that this high effective stress comes from the assumption of a deteriorated shaft seal resulting in a high permeability. Therefore, as discussed in the previous section, almost full dissipation of the excess pore pressure would occur. The preliminary design of the shaft mixture specifies mainly a sand/bentonite mixture at a 30%/70% ratio for its bottom part. Assuming a Mohr-Coulomb type of failure, with a cohesion of 0.088 MPa and a friction angle of 14° (Oswell, 1991), further shear failure is predicted for the selected seal in the bottom part of the shaft. Consequently, the engineering design of the shaft and its effectiveness as a barrier to contaminant transport should be further assessed. In contrast, the maximum vertical stresses (around 20 MPa) that can develop in the Cobourg limestone and the shale formations (Figure 6.6), i.e. the natural barrier are much lower than the strength of those rock formations. This could imply that the ice loading will not lead to the failure or fracturing of the aforementioned formations.



a) vertical effective stress at the first peak of glaciation cycle



b) vertical effective stress at the second peak of glaciation cycle

Figure 6.6. Effects of the glaciation (60,000 years, 99,000 years) cycles on the distribution of the vertical effective stress in the host rock, shaft and at the proposed DGR level

Figure 6.7 depicts the surface displacement under the impact of the two future glaciation cycles. Two main episodes of loading-unloading, with peaks at approximately 60,000 years and 100,000 years, can be identified; each one is mainly characterized by the shape of surface loading with a maximum surface displacement of about 1.1 m. The downward displacement follows primarily the time-varying ice sheet loading at the top boundary. The displacement can be attributed to the mechanical deformation and consolidation of the host rock and DGR system relative of the base of the model. As mentioned previously, it should be emphasized that the above displacement excludes the flow of the mantle underneath the earth crust, which contributes to the majority of the absolute displacement of the earth surface.

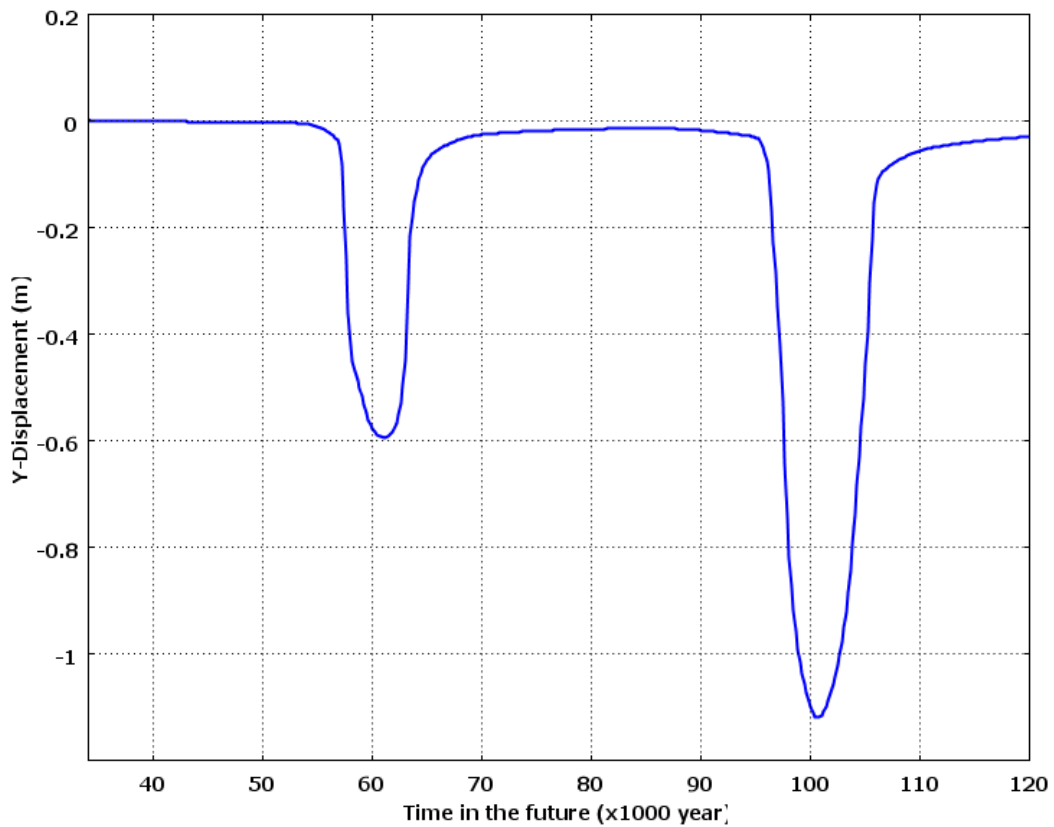


Figure 6.7. Temporal evolution of the mechanical surface displacement at the location of the study area

6.3.4 Simulation of solute transport

The objective of the present section is to study the impact of the future glaciations cycles on the solute transport within the DGR system (e.g. host rock, shaft) by using the developed THMC model. Indeed, the main objective underlying the concept of deep geological disposal of nuclear wastes is to achieve the long term containment and isolation functions. Natural processes such as future climate changes could potentially jeopardize that function. Thus, numerical simulations of the effect of ice loading cycles on the transport of a solute generated within the DGR are performed in this chapter. It should be emphasized that the aim of the present chapter is not to perform a complete numerical modeling of radionuclide transport (this is out of scope of the present project), but to provide an indication of the potential impact of the ice loading cycles on the solute transport in the study area.

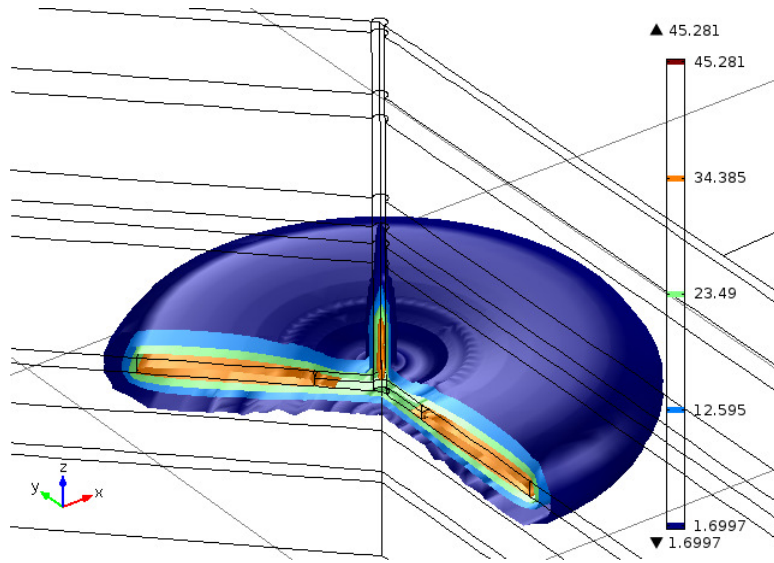
The solute transport is described by diffusion and advection, which is a simplified and/or conservative approach. Indeed, the processes affecting or controlling the transport of solute (radionuclides) from the waste matrix through the geological or engineered barrier to the biosphere may be highly complex. Besides the diffusive and advective transport, the transport of radionuclides can be affected or controlled by other factors such as retardation due to diffusion and dispersion through interconnected pores, retardation due to diffusion and sorption into a low permeability matrix, retardation due to (ad)sorption of solutes onto solids, retardation due to precipitation/co-precipitation, radioactive decay, recoil effects, complexation, colloid transport.

Up to four glaciation cycles are considered in this study, i.e. simulations are performed over 480,000 years. Model results are presented in terms of relative concentrations (%) which are normalized by the initial concentrations ($\frac{C}{C_0} \times 100$; where C_0 is the initial solute concentration at the DGR, C is the solute concentration at the time t). Initial relative concentrations of the solute in the host rock surrounding the DGR and shaft are assumed to be zero, whereas the initial solute concentration in the source (DGR level) is considered to equal to 100%. Regarding the properties of the shaft, two case scenarios are considered: (i) normal scenario; (ii) worst case scenario (shaft seal failure). The initial mechanical, hydraulic and thermal properties adopted for the host rocks and the shaft

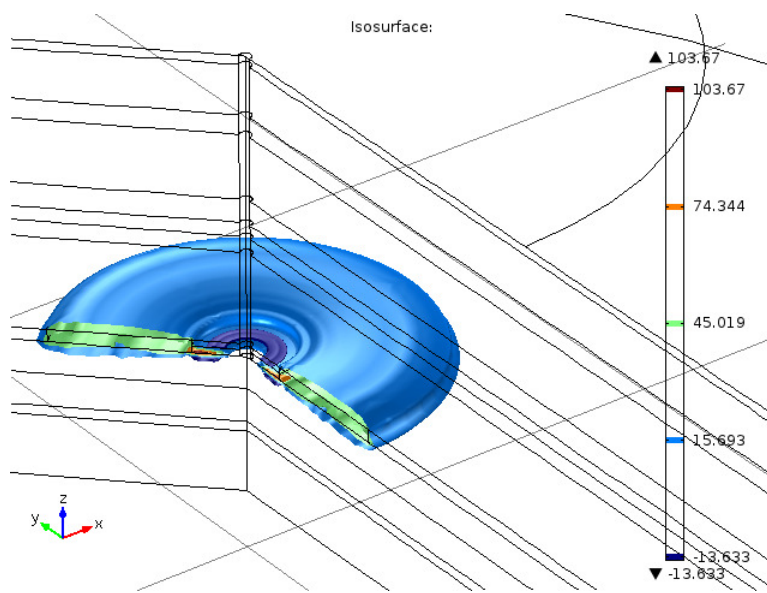
(both cases) are already given in the previous sections and in the NWMO's reports (NWMO, 2011a,b,c,d).

Several numerical simulation results have been obtained. The results obtained have shown that the solute transport in the natural limestone and shale barrier formations is controlled by diffusion. The diffusion dominant solute transport in the natural rock barriers (limestone and shale formations) was determined to be not significantly sensitive to glaciation cycles. In contrast, the results have revealed that both advective and diffusive transport occurs within the failed shaft (worst case scenario) and that the solute transport within the shaft is significantly influenced by the ice loading cycles.

The main simulation results are presented in Figures 6.8 to 6.11. These Figures illustrate the impact of the second peak of four glaciation cycles (first (Figure 6.8), second (Figure 6.9), third (Figure 6.10) and fourth (Figure 6.11)) on the relative solute concentration and distribution in the study area for the normal and worst case scenario. From these Figures, it can be seen that, regardless of the number of glaciation cycles when the shaft is intact, the migration of a solute released from the horizon of the proposed DGR will be limited and the solute will still remain in the natural shale barrier layer. This is positive with regards to the safety of the DGR and may suggest that the limestone and shale formations act as a very effective barrier with regards to radionuclide transport. In contrast, when the shaft failed, the simulation results show that the solute can reach the shallow bedrock (e.g., salina formation) groundwater zone (Figures 6.10 and 6.11). These results might imply that the failed shaft will lose much of its effectiveness and the implications have to be considered in future safety assessment and final engineering design.

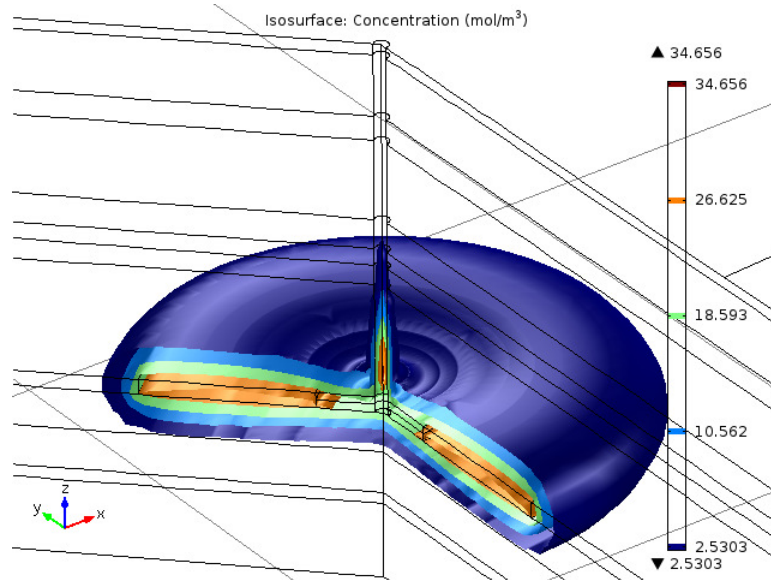


a) worst scenario

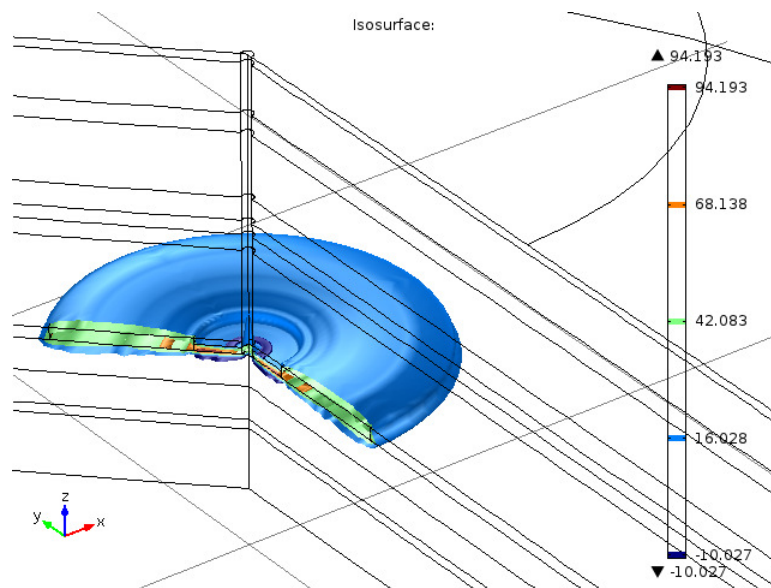


b) normal scenario

Figure 6.8. Computed relative solute concentrations at the second ice loading peak (app. 100k years) of the first glaciations cycle considering the transport by diffusion and advection

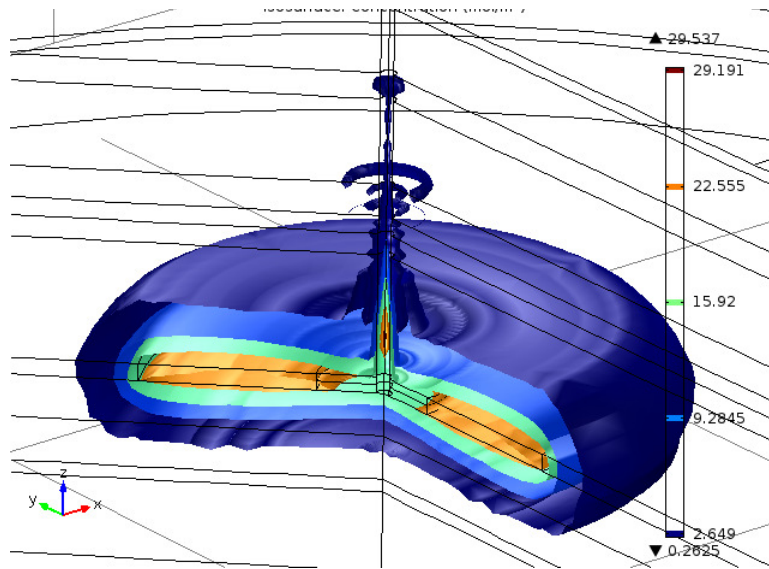


a) worst scenario

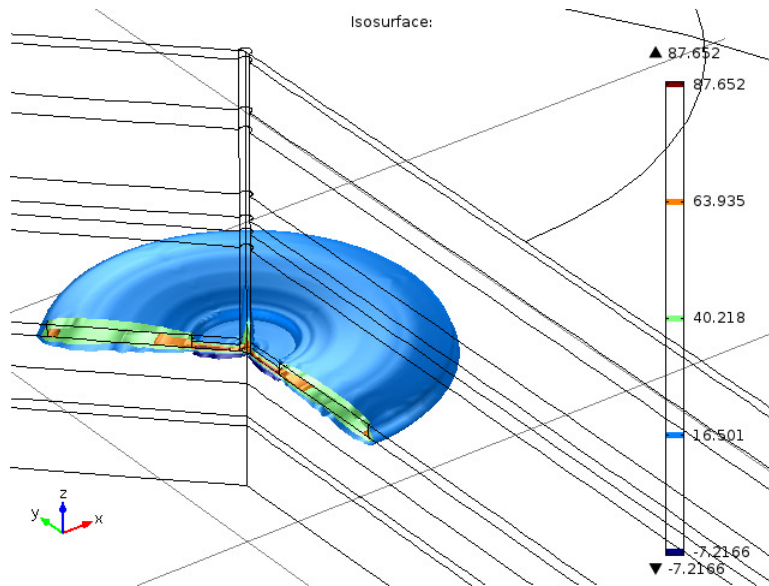


b) normal scenario

Figure 6.9. Computed relative solute concentrations at the second ice loading peak (app. 220,500 year in the future) of the second glaciation cycle considering the transport by diffusion and advection

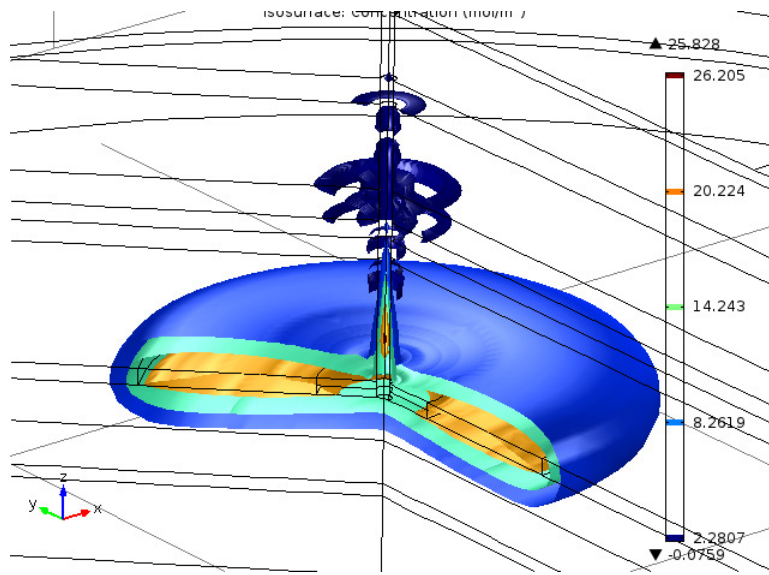


a) worst scenario

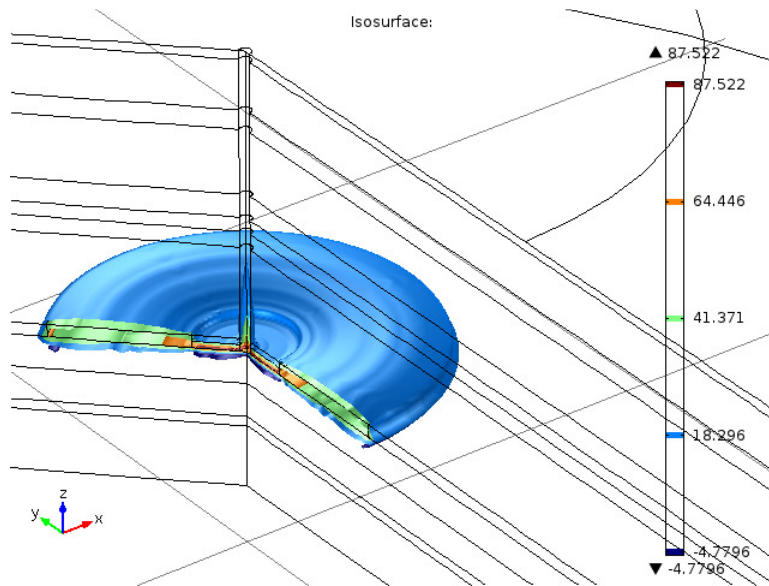


b) normal scenario

Figure 6.10. Computed relative solute concentrations at the second ice loading peak (app. 340,500 year in the future) of the third glaciation cycle considering the transport by diffusion and advection



a) worst scenario



a) normal scenario

Figure 6.11. Computed relative solute concentrations at the second ice loading peak (app. 460,500 year in the future) of the fourth glaciation cycle considering the transport by diffusion and advection

7 Conclusions

The following conclusions can be drawn:

- The analysis of the Peltier’s and Boulton’s climate change models has shown that both models, UEDIN or the U of T GMS, could be used to reconstruct past climate changes and predict future climate changes in Ontario. Each model presents certain advantages and some weakness with regards to its applicability to Ontario.
- The review and analysis of the geological and geotechnical data of Ontario’s sedimentary rocks have revealed that sedimentary rocks in southern Ontario are part of the Michigan Basin, in which some of its formations with higher horizontal hydraulic conductivity are exposed to the surface in some of the areas. It is also found that southern Ontario is “relatively” tectonically stable. However, some major fracture and fault blocks appear, dividing the region into megablocks. For more accurate and representative results, the boundaries of these megablocks could be included in the domain of the numerical model to include their impact.
- Based on the theory of porous media, a coupled thermo-hydro-mechanical-chemical model (THMC) is developed to predict the impact of past and future climate change on the sedimentary rock formations in Ontario. A set of governing equations is developed to simulate coupled heat, solute and fluid transfer or transport in deformable porous media. The governing equations are derived based on the basic laws of force equilibrium, mass conservation and heat conservation. The reliability of the prediction ability of the model is tested by comparing the predicted values with those measured in the field or obtained by using an analytical model. The model verification results have shown that there is a relatively good agreement between the predicted data and those measured in the field or obtained by using analytical procedure. Consequently, the developed THMC model can be used to simulate the effects of past and future glaciation cycles on sedimentary rocks in southern Ontario for the study area.

- A numerical study for the THMC processes associated with past and future glaciation cycles in sedimentary rocks in southern Ontario is conducted. It is found that past and future glaciations had or will have a significant impact on the pore water pressure gradient, hydraulic gradient and effective stress distribution within the sedimentary rocks in Ontario. It is also found that past or future ice loading did or will not lead to the failure or fracturing of the natural rock barrier (limestone, shale) formations. The results are consistent with the field observations. However, with regards to the past glaciations, the predicted values of underpressure are smaller than the observed values at the site, which could be attributed to additional sources, such as gas or somatic pressure.
- The results obtained have shown that the solute transport in the natural limestone and shale barrier formations is controlled by diffusion. The diffusion dominant solute transport in the natural rock was determined to be not significantly sensitive to past and future glaciation cycles. Moreover, regardless of the number of glaciation cycles, the migration of a solute released from the horizon of the proposed DGR will be limited and the solute will still remain in the natural shale barrier layer, provided that the shaft retains its integrity.
- In case the shaft seals deteriorate resulting in a substantial increase in permeability, future glaciation loads will induce solute transport within the failed shaft which will be controlled by both diffusion and advection. The simulation results show that the solute transported in the failed shaft can reach the shallow bedrock (e.g., salina) groundwater zone. Future safety assessment and the final engineering design of the shaft should take into consideration the possibility of long term deterioration of the shaft seals, that could be further exacerbated by future glaciation-deglaciation cycles.
- We have not considered the effects of data uncertainties in the present study. We intend to include those effects in the future using suitable statistical methods. Furthermore, varying and more complex (thermal, hydraulic, mechanical) boundary conditions should be incorporated in the future model to improve its analysis ability.

- The results of this research can provide valuable information that will contribute to a better understanding of the impacts of past and future glaciations on the long term performance of DGRs in sedimentary rocks.

8 References

- Boulton, G. S., G. D. Smith, A. S. Jones, and J. Newsome. 1985. Glacial geology and glaciology of the last mid-latitude ice sheets. *Journal - Geological Society (London)* 142, (3): 447-474.
- Boulton, G. S., G. Gustafson, K. Schelkes, J. Casanova and L. Moren. (2001). Palaeohydrogeology and geoforecasting for performance assessment in geosphere repositories for radioactive waste disposal (Pagepa). Luxembourg, Office for Official Publications of the European Communities. (European Commission Community Research Project report EUR19784.)
- Boulton G., Chan T, Christiansson R, Ericsson L, Hartikainen J, Jensen MR, Stanchell FW, Wallroth T. (2004). Thermo-hydro-mechanical (T-H-M) impacts of glaciation and implications for deep geologic disposal of nuclear waste. In: Stephansson O, Hudson JA, Jing L, editors. *Geo-engineering book series: coupled thermohydro-mechanical-chemical processes in geo-systems*, vol. 2. Amsterdam: Elsevier; p. 299–304.
- Chan T, Christiansson R, Boulton GS, Ericsson LO, Hartikainen J, Jensen MR, Mas Ivars D, Stanchell FW, Vidstrand P, Wallroth T. (2005). DECOVALEX III BMT3/BENCHPAR WP4. Report of BMT3/WP4 — The thermo-hydro-mechanical responses to a glacial cycle and their potential implications for deep geological disposal of nuclear fuel waste in a fractured crystalline rock mass. SKI Report 2005:28, Swedish Nuclear Power Inspectorate, Stockholm, 2005. See CD-ROM attachment entitled, DECOVALEX III BMT3/BENCHPAR WP4, the THM conditions during the dynamics of a glaciation cycle: A synthetic case based mainly on simplified data from the Whiteshell site.
- Clauser C., Huenger E. 1995. *Thermal conductivity of rocks and minerals*. Washington, DC: American Geophysical Union, pp. 105-126.
- Dziewonski, A.M., Anderson, D.L., (1981). Preliminary reference Earth model. *Physics of the Earth and Planetary Interiors* 25, 297–356.
- Eardley, A. J., (1962). *Structural geology of North America*. Harper & Row. Second Edition.

- Gartner Lee Limited, 2008. Phase I Regional Geology, Southern Ontario. Supporting technical report. OPG 00216-REP-01300-00007-R00.
- Grasby, S. E., and Z. Chen. 2005. Subglacial recharge into the western Canada sedimentary basin - impact of Pleistocene glaciation on basin hydrodynamics. *Bulletin of the Geological Society of America* 117, (3-4): 500-514.
- Hobbs M.Y., Frapce S.K., Shouakar-Stash O., Kennell L.R. 2008. Phase I Regional Hydrogeochemistry, Southern Ontario 00216-REP-01300-00006-R00, 160p.
- Jensen, M., Lam, T., Luhowy, D., McLay, J., Semec, B and Frizzel, R., 2009. Ontario Power generation's Proposed L&ILW Deep Geologic Repository: An Overview of Geoscientific Studies. Canadian Geotechnical Conference, GeiHalifax2009.
- Jeonghoon, L., Xiahong, F., Eric S. P., Anthony M. F., Susan, T. 2009. Stable isotopic exchange rate constant between snow and liquid water. *Chemical Geology* 260 (2009) 57-62.
- Karrow, P. F., and O. L. White. 2002. A history of neotectonic studies in Ontario. *Tectonophysics* 353, (1-4): 3-15.
- Lambeck, K. and Natiboglu, S. M. (1980). Seamount loading and stress in the ocean lithosphere. *Journal of Geophysical Research*, 85 (B11): 6403-6418.
- Lambeck, K., Smither, C. and Johnston, P. (1998). Sea-level change, glacial rebound and mantle viscosity for northern Europe. *Geophysical Journal International* 134, 102-144.
- Le Meur, E. and Huybrechts, P. (1996). A comparison of different ways of dealing with isostasy: examples from modelling the Antarctic ice sheet during the last glacial cycle. *Annals of Glaciology*, 23: 309-317.
- Lo, K.Y. Regional distribution of in situ horizontal stresses in rocks of southern Ontario. (1978) *Canadian Geotechnical Journal*, 15 (3), pp. 371-381.
- Lowe, J.J. and Walker, M.J.C. (1997). *Reconstructing Quaternary Environments*. Second Edition, Longman Group Ltd., London and New York, 446 pp.
- Mahaffy, M. W. (1976). A three-dimensional numerical model of ice sheets: tests on the Barnes Ice Cap, Northwest Territory. *J. Geophys. Res.* 95, 22547-22557.

- Mark, A., Maslin, a., Beth Christensen. (2007) Tectonics, orbital forcing, global climate change, and human evolution in Africa: introduction to the African paleoclimate special volume. *Journal of Human Evolution* 53 (2007) 443-464
- Maslin, M. A., & Christensen, B. (2007). "Tectonics, orbital forcing, global climate change, and human evolution in Africa". Introduction to the african paleoclimate special volume. *Journal of human evolution* 53, (5): 443-464.
- Mazurek, M. 2004. Long-term used nuclear fuel waste management - Geoscientific review of the sedimentary sequence in southern Ontario. Technical Report TR 04-01, Institute of Geological Sciences, University of Bern, Switzerland.
- McIntosh, J. C., and L. M. Walter. 2006. Paleowaters in silurian-devonian carbonate aquifers: Geochemical evolution of groundwater in the great lakes region since the late pleistocene. *Geochimica et Cosmochimica Acta* 70, (10): 2454-2479.
- McNutt, R. H., S. K. Frappe, and P. Dollar. 1987. A strontium, oxygen and hydrogen isotopic composition of brines, michigan and appalachian basins, ontario and michigan. *Applied Geochemistry* 2, (5-6): 495-505.
- Mongelli, F., M. Lodo, and A. Tramacere. 1982. Thermal conductivity, diffusivity and specific heat variation of some travale field (tuscany) rocks versus temperature. *Tectonophysics* 83, (1-2): 33-43.
- Nasir O., Fall M., Nguyen S., Evgin E. 2011. Hydromechanical response of Ontario's sedimentary rocks to past glaciations. *Engineering Geology* (in press)
- Nasir O., Fall M., Nguyen S., Evgin E. 2009. Hydro-Mechanical Response of Sedimentary Rocks of Southern. Ontario to Past Glaciations. *Comsol Conference*, Boston, 2009.
- Nguyen, T. S., V. Poliscuk, and A. P. S. Selvadurai. 1993. Effects of glaciation on a nuclear fuel waste repository. *Canadian Geotechnical Conference*: 79-88
- NWMO, 2011a, Geosynthesis, NWMO DGR-TR-2011-11, 418p.
- NWMO, 2011b, Geosphere Site Model report, NWMO DGR-TR-2011-24, 426p
- NWMO, 2011c, Hydrogeological modelling report, NWMO DGR-TR-2011-16, 261p
- NWMO, 2011d, Regional Geomechanics, NWMO DGR-TR-2011-13, 89p.

- Nguyen, T.S. (1995). Computational modeling of thermal-hydrological mechanical processes in geological media, Ph.D Thesis, McGill University, Montreal, Quebec.
- NWMO, 2011e, Postclosure safety assessment: Data, NWMO DGR-TR-2011-32, 89p
- O'Hara, N.W., Hinze, W.J. (1980) Regional basement geology of Lake Huron Geol. Soc. Am. Bull., 91, pp. 348-358.
- Oswell, J.M. (1991). Elastic-plastic behaviour of a sand-bentonite mixture. PhD thesis, University of Manitoba.
- Peltier, W.R., (1974). The impulse response of a Maxwell Earth. *Reviews of Geophysics* 12, 649–669.
- Peltier, W.R., (1976). Glacial isostatic adjustment II: the inverse problem. *Geophysical Journal of the Royal Astronomical Society* 46, 669–706.
- Peltier, W.R., (1996). Mantle viscosity and ice age ice sheet topography. *Science* 273, 1359–1364.
- Peltier, W.R. 2003. Long-term climate change – glaciation. Ontario Power Generation, Nuclear Waste Management Division Report 06819-REP-01200-10113-R00. Toronto, Ontario.
- Peltier, W.R., 2008. Phase I long term climate change study. Supporting technical report. OPG 00216-REP-01300-00004-R00.
- Peltier, W.R., 2011. Long term climate change. Technical report. NWMO DGR-TR-2011-14.
- Piotrowski, J. A. 1987. Genesis of the woodstock drumlin field, Southern Ontario, Canada. *Boreas* 16, (3): 249-265.
- Raven, K. G., K. S. Novakowski, R. M. Yager, and R. J. Heystee. 1992. Supernormal fluid pressures in sedimentary rocks of southern ontario - western new york state. *Canadian Geotechnical Journal* 29, (1): 80-93
- Ruddiman, W. F., (1997). *Tectonic Uplift and Climate Change*: New York, Plenum Press, 535 p.

- Sanford, B.V., Thompson, F.J., McFall, G.H., 1985. Plate tectonics — a possible controlling mechanism in the development of hydrocarbon traps in southwestern Ontario. *Bull. Can. Pet. Geol.* 33, 52–71.
- Siegel, D. I. 1991. Evidence for dilution of deep, confined ground water by vertical recharge of isotopically heavy pleistocene water. *Geology* 19, (5): 433-436.
- Tarasov, L., and W. R. Peltier. 1999. Impact of thermomechanical ice sheet coupling on a model of the 100 kyr ice age cycle. *Journal of Geophysical Research D: Atmospheres* 104, (D8): 9517-9545.
- Tarasov, L., and W. R. Peltier. 2002. Greenland glacial history and local geodynamic consequences. *Geophysical Journal International* 150, (1): 198-229.
- Tarasov, L., and W. R. Peltier. 2004. A geophysically constrained large ensemble analysis of the deglacial history of the North American ice sheet complex, *Quat. Sci. Rev.*, 23, 359– 388.
- Tarasov, L., and W. R. Peltier. 2006. A calibrated deglacial drainage chronology for the north american continent: Evidence of an arctic trigger for the younger dryas. *Quaternary Science Reviews* 25, (7-8): 659-688.
- Vidstrand, P., Wallroth, T., & Ericsson, L.O. (2008), “Coupled HM effects in a crystalline rock mass due to glaciation: Indicative results from groundwater flow regimes and stresses from an FEM study”. *Bulletin of Engineering Geology and the Environment*, Vol. 67(2), 187-197.
- Weaver, T. R., Frape, S. K. and Cherry, J. A. 1995. Recent cross-formational fluid flow and mixing in the shallow Michigan Basin. *Bulletin of the Geological Society of America* 107, (6): 697-707.
- Zoback, M.L., Zoback, M. State of stress in the conterminous United States. (1980) *Journal of Geophysical Research*, 85 (B11), pp. 6113-6156.

9 Disclaimer

The Canadian Nuclear Safety Commission is not responsible for the accuracy of the statements made, or opinions expressed in this publication, and do not assume liability with respect to any damage or loss incurred as results of the use made of the information contained in this publication.